A comprehensive review on advances of oil-based nanofluids for concentrating solar thermal collector application

Fazlay Rubbi[a,*], Likhan Das[a], Khairul Habib[a,*], Navid Aslfattahi[b], R. Saidur[c,d], Sanney Ul Alam[e]

[a] Department of Mechanical Engineering, Universiti Teknologi PETRONAS, 32610, Bandar Seri Iskandar, Perak Darul Ridzuan, Malaysia

[b] Department of Mechanical Engineering, Faculty of Engineering, University of Malaya, Kuala Lumpur, 50603, Malaysia

[c] Research Centre for Nano-Materials and Energy Technology (RCNMET), School of Science and Technology, Sunway University, No. 5, Jalan Universiti, Bandar Sunway, 47500, Petaling Jaya, Malaysia

[d] Department of Engineering, Lancaster University, Lancaster, LA1 4YW, UK

[e] Department of Mechanical Engineering, Khulna University of Engineering & Technology (KUET), Khulna-9203, Bangladesh

*Corresponding author: Fazlay Rubbi (mdfrs22@gmail.com) and Khairul Habib (khairul.habib@utp.edu.my).

Abstract

Nanofluids have exhibited noteworthy advancement as efficient working fluids in the last decade towards the field of solar energy conversion field to deal with escalating global energy demand. Research developments on thermo-physical, long-term stability and rheology are moving ahead to achieve practical deployment in renewable solar photo-thermal conversion sectors (i.e., solar collectors). Nevertheless, researchers and engineers are encountering many difficulties dealing with nearly infinite culpable variables impacting performance of several categories of NFs. This work attempts to offer an up-to-date review on advances and challenges of oil-based nanofluids focusing on formulation, key properties (stability, thermal conductivity, c_p, and viscosity) and effective implementation in concentrating solar collector devices. Previous experimental and numerical studies on the topics are compiled and acutely scrutinized

providing essential phenomena, mechanisms, shortcomings, responsible parameters to obtain stable and optimized thermal properties integrating with heat transfer performance. It is observed that optimization of the critical factors leads to superior behavior of the nanofluids, which in turns generates enhanced thermal performance of the solar collectors. Lastly, existing challenges are reported along with recommendations to address the issues for further developments in the field which would mobilize rapid innovation and practical engineering practice of nanofluids.

Keywords: Nanofluids, Thermo-physical Properties, Stability, Rheology, Concentrating solar Collectors.

Nomenclature

Abbreviations

NF	Nanofluid	DSC	Differential Scanning Calorimetry
NP	Nanoparticle	DLVO	Derjaguin Landau Vewey and Overbeek
BF	Base Fluid	ZP	Zeta potential (mV)
HTF	Heat Transfer Fluid	EDL	Electrical double layer
SC	Solar Collector	IEP	Isoelectric Point
TC	Thermal conductivity	DASC	Direct absorber solar collector
d_p	Particle diameter (nm)	PTSC	Parabolic trough solar collector
ECS	Energy Conversion System	PDSC	Parabolic dish solar collector
CNT	Carbon Nanotube	CPC	Compound parabolic solar collector
SWCNT	Single-walled carbon nanotube	CPV/T	Concentrated Photovoltaic/ thermal solar collector
MWCNT	Multi-walled carbon nanotube	UV-Vis	Ultraviolet–visible spectroscopy
EG	Ethylene glycol	***Greek Letters***	
SDS	Sodium Dodecyl Sulphate	μ	Dynamic viscosity (Pa.s)
SDBS	Sodium Dodecyl Benzene Sulphonate	φ	Particle concentration (%)
CTAB	Cetyl Trimethyl Ammonium Bromide	ζ	Zeta potential (mV)
GA	Gum Arabic	α	Absorptivity
PVP	Polyvinylpyrrolidone	ε	Dielectric Constant
DDC	Distearyl Dimethylammonium Chloride	***Subscripts***	
PLS	Potassium Lauryl Sulphate		
k	Thermal conductivity (W/m.K)	nf	Nanofluid
c_p	Specific heat capacity (Kj/kg.K)	bf	Base Fluid
T	Temperature (K)	np	Nanoparticle

1. Introduction

1.1. Overview on nanofluid

Nanofluids (NFs) are the superior colloids achieved from nanoscale (1-100 nm) materials dispersed into pure base fluid (BF) which is commonly a liquid. In1993, nanoscale suspensions were synthesized experimentally for the first time by Masuda, et al. [1] and later on labeled as 'nanofluid' by Choi and Eastman [2] in 1995. Due to remarkably extra-large surface area and dominant characteristics of dispersed solid particles of nanomaterials relative to BFs, NFs convey superior heat transfer properties [3]. Properties of nanoparticles (NPs) are controlled by their surfaces instead of the volume and that allows having advantageous and flexible thermal, optical, mechanical, and electrical characteristics [4]. The addition of very low weight concentration of these NPs into conventional heat transfer fluids (HTFs) remarkably enrich essential thermo-physical, optical, and chemical features of the fluids. The important thermo-physical properties include conductive heat transport and specific heat capacity of the HTFs, which have a significant impact on thermal energy efficiency of the abundant extent of liquid based thermal energy storage and energy conversion systems. Numerous studies confirm considerable escalation in thermal conductivity, specific heat capacity and heat transfer characteristics of nanofluids in comparison with the base fluids [5-7].

Among all the promising NF distinctions, colloidal stability of suspended NPs in main fluid emerges as the most critical impediment to overcome, as particles tend to congregate with the passage of time. Stable suspension time is the foremost requirement for sustainable industrial consumption of NFs in various heating and cooling applications [8]. In addition, excellent properties and suspension stability of NFs are dependent on key parameters such as types of BFs, NPs, particle concentration (φ) and morphology that can cause significant divergence in thermal characteristics. The present study focuses on the most frequently applied NFs which

are formulated using oil as a dispersion medium for multifarious NPs. Furthermore, the hybrid category of the NF has gained a lot of attention as a better form obtained by dispersing a combination of nanomaterials in the BF [9]. While water-based NFs are suitable for low temperature thermal application up to 90℃, oil-based NFs can be applied to medium-high temperature range (100-350℃) thermal energy application because of their inherent high boiling point and good thermo-physical properties at higher temperatures. In recent studies, many thermal oil-based NFs are being utilized as working fluid in thermal energy storage (TES) applications due to their potency in medium to high temperature applications in terms of thermal output. Generally, three classes of thermal oils are: petroleum-based mineral oils, chemically formulated synthetic oils and extracted vegetable oils from plants [10]. Oil-based NFs are preferable for use as HTF because they are biodegradable, have good thermal stability, are renewable, and have little environmental impact when compared to other conventional toxic liquids such as ethylene glycol, ionic liquids, and so on. Considerable research articles have been published over recent years studying relating to properties, essential factors, and future prospect of oil-based NFs in practical usage. **Fig. 1** represents previous articles published on oil, and hybrid variant of NFs in recent years (2015-2020), which indicate growing attention of oil and hybrid NFs in research and development.

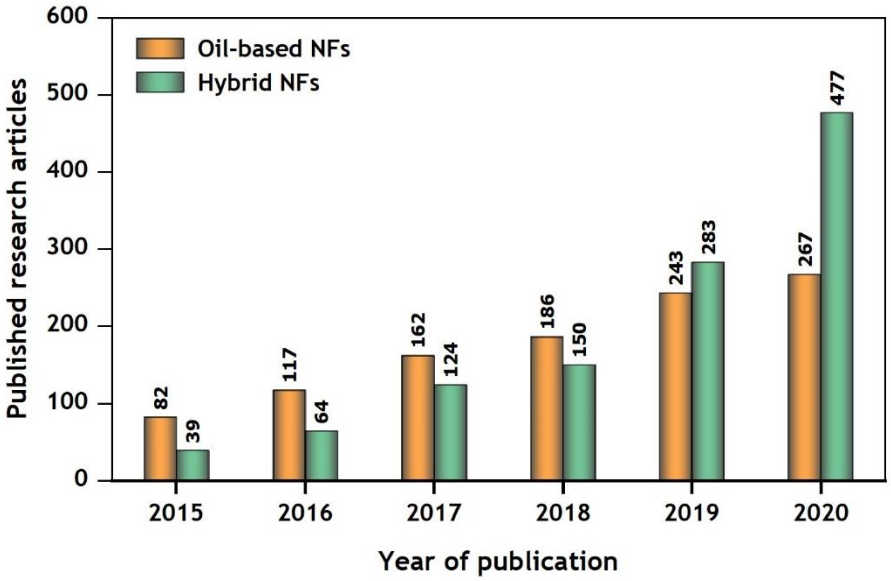

Fig. 1. Published research articles on oil and hybrid based nanofluids from year 2015-2020 (Source of data: Web of Science, using keywords: Oil based nanofluids and Hybrid nanofluids).

1.2. Application of nanofluids on solar collectors

The scarcity of sustainable energy resources has become a sophisticated challenge to meet the ever-growing global energy demand alongside depletion of carbon-based fossil energy resources and their constant threat to the environment. In this context, experts are paying attention to the pursuit of alternative sources of energy which will be adequate to achieve the massive energy requisition in the future. Since, the energy demand will keep escalating in the future, one way to compensate for the energy scarcity is by utilizing sustainable renewable energy sources. Solar energy is one of the most convenient, pollutant-free, sustainable, renewable and abundantly available energy resources [11]. A plethora of research is being conducted on solar energy systems by substituting traditional HTFs with NFs to advance the thermal energy conversion efficiency [12-14]. Concentrating solar collector (SC) systems are one of the emerging sectors of renewable energy which is growing evidently with the advancement of NFs as their working fluids [15]. Concentrating SCs are engineered systems

to harness solar radiation to produce thermal energy and electrical power for utilization in different domestic and industrial applications [16].

1.3. Aim of this review

This paper aims to provide a comprehensive review on research advances, development, and future scope of NF thermo-physical properties of oil-based NFs and their applications on concentrating SC technologies. Previously, a few articles attempted to provide a general overview of various properties (thermal and optical) and applications of NFs on SCs [17, 18], while others attempted to address NF stability issues [8, 19]. Yet, there is no comprehensive review that particularly aims to articulate overall advances on often used oil-based NFs characteristics, limitations, and application on concentrating SCs. Therefore, the aim of the current review is to put up a much-required comprehensive review of the thermo-physical properties (thermal conductivity, c_p, and rheology) and colloidal stability of the oil-based NFs. In addition, this review explicitly focuses on the extensive application of oil-based NFs on the SCs. Potential properties of the NFs are critically analyzed with causes, effects of several parameters, characterization, improvement techniques of suspension stability and finally the application of the fluids in the solar energy conversion collectors. Based on the review of substantial research on the topic, future developments, directions, and research gaps are established and important conclusions are drawn. The structure of the article is demonstrated in **Fig. 2**. This study is an essential step towards vigorous development and understanding of oil-based NFs and their application on concentrating SCs.

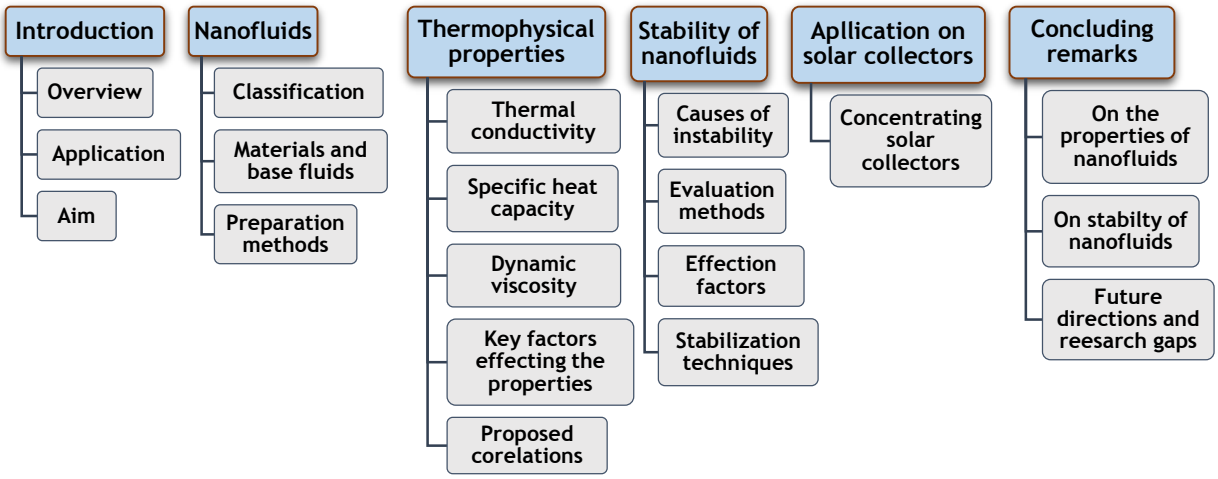

Fig. 2. Overview of structure of this review paper.

2. Nanofluids

2.1. Base fluids and nanoparticles

NFs are developed by diffusing nanostructured materials at the nanoscale range (1-100 nm) into pure conventional working fluids. Classification of NFs based on extensively used BFs and nanomaterials is depicted in **Fig. 3**. Different types of base fluids such as water, oils (thermal, synthetic, and vegetable), glycols (ethylene and propylene), and ionic liquids have been used as dispersion medium to formulate NFs based on thermal systems and their working temperature range. Each of the fluids has some advantages and disadvantages on their own while implemented on thermal systems. For low temperature applications, water-based NFs are recommended due to their superior thermo-physical properties relative to other BFs. In contrast, for medium to high temperature thermal systems, oils, glycols and liquid salts are generally utilized to prepare NFs.

Suspended nanomaterials are the most distinctive feature of NFs as these particles possess unique thermal and optical properties and significantly impact the characteristics of the BFs. Nanomaterials have at least one dimension in the nanometer range with high conductive surface to volume ratio, advanced physical, chemical, and mechanical properties relative to their bulk

form. Nanomaterials can be metallic (e.g., Ag, Cu, Ti, Fe, Al), polymers, ceramics, non-metallic (CuO, TiO_2, Al_2O_3, SiO_2) and carbon-based (SWCNT, MWCNT, graphene, MXene) materials which are formed in various geometrical shapes such as spherical, cylindrical, rod-like, and plate-like. In terms of their dimensions at the nanoscale, nanostructured materials can be divided into four categories: (a) zero-dimensional (0-D) nanomaterials with no dimensions, such as nanoparticles and graphene/carbon quantum dots; (b) one-dimensional (1-D) nanomaterials with one dimension at the nanoscale range, such as nanotubes and nanowires; and (c) two-dimensional (2-D) nanomaterials with layered nanofilaments and (d) Bulk three-dimensional (3-D) nanomaterials that are confined at nanoscale dimensions such as bulk powder, composite nanomaterials and multi-nanolayers. **Fig. 4** represents an illustration of nanostructured materials based on their dimensions at nanoscale length. Colloidal suspension comprises of a BF and one of those types of particles defined as nanofluid. If NF consists of more than one kind of particles in fluids, then it can be called hybrid NF [20]. Das, et al. [21] have discussed the utilization of a variety of traditional and advanced NPs in enhancing the optical and thermal characteristics of the working fluid for potential photo-thermal energy conversion application. An abundant number of studies are reported in literatures where types of nanomaterials are comprised of water and oils to characterize their potency in practical application. Subsequent sections of this review will cover preparation and details on characterization of the NFs.

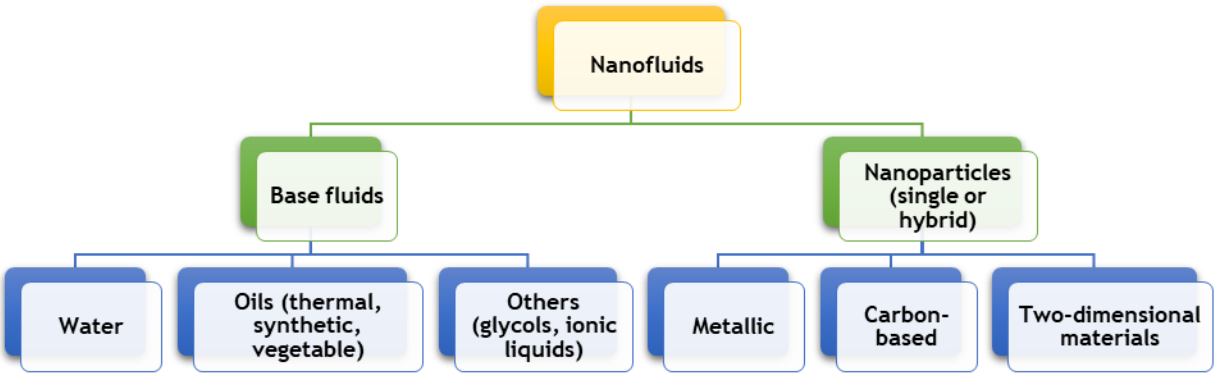

Fig. 3. Classification of nanofluids in terms of base fluids and nanoparticles.

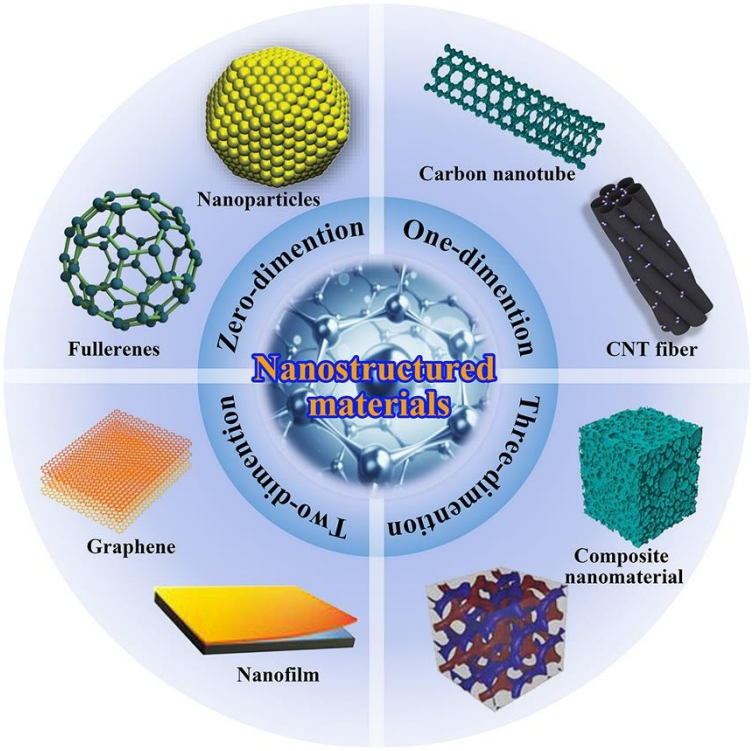

Fig. 4. Demonstration of solid nanomaterials with unique dimensions at nanoscale range [4].

2.2. Nanofluid formulation

NFs are recognized as innovative thermo-fluids because of their augmented thermophysical features, i.e., conductive heat transfer coefficient, thermal conductivity, thermal diffusivity, and heat storage capacity relative to traditional working fluids like water and oils. Exceptional properties of NFs are depicted in **Fig. 5** which are employed in various applications and performed efficiently according to their advantages over common fluids. Formulation of NF suspension is an important step as it can dictate a few important parameters, specifically the suspension stability and thermal properties. The first phase of NF formulation involves synthesis procedure of nanostructured materials and comprised with BF in the latter step. Several physical, chemical, physiochemical techniques are often utilized in nanotechnology to synthesize NPs. Moreover, NPs are assessed using different systematic approaches like transmission microscope, infrared spectroscopy, X-ray diffraction, and Raman spectroscopy during the synthesis processes.

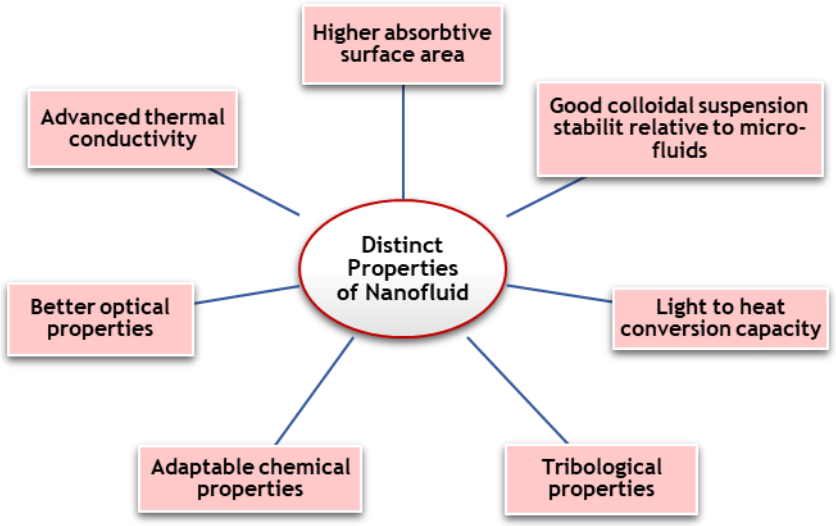

Fig. 5. Distinct advanced properties of nanofluids.

To prepare stable NFs, two standard methods are used, identified as: the single-step method, which is a combination of two individual procedures of nanoparticles fabrication and dispersion into base fluid concurrently, while the two-step method incorporates two separate processes of particle fabrication followed by dispersion utilizing several stabilization techniques. Both basic techniques have few advantages and disadvantages in terms of flexibility, thermophysical characterization, and economic aspects. Sedimentation of NPs is the major challenge in nano-powder dispersion technology even though the single-step technique is reported to produce stable NFs whereas thermal properties are found to be enhanced more when fluids are fabricated in the two-step method [22]. Details on these techniques are discussed in the later sections.

2.2.1. Formulation methods

The two-step (also recognized as top-down/dispersion) method is the simplest, cost-effective, and scalable technique to formulate NFs where solid nanomaterials are independently synthesized and subsequently suspended into a pure fluid and stabilized using chemical dispersants and/or mechanical, physical treatments. In the first step, bulk materials are broken down into suitable nano range using several approaches, such as wet-chemical etching and/or

physical procedures. The synthesis step also includes a few intermediate processes such as drying of the particles, storage, and the dispersion of the particles. The stabilization step comprises techniques like addition of several types of chemicals (electrostatic, steric, and electro-steric), physical (ultrasonication, high pressure homogenization and ball milling) treatments. However, clustering of dry NPs is inevitable while drying, storage period and during dispersion into base fluid in this method of NF formulation [23]. The major shortcoming of the two-step technique is that due to high surface energy of the NPs, the clustering and nonhomogeneous dispersion of particles which leads to short time suspension stability and weakening of expected thermo-physical properties of NFs. This disadvantage can be compensated by repeated physical treatment to break down the aggregation and stabilize the mixture consistently for longer periods. Two-step methods are the predominant techniques to formulate NFs due to their simple production procedures, flexibility with parameters and scalable production for industrial usage. These techniques are frequently used to formulate carbon-based, metallic, and oxide-based NFs in various base fluids including water and oils. In essence, the two-step method is the suitable technique to formulate and obtain thermo-physical, chemical, and optically enriched NFs at large scale production.

The single-step (also familiar as one-step or bottom-up) synthesis technique uses wet-chemistry procedures wherein fabrication of nanomaterials and dispersion into base fluid are performed concurrently to formulate NFs. Several chemical vapor decomposition methods such as plasma arc [24], spraying or sputtering [25], laser ablation [26] and electric explosion [27] techniques are employed to formulate stable nanofluid in the single step. This method eliminates the clustering issues encountered by the two-step process and produces stable suspension of NPs into base fluid. Mohammadpoor, et al. [22] formulated Cu based NFs using both single-step and two-step methods and analyzed the thermal properties and stability of the fluids. They stated that NFs formulated in the single step method are found to be more stable

than the samples prepared in two-step technique, whereas the two-step method yielded better heat transfer properties of the NFs. Nonetheless, large-scale fabrication of NFs is impractical in the bottom-up method due to the complicated procedure and extremely high production costs. Moreover, a few important parameters, including particle size and concentration, cannot be controlled in this fabrication method as it follows batch production with less control over the conditions. Formulation of NFs in single and two-step methods is summarized in **Table. 1** along with employed stabilization techniques and duration of stability.

Table. 1. Summary of recent studies on various type of oil-based NF formulation using standard single step and two-step methods.

Nanofluid(s)	**Particle size and concentration (Φ)**	**Surfactants/ Stabilization techniques**	**Formulation method**	**Stability indicator(s)**	**Reference**
Heat transfer oil/Ag	Ag (20 nm) Φ = 0.12-0.72 wt.%	none	Single step	ζ > 60 mV	Aberoumand, et al. [28]
Engine oil/Cu	Cu (40-65 nm) Φ = 0.2-1 wt.%	none	Single step	ζ = 55 to 65 mV	Aberoumand and Jafarimoghaddam [27]
Silicon oil/Ag	35 nm Φ = 0.5 wt.%	Oleic acid/stirring, ultrasonic bath, sonication, homogenization.	Two-step and Single step	> two months	Hwang, et al. [25]
Silicon oil/Functionalized Fe_3O_4	9 nm Φ = 0.75-3 mg/mL	Oleic acid (OA), and Oleyl-amine (OLA)/ Centrifugation	Two-Step	Observed stable nanofluid at low concentration.	Chen, et al. [29]
Vegetable oil-Water/ CuO	< 20 nm Φ = 1 and 20 vol.%	none	Single step	ζ = -36 mV	Seyedzavvar, et al. [30]
Kapok seed oil/MWCNT	Length: 2.5-20 µm, Diameter: 6-13 nm Φ = 0.1 wt.%	No dispersant/mechanical mixing, ultrasonic bath.	Single step	> one month	Hameed, et al. [31]
Soybean oil/MXene	Lateral size = 1-10 µm Thickness = 1 nm Φ = 0.025-0.125 wt.%	No dispersant/magnetic stirring, ultrasonication.	Two-step	ζ = -56.71 to -80.57 mV	Rubbi, et al. [32]
Therminol®66/ GO-MWCNT	GO (diameter: 0.5-5 µm, thickness: 1-3 nm) MWCNT (diameter: 20-30 nm, length: 10-30 µm) Φ = 10-150 ppm	Oleic acid/magnetic stirring, sonication.	Two-step	> two weeks	Qu, et al. [33]
Therminol®55/ Al_2O_3-TiO_2	Al_2O_3 (>80 nm), TiO_2 (15-25 nm) Φ = 0.05-0.5 wt.%	Oleic acid/magnetic stirring, ultrasonication, ball milling.	Two-step	ζ = 25 to 70 mV	Gulzar, et al. [34]
Transformer oil/Ag-WO_3	Ag and WO_3 (35-55 nm) Φ = 1-4 wt.%	None	Single step	ζ = 46 to 54 mV	[35]

3. Thermophysical properties of nanofluids

3.1. Thermal conductivity

Thermal conductivity (TC) of NFs is the most important characteristic in terms of heat transfer performance (HTP) of the NFs in thermal energy conversion and storage systems. TC of NFs is superior compared to BF due to greater thermal conductivity of solid particles compared to liquids (demonstrated in**Fig. 6**). A plethora of studies has proved the remarkable improvement of TC with the inclusion of NPs into the traditional BF. However, several parameters play an influential role in the enhancement of TC of NFs using different classes of nanomaterials and BFs.

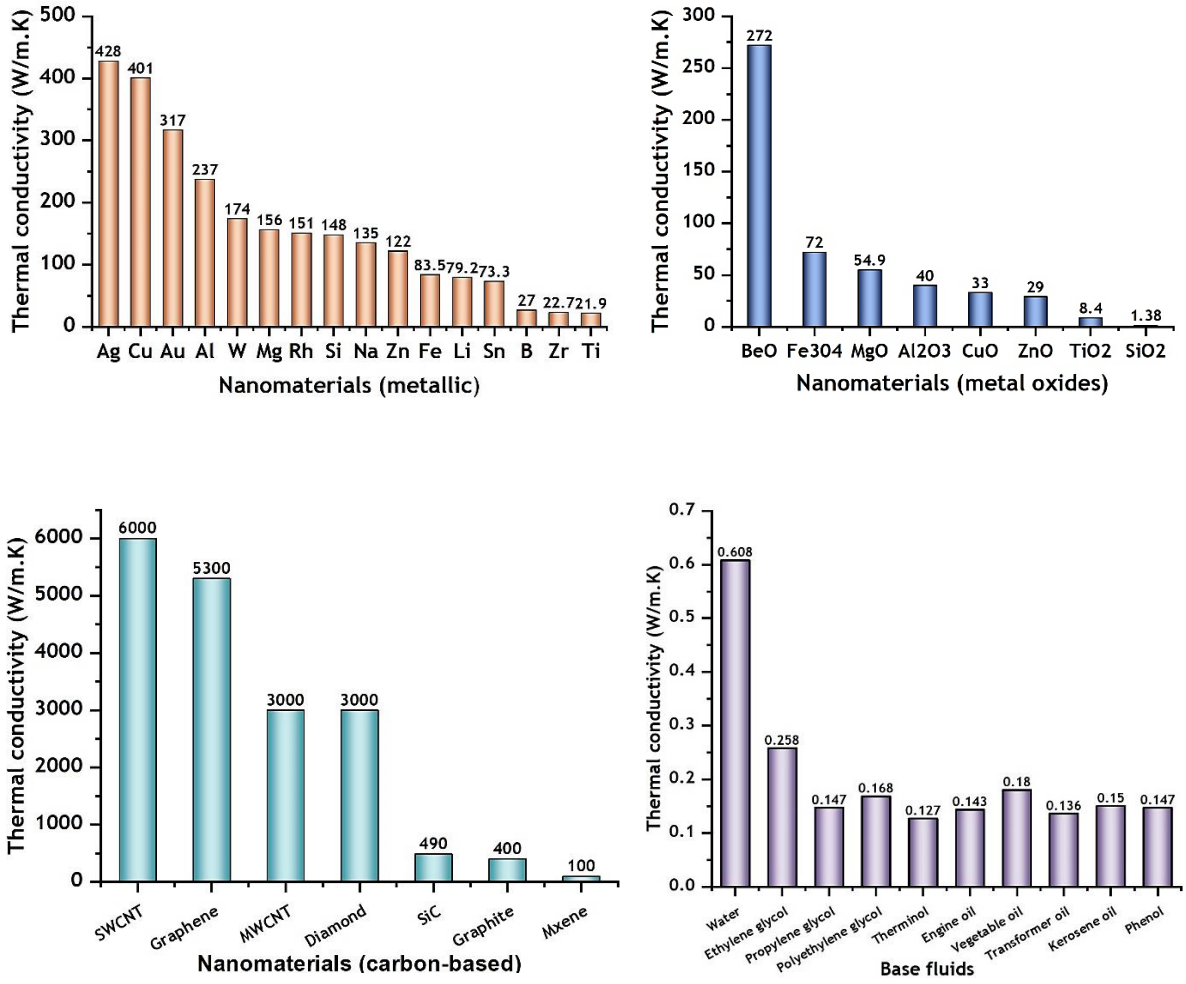

Fig. 6. Thermal conductivity of frequently used nanomaterials (metallic, metal oxides and carbon-based nanomaterials) and base fluids for synthesis of nanofluids respectively from (a) to (d).

3.1.1. Factors effecting TC of NF

TC has been rigorously studied for the last decade as being one of the key properties of advanced NFs as heat transfer fluids. However, studies with oil-based NFs are limited to some extent compared to traditional water-based NFs. The research studies on TC exhibit significant impact of inclusion of solid particles into BF for hybrid, and oil-based NFs. Furthermore, studies on TC show that the inclusion of solid particles in BF has a significant impact on NFs. Research identifies effecting factors of TC as preparation method, concentration (φ), size and shape of NPs, TC of BF, addition of chemical additives, pH of mixture, TC evaluation techniques, operating temperature and stability of dispersion are directly impacting to the effective TC and HTP of NFs represented in **Fig. 7**. Gupta, et al. [36] comprehensively reviewed the effect of several parameters on thermophysical properties of NFs using various types of NPs and dispersed mediums along with the impact of key parameters stated above. Asadi, et al. [37] summarized recent advances of formulation and thermal properties including TC of oil-based NFs which are generally utilized in domestic and industrial solar applications where water-based NFs are not applicable due to low boiling point. In addition, several mechanisms related to TC and heat convection using NFs such as: Brownian motion, particle agglomeration, dispersion stability, intermolecular forces between particles and liquid layers of BF were critically investigated by several researchers in the field [38-40]. The subsequent section is focused on recent advances on TC of widely utilized oil-based and hybrid NFs and the mechanism of TC augmentation and impacts of influential parameters along with numerical or molecular dynamics correlations to estimate the TC of NFs.

The association of φ and TC of NF is well established as it intensifies for corresponding addition of φ up to an optimum level and subsequently deteriorates due to aggregation of excess particles. TC amplification is also favorable at high temperatures due to generated intensified Brownian motion and kinetic energy of the NPs. These augmenting trends of TC established the effectiveness of NFs in elevated-temperature operations e.g., solar collectors and heating/cooling using heat exchanger [41]. NPs synthesized in different sizes and shapes depending on the used synthesis techniques and structure of the nanomaterial have been observed to cause variation in outcomes of TC of NF. Research explored that greater surface to volume ratio of NPs yields more growth in TC, which is exactly why CNT and two-dimensional NP based NFs are generally recognized as more efficient [42]. While experimentally formulating NFs, optimization of stabilizing criteria e.g., sonication time, chemical additives, pH of dispersed mixture, suspension homogeneousness and evaluation approach are the essential preconditions. TC can be measured using different techniques, for instance, transient hot-wire method, optical measurement method, temperature oscillation method and 3-□ method. Transient-hot-wire (THW) method is the most convenient technique to examine TC of NFs due to its simplicity and good precision. Theoretical correlations are also used to assess the TC of various categories of NFs.

Numerous experimental and analytical studies on NF have established the linear growth of NFs TC in response to the addition of a wide range of NPs in BF and increasing temperatures. Afrand, et al. [43] investigated TC of water/Fe_3O_4 (20-30 nm) NF at φ of 0.1-0.3 vol.% varying the temperature from 25-55 ℃. The measured TC results using THW-based KD2-pro showed addition of NPs has a dominant impact on improving effective TC (k_{nf}/k_{bf}) relative to escalating temperatures as 90% enhancement is obtained at 3 vol.% and 55 ℃. Results are consistent with other metal oil-based NFs e.g., TiO_2, Al_2O_3, CuO, SiO_2, MgO and so on (see **Table. 2**).

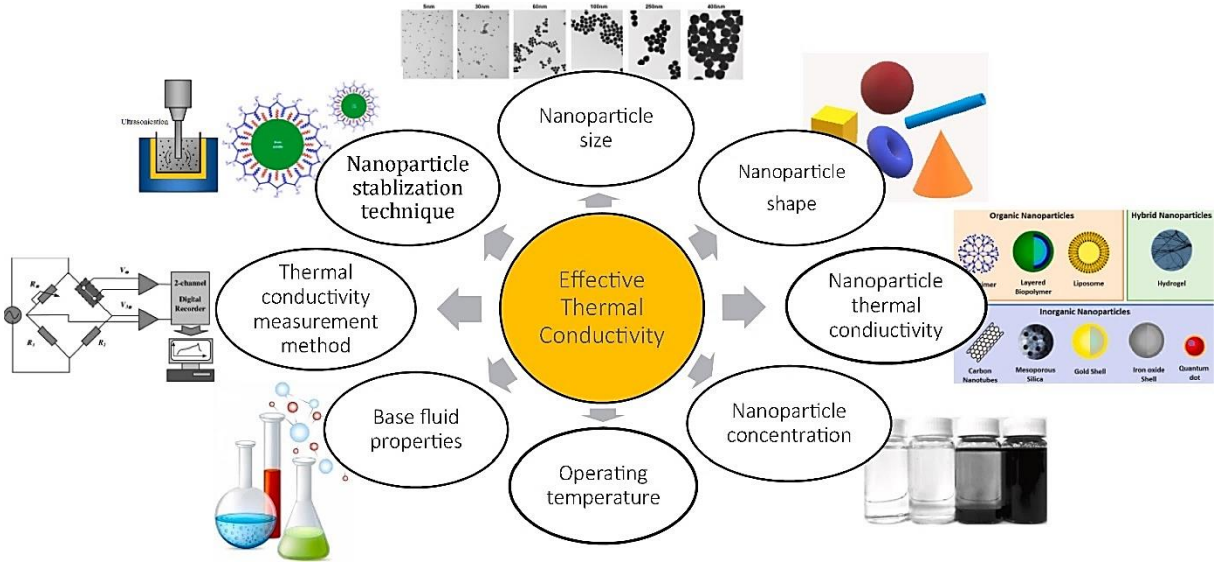

Fig. 7. Influential parameters affecting thermal conductivity of nanofluids [44].

As mentioned earlier, recent development in manufacturing of carbon-based nanomaterials (e.g., CNT, MWCNT, SWCNT, and two-dimensional Graphene) has received unprecedented attention in nanotechnology due to advanced thermo-physical and electro-chemical properties. Hence, nowadays, carbon-based nanomaterials are being utilized frequently in traditional liquids to develop innovative NF suspension with advanced TC. Asadi, et al. [45] studied the effect of solid particles addition and temperature on TC of Al_2O_3-MWCNT/thermal oil NFs. They revealed that the TC increases with the inclusion of particle loading and with rising temperatures. They also noticed that TC of the NFs was adequately influenced by rise in temperature along with particle loading and 45% augmentation is obtained at φ of 1.5 vol.% and 50℃(**Fig. 8**). Analogous trends in TC augmentation against intensifying φ and temperature reviewed in **Table. 2**.

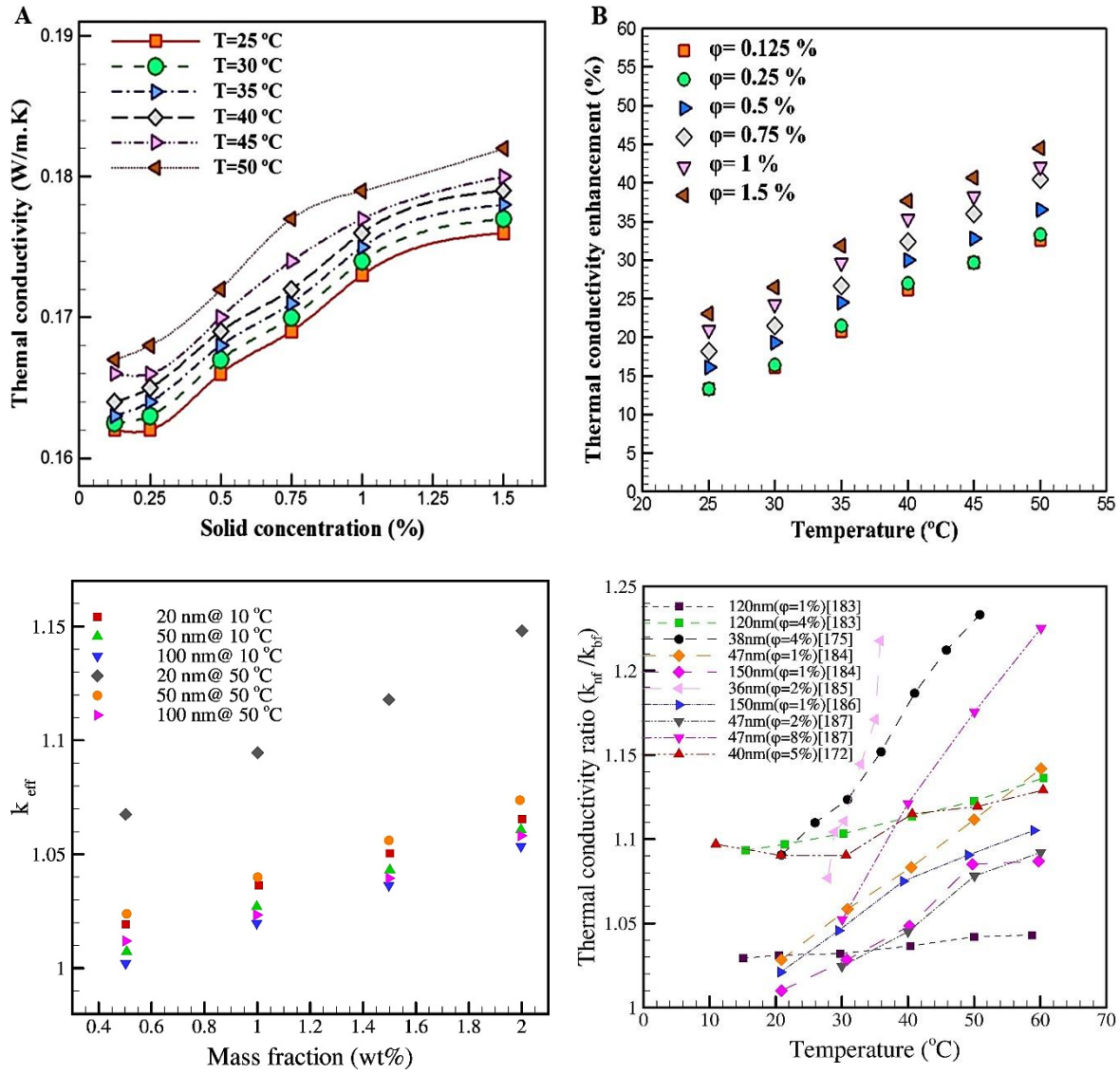

Fig. 8. Effect of particles addition and temperature on thermal conductivity variation of TC against increasing particles concentration and TC increment with respect to temperature and particle size variation (for details see [45],[46]).

Timofeeva, et al. [47] observed different mixture ratio of surfactant to NP (0.1:1-1.5:1) resulting in variation of TC using Therminol-66 oil/SiO_2 NF. They noticed that adding BAC stabilizer fosters TC to increase until an optimum ration of 1:1 and further addition does not influence TC. However, investigating the TC outcomes at rising temperatures, they observed barely an augmentation which indicates ineffectiveness of the surfactant at elevated temperatures. The parallel impact of surfactant on stability of NF is observed by Tiwari, et al. [48]. On the contrary, Colangelo, et al. [49] revealed no impact of several Oleic Acid (OA)

based surfactants on TC of Therminol-66/Al_2O_3 (0.3-0.7 vol.%) NF although they improved the stability of the suspension. Qing, et al. [50] examined the effect of pH level and particle sizes on TC of hybrid mineral oil/graphene-SiO_2 NF. They found higher TC in the pH range (9-10) away from the IEP of 2.2, and smaller particles have higher conductivities.

Garoosi [51] proposed empirical correlations considering key parameters (temperature, particle loading and size) for a wide range of NPs and BFs. The studied model is found to be more accurate with standard deviation of only 4.7% while classical models provide poor prediction of TC. The correlations are recommended for further analysis of TC in NF-based thermal engineering devices. Cui, et al. [52] performed a MDS study to analyze consequences of NP properties (materials, sizes, shapes and φ) on TC using Cu, Ag, Au and Fe nanomaterials. The proposed model predicts TC of the NFs and construed that TC improves with raising φ and smaller size of NPs. Ag NPs showed highest TC than others while, higher fraction of $\varphi > 3vol.\%$ showed reducing trend for TCs. Zendehboudi, et al. [53] reviewed widely used and effective data-driven numerical approaches to predict TC of a broad range of NFs comprised of various BFs and NPs. Recent experimental and numerical studies on TC of oil-based NFs are summarized in the following **Table. 2** and **Table. 3** respectively.

Table. 2. Summary of recent experimental studies on TC of various oil-based nanofluids with detail operating conditions.

Reference	Nanofluids	Concentration (Φ)	Surfactants/ Dispersants	Temperature range	Key findings
Fakoor Pakdaman, et al. [54]	Oil/ MWCNT	1-10 µm × 5-20 nm Φ = 0.1- 0.4 wt.%	--	40-70 °C	● TC increment is maximum 15% at particles fraction of 0.4vol.% and 70 °C and the experimental data are in accord with theoretical correlations.
Wang, et al. [5]	Oil/Graphite	20 nm Φ = 0.17-1.36 vol.%	CH-5	30-60 °C	● Maximum 36% TC augmentation is achieved at 1.36vol.% of graphite. Addition of dispersant showed remarkable enhancement in TC at all the studied concentration of nanomaterials.
Aberoumand and Jafarimoghaddam [27]	Engine oil/ Cu	50 nm Φ = 0.2-1 wt.%	--	40-100 °C	● TC enhanced for NF while pure oil showed decreasing trend. Highest increment of 49% relative to the base oil is measured at 1 wt.% and 100 °C.
Aberoumand, et al. [28]	Heat transfer oil/ Ag	20 nm Φ = 0.12-0.72 wt.%	--	40-100 °C	● 12.14% improvement of TC at 100 °C after addition of NPs is attributed to Brownian motion mechanism at escalating temperature.
Rubbi, et al. [32]	Soybean oil/MXene	1–10 µm × 1 nm Φ = 0.025-0.125 wt.%	--	25-55 °C	● TC is reported to increased up to 64.8% at highest particle loading of 0.125wt.%. ●The improvement is attributed to excellent dispersion stability of 2D MXene and oil.
Gulzar, et al. [34]	Therminol®55/Al_2O_3 / TiO_2 /Al_2O_3+ TiO_2	< 80 and 15-25 nm respectively Φ = 0. 05-0.5 wt.%	Oleic acid	15-160 °C	● Maximum TC enhanced relative to TH55 is 33.5% for hybrid NF, while slightly less 27.06 and 21% for Al_2O_3 and TiO_2 NFs, respectively. Substantial augmentation of TC leads to potential photothermal conversion in solar collectors. TC deteriorated is noticed for 0.5 wt.% over 110 °C due to aggregation of particles.
Choi, et al. [55]	α-olefin oil/MWCNT	25 nm × 50 µm Φ = 0-1 vol.%	--	n/a	● Distinct augmentation of TC is obtained dispersing nanotube in the oil medium. Highest

					160% increment is reported which is remarkably higher than predicted theoretical models.
Asadi, et al. [56]	Engine oil/ MWCNT-$Mg(OH)_2$	30 and 10 nm respectively Φ = 0.25-2 vol. %	--	25-60 °C	● Maximum TC improvement of 50% at 2 vol. %, and 60 °C. Furthermore, the NF is recommended for laminar and turbulent heat transfer applications.
Kumar, et al. [57]	Veg. oil/Cu-Zn Paraffin oil/Cu-Zn SAE oil/Cu-Zn	Both 25 nm Φ = 0.1-0.5 vol.%	SDS	30 °C	● Vegetable oil-based NF performed better effective TC relative to other two base fluids at 30 °C.
Chai, et al. [58]	Hydrogenated oil/ Graphene nanosheets	0.06-0.1 µm × 0.002-0.005 µm Φ = 25-100 ppm	--	30-50 °C	● TC improved using NF and maximum 14.4% enhancement is achieved at 50 °C and φ = 100 ppm.
Saeedinia, et al. [59]	Oil/ CuO	50 nm Φ = 0.2-2 wt.%	--	24-70 °C	● Heat transfer coefficient increased with addition of nanoparticles. Highest increment of 12.7% is obtained at φ = 2wt.%.
Taha-Tijerina, et al. [60]	Mineral oil/Nano-diamond (ND)	~ 6 nm Φ = 0.01-0.1 wt.%	--	298-373 K	● TC enhanced with addition of filler to the base oil. It intensified remarkably by 70% with 0.1 wt.% of ND at 373K.
Colangelo, et al. [49]	Therminol-66/ Al_2O_3	45 nm Φ = 0.3-1 vol.%	Oleic acid	30-50 °C	● 4% enhancement in TC is obtained adding solid particles at 1 vol.%. Surfactant had approximately no effect on TC increment of the Al_2O_3/TH-66 NF.
Farbod, et al. [61]	Oil/ CuO	61 nm Φ = 0.2-6 wt.%	--	25 °C	● TC showed dependency on morphology of dispersed particles. Leading increment of 8.3% is achieved with CuO relative to base fluid at φ= 6wt.%. Nano-rhombic and nanorod morphology are found to be less efficient relative to NPs.
Asadi and Pourfattah [62]	Engine oil/ ZnO Engine oil/ MgO	35-45 and 40 nm respectively Φ = 0.125-1.5 vol.%	--	15-55 °C	● TC enhancement for ZnO/Oil NF, 28% at φ = 1.5vol.% and 55°C.MgO/Oil NF, 32%.
Ilyas, et al. [63]	Oil/ Al_2O_3	40 nm Φ = 0.5-3 wt.%	Oleic acid, o-xylene, toluene, and ethanol.	25-55 °C	● Highest TC enhanced above 10%. The results are attributed to better stability of the NF.

Ghaffarkhah, et al. [64]	Transformer oil/ /MWCNT /MWCNT-TiO_2 /MWCNT-SiO_2 /MWCNT-Al_2O_3	10-30 µm × 10-20 nm, 20 nm, 60-70 nm, and 50 nm respectively Φ = 0.001-0.1 vol.%	--	25-65 ºC	● Solo NF performed relatively better than hybrid NFs being maximum 28.048% increment compare to pure oil.
Samylingam, et al. [65]	Palm oil/ MXene	1–10 µm × 1 nm Φ = 0.01-0.2 wt.%	--	25-70 °C	● TC of the NF improved notably with addition of nanosheets as well as with elevated temperature. Highest increment is reported about 68.5% compared to base oil with 0.2 wt.% loading at 25°C.
Li, et al. [66]	Diathermic oil/ SiC	30 nm Φ = 0.1-0.8 vol.%	--	20-50 °C	● Highest TC increment is 7.36% at φ= 0.8 vol.% and 50 °C. The improvement is attributed to high TC of SiC and well dispersion of particles in the oil.
Ilyas, et al. [67]	Thermal oil/ MWCNT	10-20 µm × 30-40 nm Φ = 0.1-1 wt.%	--	20-60 °C	● TC enhanced due to Brownian motion of nanoparticles. Maximum enhancement is reported 28.7% at φ = 1 wt.% and 60 °C.
Ettefaghi, et al. [68]	SAE 20 W50/ MWCNT	10 µm × 10-20 nm Φ = 0.1-0.5 wt.%	$SOCl_2$, DMF, Dodecyl amine and ethanol	20 °C	● Maximum TC improvement is 22.7% with 0.5 wt.% of MWCNT however, fluid is less stable at 0.5 wt.% relative to 0.1 wt.%.
Aslfattahi, et al. [69]	Silicon oil/MXene	1–10 µm × 1 nm Φ = 0.05-0.1 wt.%	n-Hexane, chloroform, toluene, and tween 40	25-150 °C	● TC enhanced due to district structure of MXene nanoflakes and excellent stability of the dispersion. Maximum increment of TC is measured 64% at φ = 0.1 vol.% and 150 °C.
Naddaf and Zeinali Heris [70]	Diesel oil/ Graphene Diesel/ Graphene-MWCNT	1-20 µm × < 40 nm Φ = 0.05-0.5 wt.%	DMF, THF, methanol, hexylamine, $NaNO_2$, and H2SO4 (98%)	5-80 °C	● TC of all the NFs exhibited higher value with inclusion of graphene and MWCNT NPs. It also raised at elevated temperature compared to pure diesel oil. Max. TC is 0.313 W/m.K at 80 °C which is much higher the base fluid.
Mukhtar, et al. [71]	Kapok seed oil/ MWCNT	2.5-20 µm × 6-13 nm Φ = 0.2-0.8 wt.%	n-Hexane	25-65 °C	● TC of the NF increased significantly from 0.35 to 1.485 W/m.K 0.8 wt.% with inclusion of MWCNT and it also intensified at elevated temperatures.

Wei, et al. [72]	Diathermic oil/ SiC /TiO_2 /SiC-TiO_2	30 and 10 nm respectively Φ = 0.1-1 vol.%	--	17-43 °C	● TC increased substantially with rising temperature and particle addition, maximum 8.39% is reported at φ= 1 vol.% and 55 °C.
Beheshti, et al. [73]	Transformer oil/ Oxidized MWCNT	30 µm × 10-20 nm Φ = 0.001-0.01 wt.%	--	20-80 °C	● Maximum TC increment is 7.7% at φ= 0.011 vol.% and 60 °C. However, TC declined for temperatures above 60 °C.
Ilyas, et al. [74]	Paraffin oil/ZnO	30 nm Φ = 0-1 wt.%	oleic acid	25-65 °C	● TC increased non-linearly with φ. Highest TC improvement obtained 18% at φ= 0.5 wt.% and 55 °C.
Li, et al. [75]	Waste cooking oil/SiC /TiO_2	30 and 10 nm respectively Φ = 0.025-0.3 vol.%	Span-80	25-60 °C	● TC increased with addition of NPs up to 0.1 vol.% of NPs and then it deteriorated abruptly. While addition of Span-80 boosted the TC by 12% relative to dispersant less NF at 0.1 vol.%.
Amiri, et al. [76]	Transformer oil/ MWNCT-HA	5-15 µm × 30 nm Φ = 0.001 to 0.005 wt.%	DMF, H_2SO_4 and hexylamine	30-70 ºC	● TC increased by 10%. with raising temperature up to 60 ºC which results augmentation in natural and forced convection heat transport coefficient by 23 and 28% respectively.
Asadi [77]	Engine oil/ MWCNT-ZnO	10-20 and 20-30 nm Φ = 0.125 to 0.1 vol.%	--	15-55 °C	● 45% TC enhancement is reported at highest φ of 1 vol.% and 55 °C. The NF is useful for laminar flow and recommended for turbulent flow regime above temperature of 35 °C.
Asadi, et al. [45]	Engine oil/ Al_2O_3-MWCNT	10-30 µm × 20-30 nm 1Φ = 0.125 to 0.1 vol.%	--	25-50 °C	● Maximum TC improvement is achieved 45% at φ φ = 1.5 vol.% and 50 °C. The oil-based NF performed advantageously in laminar flow regimes and likely to be effective in turbulent flow at solid concentration of bellow 0.1 vol.%.
Soltani, et al. [78]	Engine oil/ WO_3-MWCNT	23-65 and 20-30 nm respectively Φ = 0.05 to 0.6 vol.%	--	20-60 °C	● Highest growth in TC is 19.85% than base oil at φ= 0.6 vol.% and 60 °C. Effect of solid particles are more dominant relative to increasing temperature.
Rehman, et al. [79]	Jatropha oil/ MWCNT	2.5-20 µm × 6-13 nm Φ = 0.2 to 0.8 wt.%	n-Hexane	25-65 °C	● NF showed increment in TC due to excellent dispersion stability using surfactant. Maximum improvement is measured 6.76% at 65 °C.

Table. 3. Summary of proposed empirical correlations to estimate thermal conductivity of oil-based nanofluids.

Reference	Nanofluids	Correlation	Applicability	Accuracy
Fakoor Pakdaman, et al. [54]	Oil/MWCNT	$\frac{k_{nf}}{k_{bf}} = 1 + 304.47(1 + \varphi)^{136.35} \exp(-0.021T) \left(\frac{1}{d_p}\right)^{0.369} \left(\frac{T^{1.2321}}{10^{\frac{2.4642B}{T-C}}}\right)$	Φ = 0.1-0.4 wt.% T = 40-70 °C B = 247.8 and C = 140	Max. error = 6%
Ilyas, et al. [67]	Thermal oil/MWCNT	$k_{nf} = 0.595 - 0.4547(1 - \varphi_p) + T\left[0.7422 - 0606(1 - \varphi_p) + \frac{0.2759}{1 - \varphi_p} - \frac{0.3943}{(1 - \varphi_p)^2}\right]$	Φ = 0.1-1 wt.% T = 25 to 63.15 °C	Max. error = 3.5% R^2 =0.95
Asadi, et al. [56]	Engine oil/ MWCNT-$Mg(OH)_2$	$k_{nf} = 0.159 + 1.1112\varphi + 0.003T$	Φ = 0.25-2 vol.% T = 25-60 °C	Max. error = 2 %
Aberoumand, et al. [28]	Oil/ Ag	$k_{nf} = (3.6 \times 10^{-5}T - 0.0305)\varphi^2 + (0.086 - 1.6 \times 10^{-4}T)\varphi$	Φ = 0.12-0.72 wt.% T = 40-100 °C	Max. error = 3.5%
Ilyas, et al. [63]	Engine oil/Al_2O_3	$k_{nf} = 1.4408 - 0.829(\ln T) + 0.1588(\ln T^2) - 0.0702(1 - \varphi_p) - 0.2151(\ln T)(1 - \varphi_p) + \frac{0.5965T}{1 - \varphi_p} - \frac{0.39T}{(1 - \varphi_p)^2}$	Φ = 0.5-3 wt.% T = 24.47-54.65 °C	Max. error = ±2% R^2 =0.96
Asadi, et al. [80]	Engine oil/MWCNT-MgO	$k_{nf} = 0.162 + 0.691\varphi + 0.00051T$	Φ = 0.25-2 vol.% T = 25-50 °C	Max. error = 3%
Asadi, et al. [45]	Engine oil/MWCNT-Al_2O_3	$k_{nf} = 0.1534 + 1.1193\varphi + 0.00026T$	Φ = 0.125-1.5 vol.% T = 25-50 °C	Max. error = 2%

3.2. Specific heat capacity (c_p)

Specific heat (c_p) is one of the most essential thermo-physical properties to characterize thermal heat storage merit of various thermo-fluids. In general, while TC of NFs enhances with inclusion of NPs, c_p can either increase or decrease with dispersed solid particles relative to the fluid. This trend of c_p depends on nanomaterials type, φ, BF and temperature. This can restrict implementation of NFs on thermal systems depending on the cost and process of heat transport. Hence, it is essential to establish an explicit concept of interaction between c_p and the influential factor to characterize potential NFs. Generally, various types of thermal DSC devices are employed to experimentally measure c_p of NFs due to its convenience and technical simplicity [81-83].

Starace, et al. [84] evaluated c_p of 13 different NFs considering various BFs (including oils and water), NPs, surfactant, φ, particle size and temperature. They concluded no notable augmentation is caused by the addition of NPs as $c_{p_{nf}}/c_{p_{bf}}$ is found to be below 1 for the majority of the samples. Ilyas, et al. [63] analyzed c_p of thermal oil-based NF using functionalized Al_2O_3 (0.5-3 wt.%) at 40-160℃. The obtained data showed a significant drop in c_p values relative to BF during the addition of nanomaterial and increased with rising temperature. They found similar c_p outcomes dispersing MWCNT nanomaterial in the same base fluid [67].

In contrast, some published works claim opposite characteristics of heat capacity employing different NPs (particularly carbon-based nanomaterials), BFs and experimental conditions. For instance, Singh, et al. [85] evaluated c_p of oil TH-66/MWCNT for 0.05-0.5wt.% and a wide range of pressure (up to 70 bar) temperature from 25 to 300℃. c_p increment is obtained by adding NPs, 3.1 and 5.7% for water and oil-based NF, respectively. The results contributed to the formation of a semi-solid layer on the surface of NPs and an increase in TC, allowing NFs to store energy faster than BF. Sonawane, et al. [82] revealed that c_p of turbine oil based Al_2O_3

(0.1-1 vol.%) NF using Tween-20 and oleic acid as surfactants. Findings showed c_p increased at 0.5 vol.% of NPs then it declined at 0.1 vol.%. More experimental studies on c_p of NFs are reviewed in **Table. 4**.

Theoretical models along with experimental correlations are useful to estimate c_p of a wide range of NFs that has been proposed in literature over the years. The first model presented by Pak and Cho [86] is also known as mixture theory and is used to predict c_p of solid-liquid mixture at nonorange scale.

$$C_{p_{nf}} = \varphi C_{p_{np}} + (1-\varphi) C_{p_{bf}} \quad (1)$$

Although this model is frequently used to predict c_p of NFs, inconsistencies are also reported as the model provides considerable deviations from experimental data.

Xuan and Roetzel [87] proposed a thermal equilibrium model driven from reviewed experimental data of different NFs.

$$\rho_{nf} C_{p_{nf}} = \rho_{np} C_{p_{np}} \varphi + (1-\varphi) \rho_{bf} C_{p_{bf}} \quad (2)$$

$$where,\ \rho_{nf} = (1-\varphi)\rho_{bf} + \varphi \rho_{np} \quad (3)$$

This model is better data predictor than the mixture theory. However, discrepancies are reported up to a certain range [88, 89]. Fakoor Pakdaman, et al. [54] investigated c_p of oil based MWCNT NF and developed a correlation to predict c_p.

$$\frac{C_{p_{bf}} - C_{p_{nf}}}{C_{p_{bf}}} = (0.0128 \times T + 1.83282) \times \varphi^{0.4779} \quad (4)$$

The equation is valid for a concentration of 0-0.004wt.% and a temperature range of 313-343K. Sekhar and Sharma [90] collected data from 81 different experiments studying c_p of NFs using Al_2O_3, CuO, SiO_2 and TiO_2 to develop which can predict data with a deviation of +10% and -8%.

$$\frac{C_{p_{nf}}}{C_{p_{bf}}} = 0.8429\left(1 + \frac{T_{nf}}{50}\right)^{-0.3037}\left(1 + \frac{d_{np}}{50}\right)^{0.4167}\left(1 + \frac{\varphi}{100}\right)^{2.272} \quad (5)$$

This correlation is applicable for $0.01 \leq \varphi \leq 4.0\ vol.\%$, $d_{np} = 15 - 50\ nm$ and $T = 20 - 50℃$.

Table. 4. Summary of studies focusing on specific heat capacity (c_p) of water and oil-based nanofluids.

Reference	Nanofluids	Particle dimension and concentration	Surfactants/ Dispersants	Temperature range	Key findings
Fakoor Pakdaman, et al. [54]	Oil/MWCNT	1-10 µm × 5-20 nm Φ = 0.1- 0.4 wt.%	--	40-70 °C	● c_p increased with raising temperature for the NFs whereas, it declined adding NPs. 42% reduced c_p is measured at 0.4 wt.% and 40 °C.
Rubbi, et al. [32]	Soybean oil/MXene	1–10 µm × 1 nm Φ = 0.025-0.125 wt.%	--	25-80 °C	● Non-linear relationship is elucidated throughout the temperature range and highest c_p enhancement is measured 24.49% greater than oil at 25 °C.
Ilyas, et al. [63]	Oil/Al_2O_3	40 nm Φ = 0.5-3 wt.%	Oleic acid, o-xylene, toluene, and ethanol.	40-160 °C	● c_p increased notably with rising temperature but reduced adding alumina particles to the oil. Temperature dropped by 8 °C adding solid particles.
Singh, et al. [85]	Therminol-66/MWCNT	30 nm Φ = 0.05-0.5 wt.%	Oleic acid	25-300 °C	● c_p enhanced with increasing dispersed particles; highest augmentation is noted 5.7 % relative to water. The progress is attributed to semi-solid layer developed on the surface of nanomaterial.
Gil-Font, et al. [91]	Therminol-66/Sn	< 300 nm Φ = 0.137 vol.%	Oleic acid Virgin olive oil	80-140 °C	● c_p slightly deteriorated by 2.5% relative to Therminol-66 due to addition of tin particles. Surfactant also had negative effect on heat capacity of the fluids.
Akhter, et al. [92]	Therminol-66/Titania	30 nm Φ =0.25-1 wt.%	--	30-130 °C	● c_p augmented with increasing temperature for base oil and NF samples but deteriorated due to low c_p property of solid titania nanomaterial.
Nelson, et al. [93]	Polyalphaolefin (PAO)/Exfoliated graphite	20 µm × 100 nm Φ = 0.3-0.6 wt.%	--	40-100 °C	● c_p of the nanofluid was found to be improved by 50% at 0.6 wt.% relative to PAO. Remarkable rise is explained based on parallel increase in c_p of nanomaterials.
Safaei, et al. [94]	Therminol-66/SiO_2 /Al_2O_3	20-50 nm and 60-120 nm respectively Φ = 0.1 wt.%	Dimethylformamide, CTAB and Benzalkonium Chloride	25-325 °C	● c_p of the NFs improved considerably with increasing temperatures until BF started degradation. SiO_2 based NF performed better than Al_2O_3 NF specially at elevated temperature.

4. Colloidal stability of nanofluids

The stability of nanofluids is the most crucial hinder to widespread application of nanofluids for industrial purposes. Stability of nanofluids is defined as the ability to resist permanent deformation i.e., resultant of attraction and repulsion forces (between particle-particle and particle-fluid interface) over a certain period. The effectiveness of nanofluids highly depends on the suspension stability of nanoparticles dispersed in base fluid. NPs tend to destabilization and form aggregation caused by various forces, for instance, Van der Waal attraction force, magnetic force, electrostatic force, bouncy and gravitational force. These forces act against the stability of colloidal suspension and cause formation of large clusters leading to deterioration of nanofluid performance. The proclivity of NPs to form clusters causes nanofluid suspension destabilization. The tendency of agglomeration is attributed to higher surface area as well as surface activity of nanofluids with the addition of NPs. Therefore, such propensity to agglomeration must be prevented to prepare stable nanofluid maintaining stable dispersion of NPs in the base fluid. The mechanism of dispersion of colloidal suspension is explained by the DLVO theory of particle dispersion [95]. The DLVO theory is based on Van der Waal attractive force and electrostatic repulsive force existing in between the particles in the colloidal suspension. The net attraction or repulsion force depends on the distance between particles and the summation of Van der Waals attraction force and electrostatic repulsion force. However, this colloidal theory of nanoparticle dispersion is based on few key assumptions: (1) Particle dispersion is homogeneous and dilute, (2) Van der Waals forces and electrostatic force are the only forces acting on the suspension, (3) buoyancy and gravity forces are negligible, and (4) ion distribution in the suspension is controlled by factors such as Brownian motion, electrostatic force, and entropy influenced dispersion.

$$F_T = F_{VdW} + F_{ES} \qquad (6)$$

Where F_{VdW} and F_{ES} are the attractive and repulsive potential between the particles. The expressions of Van der Waals attractive potential and electrostatic repulsive potential for particles of different size and shape. If the attractive force is stronger than the repulsive potential, suspension will not be defined as unstable. From **Fig. 9**, it can be understood that when total interaction potential is high (i.e., potential barrier is high), NPs are likely to remain stable preventing clusters due to higher separation distance, whereas low net interaction potential will result in unstable suspension. Nevertheless, if the particles collide beyond the potential barrier being affected by influential factors (e.g., temperature, chemical additives) than attractive potential will dominate (i.e., separation distance is less) and form agglomeration (low zeta potential) to deteriorate suspension homogeneousness. Hence, the separation distance would be low, and it will cause to emerge secondary minima which leads to further aggregation. Electrostatic repulsive potential must be predominant over the attraction force to formulate stable NF. However, mathematical expressions of Van der Walls attraction force and electrostatic repulsive force vary depending on particle's concentration, size, and shape of the particles.

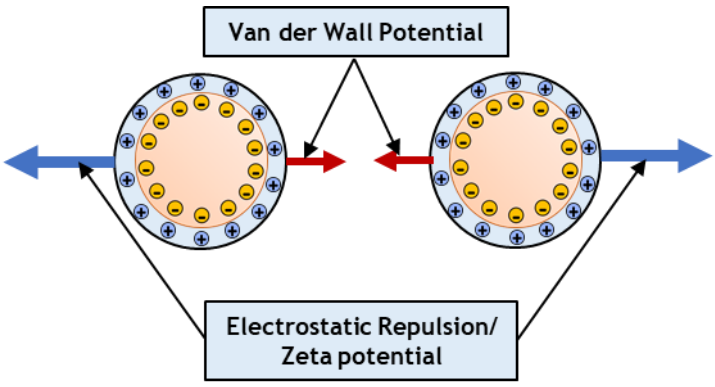

(a)

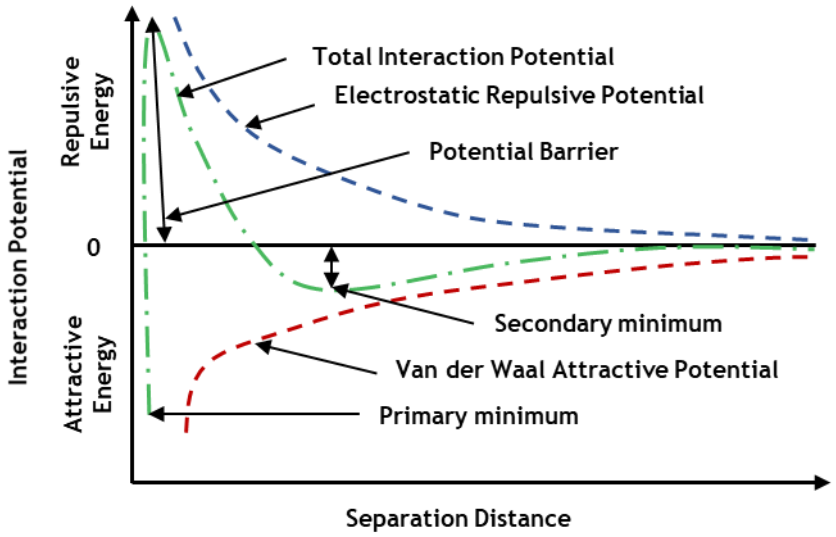

(b)

Fig. 9. (a) Interaction between two particles of NF dispersed in a BF (b)Schematic of interaction energy of typical stable NFs as a function of separation distance between the particles.

4.1. Influential factors of nanofluids stability

Several factors have noteworthy effects on the colloidal stability of NF suspension. The mechanism of some crucial factors influencing the colloidal stability of NF such as dielectric constant of BFs, φ, pH value, particle shape and size, temperature, zeta potential (ζ), stabilizing additives, stability evaluation techniques, and so on. For instance, various types of base fluids are used to formulate NFs based on the potential application of that fluid in low to high temperature thermal heat transfer systems. The dielectric potential of fluids is an important property as it is directly related to repulsive potential which determines the stability of the fluid. The higher value of the dielectric constant for fluid implies higher stability in suspension. Water has a dielectric constant of approximately 78.5 at room temperature which is maximum among the generally used base fluids such as; ethylene glycol, acetone, thermal oils, vegetable oils, ethanol and benzene [96]. The degradation of NF suspension stability due to NP dispersion is a chemical phenomenon, i.e., the more solid particles in BF, the lower the suspension

stability [8, 97]. Therefore, techniques are necessary to improve the dispersion property of NF for sustainable application in various sectors. Zeta potential (ζ), surfactant and pH value of suspension have significant effects on the dispersion stability. When NPs are dispersed into BF, the fluid layers surrounding the particles form stern and diffuse layers to establish an electric doble layer (EDL) combining the layers and charges (+ve and -ve). EDL yields potential difference which is known as zeta potential to increase the repulsion among the distributed particles. Suspensions having a ζ value of more than ± 30 mV are considered electrostatically stable and above ± 60 mV indicate very good stability. Suspensions having ζ value in the range of ± 15 mV are considered unstable. However, it should be noted that, in contrast to common practice regarding stability of NFs, zeta potential should not be taken as the ultimate indicator of suspension stability of NFs unless the NFs are stabilized by electrostatic repulsion between the particles. At a certain pH value of nanosuspension, zeta potential becomes zero and it is called isoelectric point (IEP). Dispersed particles stay in an electrophoretic immobility at the IEP. When the pH of the suspension is greater or lower than the IEP, electrostatically stabilized NF can be produced.

Tiwari, et al. [48] studied stability of four separate BF (water, EG, therminol-VP1 and silicon oil) based MWCNT-CeO_2 NFs using six unique surfactants (BAC, ALS, CTAC, Bri-700, PLS and Span-80) and substantial rang of ultrasonication period (30-240 minutes) for stabilize the suspensions (**Fig. 10**). The obtained data elucidated that BAC was the most efficient stabilizer as it produced better improvement to stability indicator (ζ) relative to other surfactants. Increment of ultrasonication time provides more homogenous suspension up to an optimum an optimum limit after which additional ultrasonication deteriorates dispersion stability caused by sedimentation at excess ultrasonication. Using BAC as surfactant, silicon oil-based NF performed best stability in terms of ζ, duration and sonication time (66 mV, 30 days, 60 min) followed by EG (61 mV), water (57 mV) and therminol-VP1 (45 mV) based NFs at identical

0.75 vol.% of MWCNT-CeO_2. The effect of increasing temperature (25-50℃) on stability had a negative impact in this experiment which might have been caused due to limitations of the stabilizers at higher temperature [98]. The same cationic surfactant (BAC) utilized in experimentation with therminol-66/SiO_2 NF revealed analogous findings on stability [47].

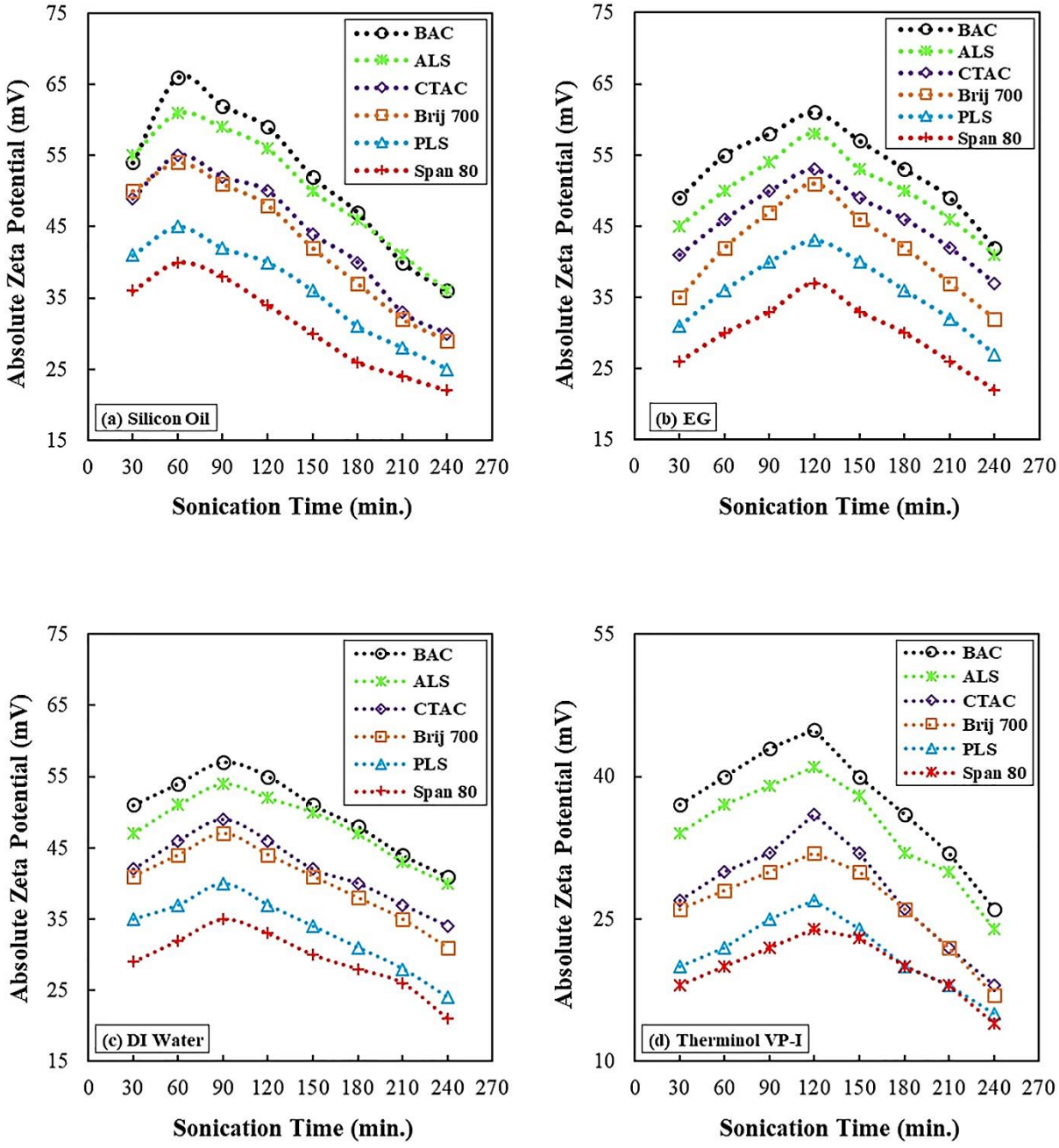

Fig. 10. Effect of several BFs, surfactants and sonication period on suspension stability of hybrid NFs using MWCNT-CeO_2 nanocomposite and different BFs, investigated by [48].

Gao, et al. [99] experimentally studied the impact of six different surfactants (APE-10, CTAB, OP-10, SDBS, SDS and TTAB) on the dispersion method of palm oil/CNT NF at 3wt.% loading. Among the stabilizers, APE-10 implied superior dispersion of the suspension with the lowest frictional coefficient of 0.121. Colangelo, et al. [49] observed that the inclusion of oleic acid as surfactant in dispersion of TH-66/Al_2O_3 NF improved the stability, and it is effective for long-term stability. Also, they stated stability as a function of temperature as sedimentation is observed to be inversely related to temperature. Gulzar, et al. [100] examined the stability of hybrid TH-55/Al_2O_3-TiO_2 NF using oleic acid for concentrating SC application. The results indicated NP distribution without agglomeration and NF samples were stable for more than a week as the zeta potential value was from 34.43-54.52 mV after seven days from the formulation. Analogous findings reported by Ilyas, et al. [63] deploying thermal oil/alumina NF. Mesgari, et al. [101] investigated the stability of TH-55 oil-based NFs from 20-250℃ dispersing several NPs (SWCNT, DWCNT and MWCNT) and stabilizers (Potassium persulphate, acid and SDBS) separately. The potassium persulphate functionalized TH-55/MWCNT NF is implied as the most stable suspension up to 250℃and a potential alternative for concentrated SC implementation. Dhanola and Garg [102] studied dispersion of TiO_2 NPs in canola oil utilizing different nonionic (TX-100, oleic acid) and ionic (SDS, Tween-20) surfactants at various NP to surfactant ratio and 0.04 vol.% particle loading. Optimized stability is achieved for TX-100 induced TiO_2 NF, over 30 days at 1:3 ratio.

Table. 5 represents summary of reviewed experimental works on stability of various NFs with specifications on NP, φ, surfactants, stability indication and stabilization techniques. Details on stability evaluation methods and stabilization techniques are covered in **section 4.2 and section 4.3**, respectively.

Table. 5. A summary of experimental studies on stability of oil-based nanofluids with deployed stabilization techniques.

Reference	**Examined nanofluids**	**Particle size and concentration (φ)**	**Surfactant or chemical additives**	**Stability or Zeta potential (ζ)**	**Stabilization techniques**
Gulzar, et al. [34]	Therminol®55/Al_2O_3 /TiO_2 /Al_2O_3-TiO_2	Al_2O_3 (>80 nm) TiO_2 (15-25 nm) Φ = 0.05-0.5 wt.%	Oleic acid	> one week ζ = 25-60 mV	Steric stabilization magnetic stirring, ultrasonication, ball milling.
Javed, et al. [103]	Waste palm oil/CuO	25 nm Φ = 0.1-0.9 wt.%	none	> 6 months	Steric stabilization magnetic stirring, ultrasonication.
Chen, et al. [29]	Silicon oil/ Functionalized Fe_3O_4	9 nm Φ = 0.75-3 mg/mL	Oleic acid (OA), and Oleyl-amine (OLA)	Stable nanofluids at 0.75 mg/mL loading.	Physical stabilization: centrifugation
Amiri, et al. [104]	Turbine oil/MWCNT	5-150 μm×< 30 nm Φ = 0.001-0.1 wt.%	hexylamine	> 6 months	Electrostatic stabilization Functionalization, ultrasonication
Rehman, et al. [79]	Jatropha oil/ MWCNT	d 2.5-20 μm × 6-13 nm Φ = 0.2-0.6 wt.%	--	> one month ζ = -38.6 to -52.3 mV	Steric stabilization mechanical mixing and ultrasonication.
Mukhtar, et al. [71]	Kapok seed oil/MWCNT	2.5-20 μm × 6-13 nm Φ = 0.2-0.8 wt.%	--	> one month	Steric stabilization mechanical mixing and ultrasonication.
Wang, et al. [5]	Oil (LD320)/ Graphite	10-30 nm Φ = 2 and 4 wt.%	CH-5	< 36 h	Steric stabilization addition of non-ionic dispersant.
Rubbi, et al. [32]	Soybean oil/Ti_3C_2	1-10 μm × 1 nm Φ = 0.025 and 0.125 wt.%	--	ζ = -56.71 to -80.57 mV	Ultrasonication and magnetic stirring
Qu, et al. [33]	Therminol®66/ GO-MWCNT	0.5-5 μm × 1-3 nm) 10-30 μm × 20-30 nm Φ = 10-150 ppm	Oleic acid	> two weeks	Steric stabilization magnetic stirring, sonication.
Kumar, et al. [57]	Veg. oil/Cu-Zn Paraffin oil/Cu-Zn SAE oil/Cu-Zn	Both 25 nm Φ = 0.1-0.5 vol.%	SDS	72 h	Steric stabilization Ultrasonication
Akhter, et al. [105]	Therminol-55/CuO	40 nm Φ = 0.25-1 wt.%	--	few days	Ultrasonication
Hwang, et al. [25]	Silicon oil/Ag	35 nm Φ = 0.5 wt.%	Oleic acid	two months	Steric stabilization technique is used to characterize the stability.

Nabeel Rashin and Hemalatha [106]	Coconut oil/ZnO	26 nm Φ = 0.08-0.48 vol.%	--	> 7 days	Steric stabilization
Ilyas, et al. [67]	Thermal oil/MWCNT	10-20 µm ×30-40nm Φ = 0-1 wt.%	--	> 3 months	Ultrasonication of the nanofluids observed to be excellent choice without any chemical additives for this oil-based nanofluids.
Shariatmadar and Pakdehi [107]	Kerosene/Boron	1-5 µm Φ = 0.5 wt.%	oleic acid, propylene glycol, CTAB	57 h	Achieved a strong repulsive force due to the extended hydrophobic end of surfactants.
Amiri, et al. [76]	Thermal oil/ MWCNT	5-15 µm ×< 30 nm Φ = 0.001 and 0.005 wt.%	hexylamine	> one month ζ = -38.6 to -52.3 mV	Stabilization is obtained using mechanical shaking and sonication mechanism with fluctuating values of zeta potential.
Yu, et al. [108]	Kerosene/ Fe_3O_4	Size: 15 nm Φ = 1 vol.%	oleic acid	6 h	Nanofluids are less stable despite of ultrasonication. Temperature independent thermal conductivity reveals little stability of the nanofluids.
Loni, et al. [109]	Thermal oil/ Alumina	30-40 nm Φ = 0.8 wt.%	Gum Arabic, Bromide Chloride, Texapon, Aniline, and Sodium dodecyl sulfate (SDS)	4 h	Several surfactants along with ultrasonication technique are employed to observe stability of nanofluids stability.
Colangelo, et al. [49]	Diathermic oil/ Al_2O_3	40-50 nm Φ = 0.3-1 wt.%	oleic acid	--	Implementation of surfactant and sonication increases the stability of the nanofluid sample.
Asadi [77]	Engine oil 10W40/ MWCNT-ZnO/	20-30 and 10-20 nm Φ = 0.125-1 wt.%	--	> 14 days	Steric stabilization mechanical stirring and ultrasonication.
Ilyas, et al. [63]	Thermal oil/ Alumina	40 nm Φ = 0.0.5-3 wt.%	oleic acid	> 1 month	Steric stabilization ultrasonic homogenization.
Ettefaghi, et al. [68]	Engine oil/ MWCNT	10 µm ×10-20 nm Φ = 0.01-0.5 wt.%	Dodecyl-amine functionalization	720 h	Steric stabilization Ultrasonic bath and ball milling.
Wei, et al. [110]	Diathermic oil/ TiO_2	10 nm Φ = 0.1-1 vol.%	Oleic acid	10 days ζ = 52 mV	Steric stabilization Magnetic stirring, ultrasonic homogenization.
Li, et al. [111]	Kerosene oil/ Ag	5 nm Φ = 0.1-5 vol.%	Oleic acid, n-Butylamine	720 h	Steric stabilization

4.2. Stability evaluation methods

Different techniques are employed in investigation for the assessment of nanofluids suspension stability, i.e., sedimentation and centrifugation, zeta potential measurement, transmission electron microscopy, spectral absorbance, and transmittance measurement, 3-ω method and dynamic light scattering presented in **Fig. 11**. In the following sections, stability measurement methods will be discussed briefly.

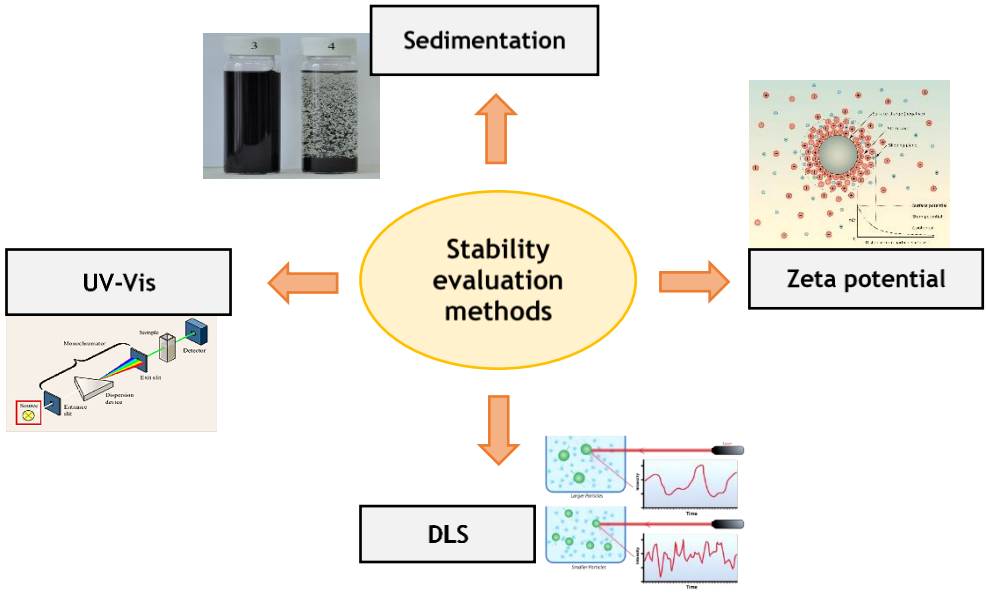

Fig. 11. Effective stability evaluation techniques for nanofluids.

4.2.1. Sedimentation

Sedimentation of NFs is significantly important as it is directly associated with suspension stability of NFs. This method is based on visualization of static nanofluid photographs in a set of sample columns to evaluate settling behavior of NFs due to gravitational force and internal solid-liquid interactive between dispersed particles and BF. In this technique, stability is assessed in terms of time taken to form precipitation by the NF sample. Several investigations regarding stability characterization of NFs are carried out using sedimentation technique [112-114]. This technique is useful and cost-effective relative to other stability characterization

methods for instance Zeta potential, UV-vis and electron microscopy. Rehman, et al. [79] investigated the stability of MWCNT/Jatropha oil nanofluids by sedimentation method. The nanofluids exhibited no visual sedimentation for up to three weeks and they observed excellent stability over one month. Ilyas, et al. [63] studied the stability of Al_2O_3/thermal oil NFs in natural and functionalized conditions. They revealed that functionalized NFs exhibit suspension stability of more than 4 weeks whereas, natural samples aggregation within a few hours from the formulation of NFs. The settling of spherical shaped particles due to gravity can be determined by Stokes law:

$$V_t = \frac{2r^2(\rho_p - \rho_b)g}{9\mu} \qquad (7)$$

where V_t, r, ρ_p, ρ_b, g and μ represent terminal velocity of spherical particles, radius of the particles, density of solid particles, density of base fluid, gravity, and dynamic viscosity of the base fluid. The equation indicates that with smaller particles, terminal velocity will be less and the sedimentation process will be slower compared to larger nanoparticles dispersed into base fluid. It also clearly shows that dynamic viscosity of base fluid and density of nanoparticles and base fluid are key parameters to obtain stable nanofluids. In this technique, stability can also be evaluated by measuring the height of the sedimented layer with respect to duration.

4.2.2. Zeta potential (ζ)

The ZP indicates the potential difference between the stationary layer (stern layer) of mobile particles and the layer of dispersant (diffuse layer) around the particles at the slipping plane. The stern layer is strongly bonded with oppositely charged ions on the surface of the particles relative to inner surface charge while ions are weakly bonded in the diffuse layer and consist of both neutrally distributed positive and negatively charged ions (demonstrated in **Fig. 12**). The ZP can be calculated using the following equation:

$$\mu_e = \frac{V}{E} \qquad (8)$$

where $V =$ particle velocity (μm/s), E = electric field strength (Volt/cm). The ZP(ζ) is then calculated from the obtained μ_e by the Henry's equation.

$$\mu_e = \frac{2\varepsilon_r \varepsilon_0 \zeta f(ka)}{3\eta} \qquad (9)$$

where $\varepsilon_r =$ relative permittivity/dielectric constant, $\varepsilon_0 =$ permittivity of vacuum, $f(ka) =$ Henry's function and $\eta =$ viscosity at experimental temperature. The ZP value significantly effects the colloidal stability of nanofluids [115]. A higher absolute value of ζ indicates more stable suspension, whereas low ζ depicts unstable nanoparticles distribution into the pure fluid [116]. A stable nanofluid possesses higher repulsive force among the dispersed particles because of higher absolute potential difference. According to the most widely accepted DLVO theory, colloid stability depends on the sum of van der Waals attractive forces and electrostatic repulsive forces due to the EDL. However, the limitations of this theory is stated by Bhattacharjee [117] as it does not provide details on Van der Waal interactions among the dispersed particles. In addition, it should be noted that, in contrast to common practice regarding stability of NFs, ζ value should not be taken as the ultimate indicator of suspension stability of NFs unless the NFs are stabilized by electrostatic repulsion between the particles.

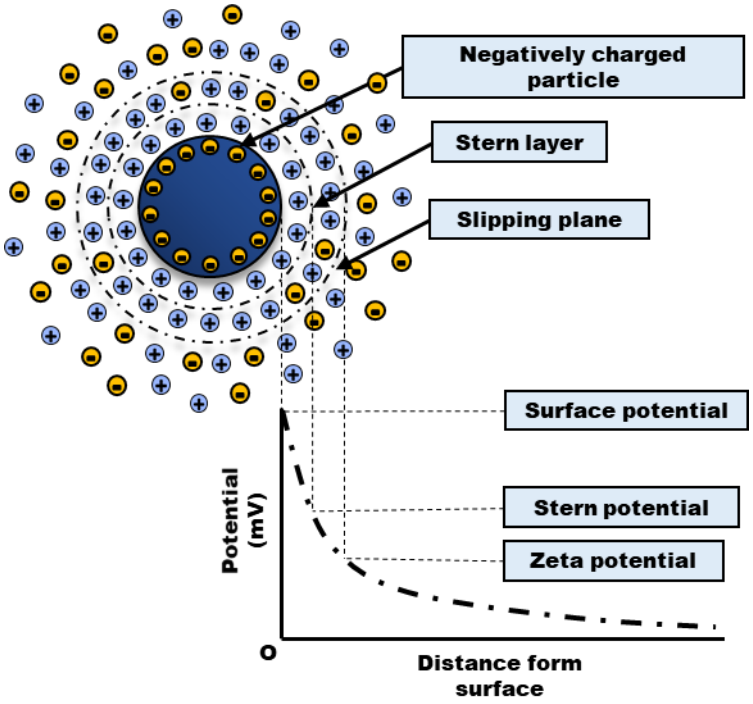

Fig. 12. Charged layers of nanoparticle dispersed in bulk base fluid.

4.2.3. Dynamic light scattering (DLS)

The DLS technique can be utilized to determine particle size distributing of any colloidal solution transmitting a monochromatic beam of light across suspension containing nanoparticles. Light diffuses in all directions depending on the size and shape of dispersed particles. The intensity of scattered fluctuates due to Brownian motion of the particles and then investigated by photon detector to evaluate the particle size distribution analyzing diffusion coefficient (D_τ) which is function of crucial parameters such as hydrodynamic size of particles, temperature, and absolute viscosity of the NF. D_τ can be calculated using Stokes-Einstein equation [117]:

$$D_\tau = \frac{k_B T}{6\pi\mu R_h} \qquad (10)$$

where k_B, T, μ and R_h are Boltzmann constant, temperature, viscosity hydrodynamic radius of particles. Particle size distribution of a suspension indicates dispersion stability by measuring cluster size of the distributed particle over intervals of time. Large cluster size of particles

implies instability of suspension, hence leading to sedimentation and agglomeration of dispersed particles. Investigations with nanofluids, DLS technique is being used to successfully determine the particle distribution in order to define suspension stability. Anushree and Philip [118] observed the hydrodynamic size of α-Al_2O_3 and TiO_2 NFs decreases significantly with time, implying significant sedimentation and unstable dispersion of the nanofluids. Navarrete, et al. [119] experimentally measured particle size distribution for molten salt-based NFs using a DLS set-up which is designed to perform up to 500ºC. The study revealed that Al/Cu NF exhibited a better dispersion rate than Silica NFs at high temperatures.

4.2.4. Spectral absorbance measurement

NFs stability can be assessed by measuring spectral absorbance for a band definite range of wavelengths. UV-Vis spectral investigation is commonly used to assess stability by evaluating spectral absorption between the wavelength of 190 to 1100 nm [120]. In this technique, stability is determined by examining absorption profiles of NF samples with various solid concentrations over a certain period. An UV–vis spectrophotometer uses the fact that the light intensity turns out to be different by absorption and scattering of light passing through a fluid. Stability is evaluated by assessing the variation in absorption peak characteristics for the fluid against time. Lower value of absorbance after a certain period indicates instability of NF suspension. Absorbance (A_λ) can be estimated using the following equation:

$$A_\lambda = \log_{10}(I_0/I) = \alpha \times l \times c \qquad (11)$$

Absorbance (A_λ) is proportional to particles concentration (c), absorptivity (α) distance traveled by the light source. I_0 and I are the intensities of light beam before and after passing through the fluid sample. The reduction of solid concentration in the suspension with time is reflected in decreased absorbance due to agglomeration in the suspension. The method is used to evaluate the stability of NF effectively, reported by several investigations [79, 121]. However, the technique is not effective for high concentration NF samples or for dark

suspensions as it is difficult to differentiate sediment visibility at high solid concentrations [122].

4.3. Nanofluids stabilization techniques

A comprehensive understanding of dispersion mechanism in colloidal science is imperative to explain the suspension stability of NFs. Dispersion behavior or suspension stability of NF is explicitly associated with inter-particle interaction and active microscopic forces acting on nanoparticles dispersed into the base fluid. NFs are inherently unstable due to gravitational force acting on single NP which causes sedimentation of the particles. However, random thermal motion, i.e., Brownian motion of NPs can counterbalance the sedimentation and stabilize the suspension. Along with the acting forces on each NP, interaction forces between the particles in the suspension play a dominant role in the dispersion characteristics of NF [19]. During inter-molecular interaction among adjacent particles, NPs tend to form aggregation due to ubiquitous Van der Waals attraction forces (F_{VdW}). The magnitude of F_{VdW} depends on different factors such as; dielectric constant of the solvent, interfacial interaction between the NP and dispersion medium [123]. In contrast, electrostatic potential among neighboring particles stabilizes the colloidal suspension due to repulsive intermolecular interaction. The resultant potential of these inter-molecular forces is a function of few key parameters. Different effective stabilization techniques for improved stability of NF are summarized and classification of the techniques is shown in **Fig. 13**. In the following sections, these stabilization techniques are enlightened.

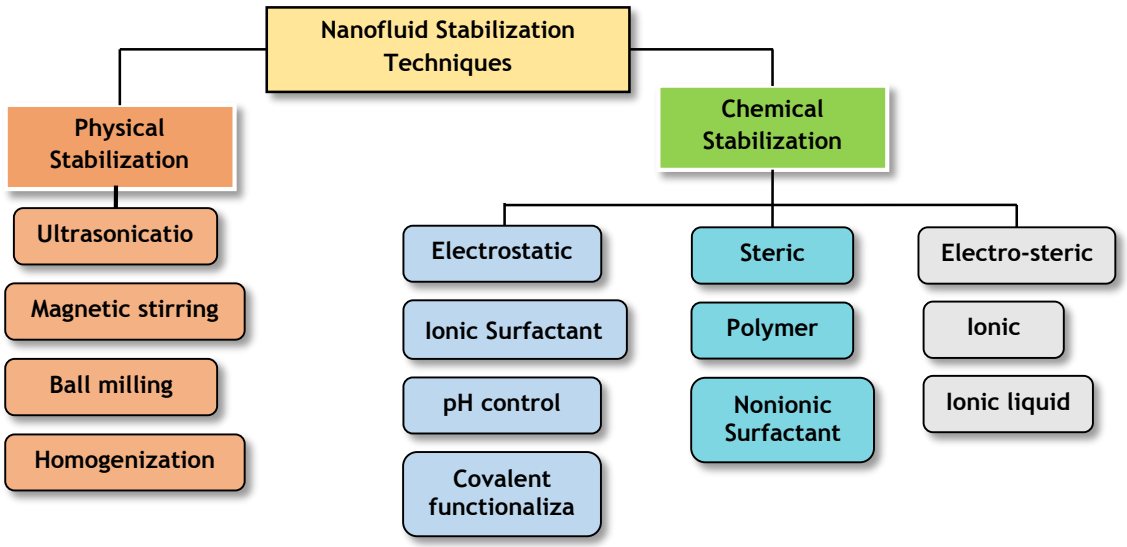

Fig. 13. Stability enhancement techniques for nanofluids.

4.3.1. Physical stabilization

Different physical methods are commonly utilized to stabilize NF suspension. Mechanical techniques such as ultrasonic vibration, magnetic stirring and homogenization are commonly employed for homogenous dispersion of colloidal mixture.

Ultrasonication is one of the effective mechanical dispersion techniques for homogenous mixture of NPs into base fluid. Direct (ultrasonic bath) and indirect (probe sonicator) ultrasonication techniques can be applied to stabilize colloidal suspension by breaking particle clusters and lowering the average particle size distribution. The indirect ultrasonication method using high frequency probe sonicator shows dominant performance reported in different investigations regarding NF dispersion. Ultrasonication of colloidal suspensions provides homogenous distribution of NPs within the mixture and reduces the average cluster size, which in turns remarkably influences the heat transfer properties of the NP [124]. Asadi, et al. [125] reviewed the remarkable impact of ultrasonication treatment on colloidal dispersion and heat transfer characteristics of NFs. In addition, they reported a notable effect of variation in ultrasonication time and power on effective dispersion of NPs into BF. However, beyond a certain limit of ultrasonication period, dispersion characteristics tend to deteriorate

significantly. Chen and Guo [126] revealed that the average particle size of NPs remains constant after an optimum period of effective ultrasonic vibration in the colloidal suspension. Magnetic stirring is one of the basic techniques implemented to prepare homogenous dispersion of NPs into base liquid solvent. In this method, a rotating magnetic bead rotates at high-speed using external magnetic field to break down the clusters and disperse the NPs. Studies have shown that an effective stirring technique depends on two crucial parameters such as stirring speed and stirring time. Generally, higher stirring speeds and longer stirring times result in better performance dispersing NP clusters. At elevated speed and longer stirring time, more NPs can come into contact with the magnetic bead and break apart into smaller particles. Chen, et al. [127] investigated dispersion stabilization of Al_2O_3/liquid paraffin NF at different stirring periods. They discovered that stirring for a longer period increases stability by using stirring in two stages of the stabilization process. They noted that increasing stirring time by 30 to 40 minutes yields 3.14% more thermal conductivity for the studied NFs. In addition, stirring is found to be more effective at elevated temperatures and lower concentration of NPs. To formulate stable NFs, few other effective stabilization methods, for instance; high-pressure homogenization and ball milling are employed in various studies and found prominent improvement of dispersion characteristics [128-130].

4.3.2 Chemical stabilization

Chemical techniques for stabilization i.e., electrostatic, steric, or electro-steric strategies include surface functionalization, surfactant inclusion, pH control, polymer addition, acid treatment and so on. The latter sections provide comprehensive insight of these stabilization techniques.

4.3.2.1. Electrostatic stabilization

Electrostatic stabilization of NFs can be obtained when attractive Van der Wall force is stabilized by reciprocal repulsive potential between the identically (positive or negative) charged particles demonstrated in **Fig. 14**. The surface charges of the NPs can be induced by several approaches such as: (a) ionization of surface groups, (b) adsorption of ions from ionic surfactants, (c) substitute of ions, (d) dissociate surface charged parts, (e) physically adsorbed ions, (f) accumulation or depletion of electrons at surfaces. In liquid suspension, charged NPs are surrounded by opposite charges to sustain charge neutrality of the dispersion and to form electric double layer (EDL) with strongly bonded stern layer and diffuse layer. The stern layer contains opposite ions whereas, diffuse layer consists of weakly attached both positive and negatively charged ions due to electrostatic force of the particles. The electric potential is maximum at the surface of the particles and drops steadily away from the surface to EDL. The electric potential at the outer layer of EDL is defined as Zeta potential (ζ) which value is used to estimate the dispersion stability of NF suspension. The objective of electrostatic stabilization is to increase the electric potential between the particles to minimize the attraction force so that particles cannot form agglomeration and disperse homogenously in the liquid medium. The higher the potential, the higher the dispersion stability of NFs.

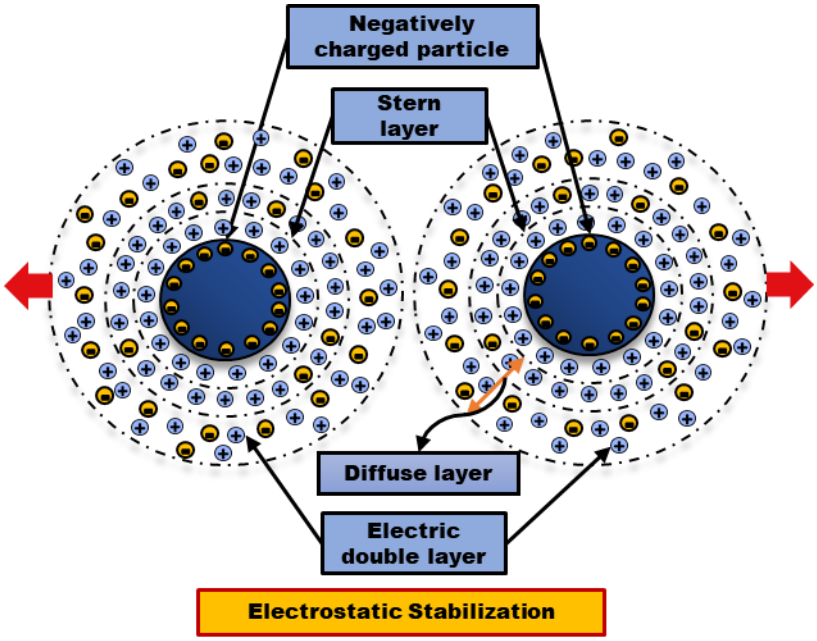

Fig. 14. Electrostatic stabilization technique for nanofluid suspension.

Electrostatic stabilization includes the addition of ionic surfactants to the NF. Several categories such as cationic, anionic, non-ionic, and amphoteric surfactants are employed in NF to stabilize the suspension [131-134]. Amphoteric surfactants, also known as zwitterionic, are surfactants containing both cationic and anionic hydrophilic functional groups in its chemical structure. This class of surfactants can produce cations and anions depending on the acidity (pH) of the suspension. These surfactants exhibit low toxicity, good anti-bacterial characteristics, resistance to the hardness of water and are well-suited with other forms of surfactants. Amiri, et al. [134] reviewed stable liquid-phase exfoliation of two-dimensional graphene using several classes of ionic and non-ionic surfactant stabilizers such as pluronic P-123, Triton X-100, Polyvinylpyrrolidone (PVP), n-Dodecyl β-D-maltoside, Polysodium4-Styrenesulfonate (PSS), Sodium deoxycholate (DOC), Sodium taurodeoxycholate hydrate and so on.

Pyrene derived stabilizers are also considered as anionic surfactants and used as a non-covalent functionalization method of NF stabilization. Ionic and non-ionic surfactants are used to obtain electrostatic and steric stabilization of NF dispersion. Non-covalent functionalization can be

accomplished in various ways, such as anionic and cationic surfactant, non-ionic surfactant, polymer, and aromatic surfactant. For carbon based nanofluid, the main shortcoming of non-covalent functionalization is the formation of foam inside thermal apparatus leading to lessening in effective heat transfer and thermal performance [135, 136]. In contrast, covalent functionalization of carbon-based NF can overcome these shortcomings [137, 138]. The most frequently utilized stabilizers for covalent functionalization of carbon-based NPs are Sodium Dodecyl Sulfate (SDS), Sodium Dodecyl Benzene Sulphonate (SDBS), Gum Arabic (GA) and Triton X-100.

Stability of NFs can also be obtained by substituting the functional groups on the surface of NPs using acid or alkali solution and employing plasma treatment as well. Several functional groups, for instance; hydroxyl ($-\mathrm{OH}$), carboxylic ($-\mathrm{COOH}$), carbonyl ($\mathrm{C}=\mathrm{O}$), sulphate (SO_4^{2-}) and amine ($N-H$) lead to advanced suspension stability in the polar solvents. Such form of functionalization is identified as covalent functionalization [134, 139]. Amiri, et al. [137] investigated the effect of covalent and non-covalent functionalization of CNT NPs using Gum Arabic and Cysteine, respectively. The pH of NF suspension plays an essential role in terms of stability of the dispersion. Therefore, pH adjustment of the NF mixture leads to attaining considerable homogenous dispersion characteristics of the mixture. To obtain good suspension stability, pH should be controlled either at higher value or lower value with respect to pH value of isoelectric point (IEP) for the suspension. At IEP, zeta potential for any suspension is zero which implies absence of repulsive force in the mixture. Hence, the mixture is at unstable state in terms of homogenous dispersion. Lee, et al. [140] showed colloidal mixture performs better suspension stability and thermal performance at pH value far from the value of IEP using CuO NF. They concluded surface charge as a basic key parameter towards improved thermal performance of NFs. Investigations on the effect of pH control on dispersion stability of NF are performed to evaluate optimum pH value for NF under which it performs

better suspension stability [141-144]. Several oxidizing agents such as; HNO_3, $K_2S_2O_8$, H_2SO_4, $KMnO_4$ and so on are utilized to improve dispersion stability of colloidal mixture [145, 146]. Ghozatloo, et al. [147] used $K_2S_2O_8$ and KOH solution as oxidizer and pH control agent respectively for alkaline functionalization of hydrophobic graphene nanosheets into hydrophilic structure. The results exhibited improvement in dispersion as well as in thermal conductivity due to the inclusion of $-\mathrm{OH}$, $-COOH$, $-\mathrm{COOK}$ functional groups in the formulated NF.

However, electrostatic stabilization has some restrictions regarding the applicability of this dispersion technique in different mediums as follows; (a) this technique is applicable for non-aqueous colloidal suspension, (b) limited to dilute nanoparticle dispersion, (c) not suitable for systems containing metal ions and saline medium and (d) stable dispersion of the agglomerated particles is not possible in this method of stabilization.

4.3.2.2. Steric stabilization

The steric or polymeric technique of stabilization for colloidal suspension can be defined as the addition of polymeric chains onto the particle surface to generate repulsive forces between the dispersed particles for better stability of the suspension. The polymer molecules prevent particles from coming near to each other by steric hinders (see **Fig. 15**). The steric stabilization of NFs can be attained using non-ionic surfactants and polymers under non-covalent stabilization [134, 148-150]. In steric stabilization technique, NFs can be stabilized at higher particle loading which is not possible in electrostatic stabilization.

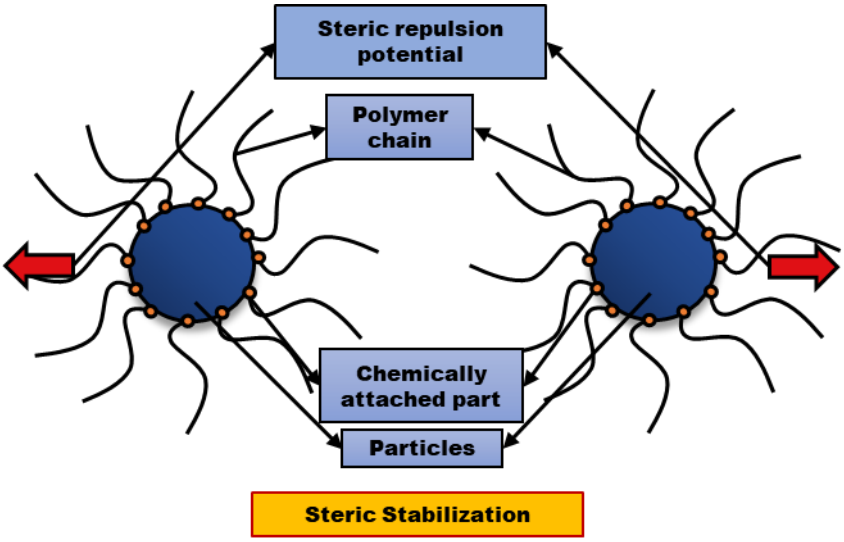

Fig. 15. Steric stabilization technique for nanofluids stabilization.

Grafting of polymers or macromolecules on the surface of NPs forms a steric barrier between the dispersed particles which significantly reduces the inter molecular van der Waals potential [19, 151]. The polymers are weakly attached to the NP surface through chemical or physical adsorption. When the polymers are grafted to the particle's surface, it limits particle movement in the base fluid, which provides barrier potential to prevent aggregation of particles [152]. The compatibility of polymeric additives into BF is an important factor to consider for effective stabilization. Absorption characteristics and length of polymeric chains have an important role in the effectiveness of steric stabilization. For instance, better absorption of the polymers in the NP surface ensures higher grafted surface, hence, can provide improved steric effect in the dispersion. The length of polymeric chains is important because polymers with short lengths have poor absorption properties. Therefore, longer polymeric chain and good absorption properties through strong bonding to the NP surface are essential requirements for effective steric stabilization.

Polymers employed in steric stabilization technique are either homo-polymer containing the same monomer or co-polymer containing two non-identical monomers, in the same polymeric chain. Co-polymers can be divided into three different types according to the arrangement of

the monomers such as random, block and graft co-polymers. Random co-polymers consist of several groups of monomers randomly arranged together, whereas a block co-polymer is formed with two monomer blocks of repeating units. Graft copolymer differs from random and block co-polymer in that the linear backbone is made up of one monomer and another monomer attached to the side chain. Grafted and amphiphilic block polymers are optimum for potential steric stabilization. The standards for selecting co-polymers for steric technique are to have one part attracted to the particle surface and another part compatible with the base fluid medium. Gum Arabic, Oleylamine, Triton X 100, Tween 20, Span 80, PVP, Oleic acid are extensively used polymers for steric stabilization [153-155].

4.3.2.3. Electro-steric stabilization

Electro-steric stabilization is the combination of electrostatic and steric stabilization. In this technique, ionic polymers are absorbed by charged particle surface and lead to produce steric barrier and electrostatic hinders to prevent agglomeration of dispersed NPs. Besides steric repulsion, the electrostatic double layer formed in this method further improves the dispersion of NFs. Electro-steric stabilization is generally attained utilizing ionic polymers that include charged anchor segment and ionic polymeric chain to provide electrostatic and steric stabilization at the same time (illustrated in **Fig. 16**).

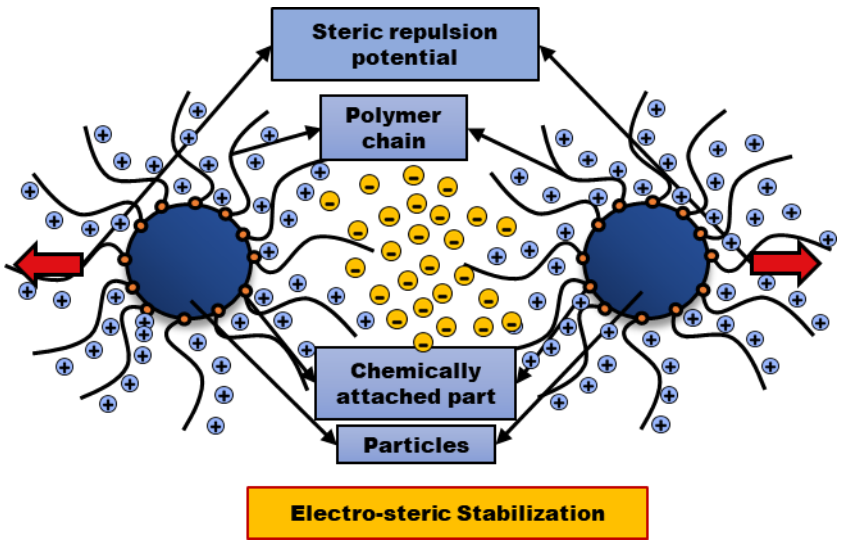

Fig. 16. Electro-steric stabilization for nanofluid suspension.

The polymer used in this method is identified as polyelectrolyte which is an amalgamation of repeating polymer units attached with at least one ionized functional group (such as; carboxylic, sulfonic acid group and so on) and different molecular structure [156]. The most used polyelectrolytes for the electro-steric stabilization of NPs in suspension are poly (styrene sulfonic acid) (PSS), polyacrylic acid (PAA) and poly (1-vinylpyrrolidone-co-acrylic acid) (PVcA) as anionic block co-polymers, poly (vinyl sulfonic acid) (PVSA), and polyethyleneimine (PEI) as cationic polyelectrolyte [156, 157]. The ionized function groups attached to the polymers dissociated into the base fluid to form EDL between the approaching particles. To obtain effective stabilization, ionic polyelectrolytes and NP should contain opposite charges. Polyampholyte, which consists of both anionic and cationic functional groups, can be used for electro-steric stabilization as well. Ionic liquids are used for stabilization of NFs due to their high charge density and strong chemisorption on the NP surface to provide electrostatic repulsion and steric stabilization respectively [158]. Kong, et al. [159] used melamine formaldehyde sulfonate (MFS) as a strong anionic polyelectrolyte to stabilize cement and deionized water suspension.

4.4. Behavior of surfactants below and above CMC

The critical micelle concentration (CMC) is the temperature at which micelles begin to form because of the presence of surface-active agents (i.e., surfactants) in a solvent or colloidal suspension. Prior to that critical concentration, surface tension of a suspension reduces strongly (i.e., higher slope) with the addition of surfactant additives, while at CMC, surface tension of a suspension becomes relatively steady (i.e., lower slope). Further addition of surfactant does not shift the surface tension of the suspension and forms clusters of micelles. Several parameters, such as base fluid, temperature, pH, and particle concentration effect the CMC of

surfactants in a colloidal suspension (i.e., nanofluid) and thus, the behavior of surfactants varies below and above the critical concentration.

Generally, various types of surfactants (i.e., anionic, and cationic) are utilized as stabilizing agents in nanoscale suspensions to achieve long-term dispersion stability of nanofluid. Cacua, et al. [160] investigated the impacts of surfactant's concentration and pH on the stability of alumina nanofluids using anionic SDBS and cationic CTAB at 0.5 and 1 CMC. The absorbance characteristic of the NF samples exhibited less sedimentation at 1 CMC, while lower absorption behavior is identified for both surfactants at 0.5 CMC due to higher sedimentation (**Fig. 17**). At concentration below CMC, surfactants are unable to completely cover the surface of the particles and thus fail to produce sufficient electrostatic repulsive force to stabilize the particles in the suspension. Furthermore, particle distribution analysis and zeta potential measurements confirm the observed results, indicating the existence of nanoparticles and a standard potential of around -30 mV for SDBS stabilized samples at 1 CMC regardless of the pH value. However, the effects of surfactant with a CMC greater than one are not reported in this experiment.

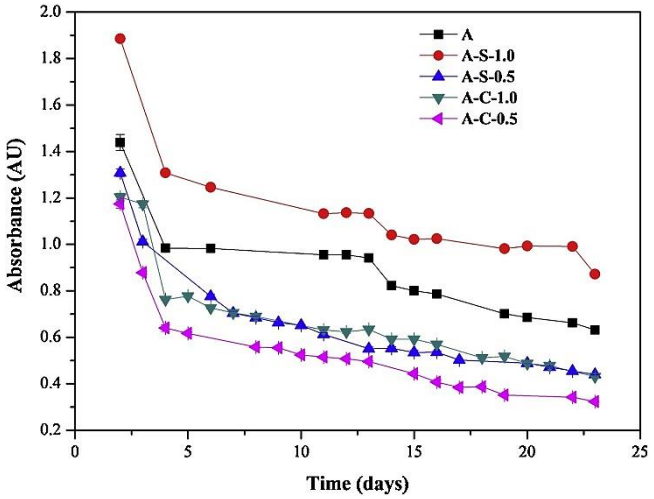

Fig. 17. Variation in absorbance of alumina nanofluids with surfactants at different CMC.

Al-Anssari, et al. [161] revealed the behavior of surfactants (CTAB and SDS) stabilizing saline silica nanofluids at below and above CMC. The effect of concentration variation of cationic CTAB (0.1-5 CMC) and anionic SDS (0.1-3 CMC) showed significant fluctuations in

sedimentation height. The cationic surfactant showed poor dispersion due to formation of double positive layers on the surface of the particles and sedimentation at both below and above CMC. On the other hand, anionic SDS produces robust stability of the suspension at 2450 mg/l (1 CMC) as the absorbed monomers on the surface form negatively supercharged nanoparticles with sufficient repulsive force among the nearby NPs. However, dispersion quality deteriorated at higher concentrations, up to 7350 mg/l (3 CMC). Furthermore, the surfactants have been shown to be effective in a saline environment of NaCl (1-5wt.%). Along with stability, Ma, et al. [162] studied the rheological and thermo-physical properties of hybrid NFs (water/Al_2O_3+CuO and water/Al_2O_3+TiO_2) using several surfactants (SDS, PVP and CTAB) at various concentrations (0.005-0.5wt.%) and temperatures (20-60℃). UV-vis and TEM analysis are performed to characterize the stability of NFs with and without the surface-active agents. The obtained results suggest that the addition of the surfactants significantly reduces the aggregation of the NPs and produces better dispersion and absorption behavior. The non-ionic PVP was found as the most effective additive in both NFs with least agglomeration, improved absorbance, and lowest cluster size of 63 nm. In addition, dispersion characteristics improved with increasing concentration of the surfactants from 0.005 to 0.05wt.% and beyond 25 days of stability is achieved at 0.05wt.%. Nevertheless, concentration of PVP above 0.005 and 0.1wt.% negatively impacts the thermal conductivity and viscosity of the Al_2O_3+CuO and Al_2O_3+TiO_2 NF, respectively. To stabilize the alumina NF, Cacua, et al. [163] observed that a higher concentration of anionic SDBS (5 CMC) additive is required relative to cationic CTAB (1 CMC) at constant ultrasonication time (30 minutes) and tip amplitude (50%). Chen, et al. [164] used Gemini surfactant (12-3-12,2Br^{-1}) up to 60 CMC to stabilize the MWCNT nanofluid. The Zeta potential and visual sedimentation results indicate substantial improvement in dispersion. Nevertheless, Zeta potential dropped at the increasing pH values from 2 to 12. Gao, et al. [99] investigated the dispersion and tribological behavior of pure palm

oil-based CNT nanofluid employing a broad range of surfactants such as APE-10, OP-10, SDBS, SDS, CTAB and TTAB. At a constant concentration of 3wt.%, non-ionic APE-10, OP-10 and cationic TTAB exhibited superior stability and tribological performance in terms of viscosity and factor. The stabilization is obtained by reduced free energy due to absorption of surfactant on the surface of the NPs and reversed micellization effect in non-aqueous base fluid like oil. But the impacts of the additives beyond the constant concentration is not reported in the investigation. Colangelo, et al. [49] studied properties (stability, thermal conductivity, and viscosity) of Therminol/Al_2O_3 NF using Oleic acid as surface-active agent at multiple CMC (1 to 7). According to the results, the stabilization effect is prominent at lower particle concentrations (0.03-0.07wt.%) and CMC (1-2). The Oleic acid reduced the sedimentation factor, providing substantial repulsive forces by being absorbed on the NP's surface. But at higher CMC (3-7), excess Oleic acid deteriorates the dispersion quality due to the formation of double chain layers on Al_2O_3 particles. However, using surfactant, no major effect is found on thermal conductivity and viscosity.

From the above discussion, it is evident to state that CMC of surfactants has crucial impacts on NF's suspension stability and thermophysical properties. Yet, the effects of crucial parameters such as temperature variation and NP morphology (size and shape) on CMC for nanofluids (particularly non-aqueous i.e., oil-based suspensions) are not studied comprehensively and can be further investigated in future research. In addition, interaction of various essential parameters (NP type, NP concentration, base fluid type, temperature, and stability) of NF with CMC of surfactants should be determined to effectively utilize them in photo-thermal applications.

5. Rheology of NFs

Rheology is the study of the flow behavior of fluids flowing against applied tensions. Rheological behavior for flow is evaluated by the relationship between shear stress and

corresponding shear rate. Shear stress is defined as the applied force per unit area while shear rate can be calculated by measuring the rate of change in strain. The ratio of these two parameters is defined as viscosity (μ) and it is one of the key parameters for rheological characteristics of fluids.

5.1 Viscosity (μ), Newtonian and non-Newtonian behaviour

The resistance force to deformation on fluids in the opposite direction of the flow is defined as dynamic viscosity. It is one of the key properties of NFs which has a significant effect on convective heat transfer performance during implementation on thermal energy conversion systems due to its direct association to pressure drop and pumping power. Rheometers and different viscometers are commonly utilized to experimentally evaluate the dynamic viscosity of NFs [165-168]. A rheometer is appropriate to assess noteworthy flow behavior of fluids for a wide range of shear rates and temperatures, whereas a viscometer is a device which only allows to determine the viscosity of fluids.

Considering the relationship between shear stress and shear rate, rheological behavior of fluids can be categorized into Newtonian and non-Newtonian nature. It is established that Newtonian fluids follow linear variation in shear stress against corresponding shear rate or the ratio of shear stress and shear rate i.e., dynamic viscosity (μ) of Newtonian fluids remain unchanged with variation of shear rate. Whereas the non-linear relationship of shear stress and shear rate i.e.., variation of μ against corresponding shear rate results in non-Newtonian behavior of fluids. Rheological behavior along with μ of NFs is affected by several vital parameters depicted in **Fig. 18**. Numerous experimental and theoretical investigations are performed to scrutinize and estimate rheological characteristics and dynamic viscosity of various NFs. Studies enlighten that dynamic viscosity of NFs generally increases with inclusion of solid particles, however the flow characteristics i.e., rheology depends on several parameters and operating conditions [169-171]. For instance, NFs prone to behave as Newtonian fluid at low

particles concentration, high shear-rates and without surfactants or stabilizers while they act as non-Newtonian fluids at higher dispersed particles, low shear-rates, and addition of surfactants.

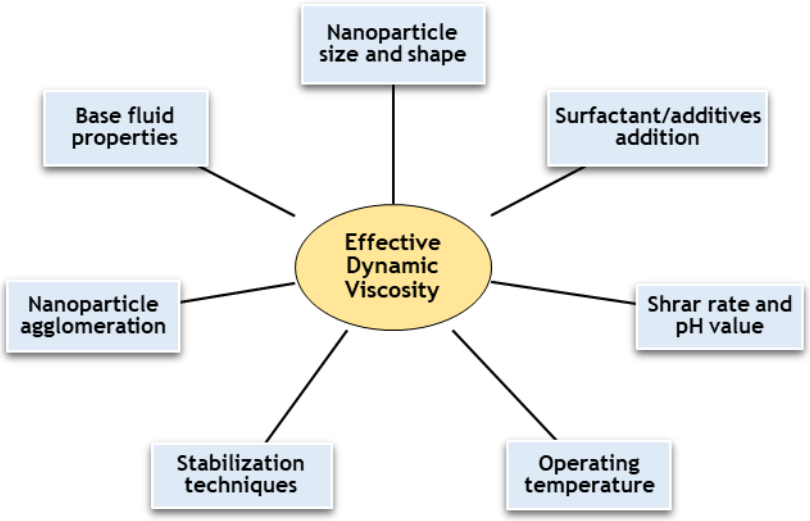

Fig. 18. Key parameters effecting dynamic viscosity of nanofluid.

In a systematic experimental approach, Minakov, et al. [172] studied several NFs based on three different base fluids (water, glycol and oil) dispersing seven different nanomaterials (Al_2O_3,TiO_2, ZrO_2, CuO, Fe_2O_3, Fe_3O_4 and diamond NPs). The NFs are created in two steps, with the NPs dispersed at a concentration of 0.25-8 vol.% and the nanomaterials ranging in size from 5-150 nm. Considerable augmentation in μ is reported for all the samples when it was higher for oil-based NFs due to greater viscosity of oil as BF. Furthermore, rheological analysis of the NFs revealed that using smaller NPs and higher particle loading can change Newtonian behaviour to non-Newtonian behaviour, whereas using identical size NPs of different classes of nanomaterials can also show significant divergence in rheological behaviour.

Asadi, et al. [80] investigated the influence of temperature and φ with hybrid MWCNT-MgO/Engine oil NFs demonstrated in **Fig. 19**. The results revealed that the addition of nanomaterials caused a 65% increment in NF viscosity (μ_{nf}) and elucidated an exponential drop against raising temperature from 25-50 ℃. Furthermore, Newtonian flow trait is identified

with the NF as μ_{nf} remains constant for studied range of shear-rate and temperature. Koca, et al. [173] reviewed the impact of NP sizes on the viscosity of NFs based on data from the literature. They concluded inconsistencies among the studied investigations regarding different particles sizes at similar concentration and altering the NP size could results in either increase or decrease in NF viscosity by 40%. Timofeeva, et al. [174] experimentally studied the effect of four different NP shapes (platelets, blades, cylinders, and bricks) and solution pH for alumina NFs. They revealed that with addition of NPs at 1-7 vol.%, platelet-like particles exhibited largest μ_{nf} followed by cylindrical, bricklike, and bladelike particles. NFs using identical NP concentration, NFs comprised with platelet-like and blade shaped particles showed Newtonian property while cylindrical and bricklike NP contained NF signifies shear-thinning characteristic above loading of 3 vol.%. Maximizing the pH value resulted in a substantial 31% reduction in μ_{nf}.

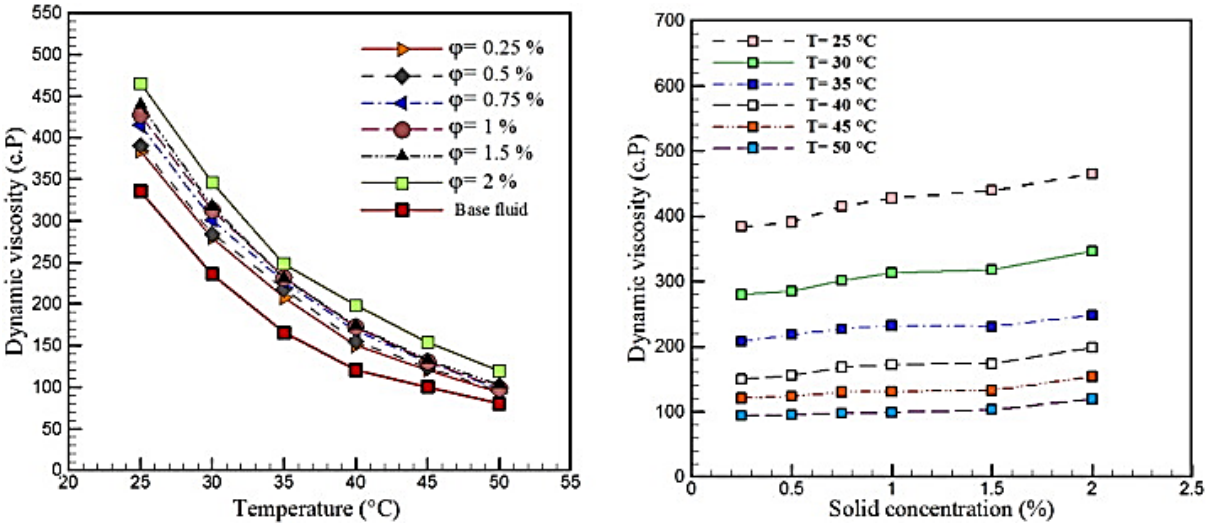

Fig. 19. Dynamic viscosity of MWCNT-MgO/Engine oil nanofluids with respect to increasing temperature and solid particle loading [80].

Frequently studied carbon-based nanomaterials (e.g., CNT and MWCNT) perform both Newtonian and non-Newtonian features depending on the variation of particle concentration, dispersed medium, size and shear-rate. Samylingam, et al. [65] revealed that palm oil/MXene (0.01-0.1 wt.%) NF shows Newtonian behavior at 25-75℃ for shear-rate up to 100 s^{-1}. Similar

findings are observed by Aslfattahi, et al. [69] examining Silicon oil based NF. Hemmat Esfe and Abbasian Arani [175] dispersed MWCNT and SiO_2 NPs in engine oil at 0.05-1 vol.% to experimentally evaluate viscosity and rheological performance of the formulated NF. All the fluids including the base oil exhibited dominant shear thinning flow behavior for the shear-rate of 666.5-10664 s^{-1} at 5-55℃. In contrast, Aghahadi, et al. [176] revealed Newtonian rheological property of engine oil based NF dispersing MWCNT-WO_3 nanocomposite even at low shear-rate (0-25 s^{-1}) and studied temperatures (20-60 ℃). In a recent 3S research, Tiwari, et al. [48] evaluated impacts of several surfactants (BAC, CTAC, ALS, PLS, Brij 700 and Span 80), base fluids (water, EG, Therminol VP-1 and silicon oil) and sonication time on viscosity of hybrid MWCNT-CeO_2 nanocomposite based NFs. Measurements revealed that increasing ultrasonication time for the samples decrease $\frac{\mu_{nf}}{\mu_{bf}}$ up to an optimum period and further ultrasonication offers opposite consequences due to formation of clusters at longer sonication periods while addition of nanocomposite (0.25-1.50 vol.%) and surfactants reasonably rises the $\frac{\mu_{nf}}{\mu_{bf}}$. Silicon oil and Therminol VP-1 based NFs resulted in higher viscosity ration than other BFs. In addition, pH 6-8 exhibited optimum viscosity ratio for all the examined NFs.

In parallel to experimental development on NF rheology, numerical simulations and molecular dynamics methods have also contributed to the advancements in this area of research. Wu, et al. [177] performed numerical study on rheology of graphene-PAO NF using nonequilibrium molecular dynamics analysis utilizing statistical data from previous experimental and numerical works. The model was validated, and results confirmed improvement in μ_{nf} at higher temperature and shear thinning property is identified for oil and NF samples.

Studies on viscosity and rheology of NF are somewhat inconsistent and unorganized in terms of key influential parameters and characteristics of a particular NF. This section demonstrates a comprehensive review of advances made by works in this area. **Table. 6** represents a summary of reviewed works on rheology and viscosity of oil-based NFs using a wide range of

NPs and **Table. 7** and **Table. 8** demonstrate summary of empirical and classical correlations obtained from available studies on this topic respectively.

Table. 6. Summary of reviewed experimental studies on viscosity and rheological behavior of oil-based nanofluids.

Reference	**Nanofluids**	**Size and concentration (φ)**	**Temperature range**	**Surfactants**	**Rheological behavior and shear rate (1/s)**	**Key findings**
Fakoor Pakdaman, et al. [54]	Oil/ MWCNT	1-10 µm × 5-20 nm Φ = 0.1 to 0.4 wt.%	40-100 ºC	--	Newtonian 20 to 520	● Maximum μ_{nf} rises 67% @ T = 40 °C and φ = 0.4 wt. %. However, it dropped considerably at elevated temperatures.
Wang, et al. [5]	Oil/Graphite	10-30 nm Φ = 0.17-1.36 vol.%	30-60 °C	CH-5	Newtonian 0.1-1000	● All the samples except graphite at 1.36 vol.% exhibited non-Newtonian behaviour due to formulation of cluster of nanomaterials at higher concentration and lower shear rate.
Aberoumand and Jafarimoghaddam [27]	Engine oil/ Cu	50 nm Φ = 0.2 to 1 wt.%	25-60 °C	--	Newtonian and Non-Newtonian 0-25	● Inclusion of solid particles resulted non-Newtonian behaviour and increase in μ_{nf} for the NFs. However, NFs showed Newtonian behaviour over 35°C.
Aberoumand, et al. [28]	Oil/Ag	20 nm Φ = 0.12 to 0.72 wt.%	25-60 ºC	--	Newtonian to Non-Newtonian 5-30	● Base oil exhibited Newtonian behavior whereas, non-Newtonian behavior appeared with inclusion of particles and at temperatures below 35 ºC. Maximum μ_{nf} enhances 41% at T 25°C and φ = 0.72 wt. %.
Rubbi, et al. [32]	Soybean oil/MXene	1–10 µm × 1 nm Φ = 0.025-0.125 wt.%	25-85 ºC	--	Newtonian 30-100	● Maximum μ_{nf} rises of 13.28% at T = 25°C and 0.125 wt. %. It also decreased remarkably at elevated temperatures.
Kumar, et al. [57]	Veg. oil/Cu-Zn Paraffin oil/Cu-Zn SAE oil/Cu-Zn	Both 25 nm Φ = 0.1 -0.5 vol.%	30 °C	SDS	Newtonian 10-100	● Veg. oil base NF elucidated higher relative μ_{nf} with rise in loading of hybrid nanoparticle incorporation and mor dominant Newtonian behaviour than paraffin and SAE oils.
Asadi, et al. [56]	Engine oil/ MWCNT-$Mg(OH)_2$	30 and 10 nm respectively Φ = 0.25-2 vol.%	25-60 °C	--	Newtonian Rotational speed (100-600 rpm)	● Maximum μ_{nf} rises 50% at 60 °C and 2 vol. %. Minimum viscosity increases 5% at 25 °C and 0.25 vol. %.

Chai, et al. [58]	Hydrogenated oil/ Graphene	0.06-0.1 µm × 0.002-0.005 µm Φ = 25-100 ppm	30-50 ºC	--	Non-Newtonian	● Maximum μ_{nf} increases of 33% have been reported at temperature of 30 °C.
Saeedinia, et al. [59]	Oil/CuO	50 nm Φ = 0.2 to 2 wt.%	20-70 ºC	--	Newtonian 1-17	● Considerable increment in μ_{nf} is observed with addition of CuO particles and it dropped at elevated temperatures. Highest 20% rise is measured at 20 °C.
Taha-Tijerina, et al. [60]	Mineral oil/Nano-diamond (ND)	~ 6 nm Φ = 0.01-0.1 wt.%	298-373 K	--	Newtonian 0-6000	● It is observed that increment of μ_{nf} is very less (<6%) with addition of maximum 0.1 wt.% of ND into the oil.
Colangelo, et al. [49]	Diathermic oil/ Al_2O_3	45 nm Φ = 0.3-1 vol.%	30-50 ºC	Oleic acid	Non-Newtonian 0-250	● The effect of surfactant addition on rheological behavior has been investigated and found that the μ_{nf} increase is not noticeable in the samples containing Oleic Acid surfactant.
Farbod, et al. [61]	Oil (20W50)/ CuO	61 nm Φ = 0.2-61 wt.%	10-70ºC	--	Newtonian 0-70	● Nano-rhombic morphology of particles exhibited less μ_{nf} relative to nanorods and nanoparticles. Maximum μ_{nf} was found for 0.2 wt.% of nanorods nanofluids.
Asadi and Pourfattah [62]	Engine oil/ MgO /ZnO	35-45 and 40 nm respectively Φ = 0.125-1 vol.%	5-55 ºC	--	Newtonian Rotational speed (100-800 rpm)	● Maximum μ_{nf} increases 124.3% for ZnO and 75% for MgO at 55 °C and φ = 1.5 vol. %.
Ilyas, et al. [63]	Oil/ Al_2O_3	40 nm Φ = 0.5-3 wt.%	25-90 °C	Oleic acid, o-xylene, toluene, and ethanol.	Non-Newtonian 100-2000	● μ_{nf} increased with addition of NPs and decreased at higher shear rate. Leading increment is almost 20% at 25 °C and 100 s^{-1} shear-rate.
Ghaffarkhah, et al. [64]	Transformer oil/ /MWCNT /MWCNT-TiO_2 /MWCNT-SiO_2 /MWCNT-Al_2O_3	10-30 µm × 10-20 nm, 20 nm, 60-70 nm, and 50 nm respectively Φ = 0.001-0.1 vol.%	25-65 ºC	--	Newtonian 26.4-237.6	● μ_{nf} increased slightly with addition of nanoparticles whereas, significant decrease is noted with increasing temperature. Maximum μ_{nf} rises of 13.618% for MWCNT-Al_2O_3 nanofluid.
Li, et al. [66]	Diathermic oil/SiC	30 nm Φ = 0.1-0.8 vol.%	25-60 °C	--	Newtonian 0-1000	● μ_{nf} increased substantially adding NPs and decreased drastically at increasing temperature.

Aslfattahi, et al. [69]	Silicon oil/MXene	1–10 µm × 1 nm Φ = 0.05-0.1 wt.%	25-125 °C	n-Hexane, chloroform, toluene, and tween 40	Newtonian 0-100	● μ_{nf} of the NFs remained constant throughout the temperature range and shear-rate. It decreased by 127% at 125 °C relative to the viscosity at 25 °C and remained almost constant after adding NPs.
Wei, et al. [72]	Diathermic oil/ SiC /TiO_2 /SiC-TiO_2	30 and 10 nm respectively Φ = 0-1 vol.%	25-60 ºC	--	Newtonian 0-1000	● They informed an increasing trend in the μ_{nf} by increasing the solid fraction and decreasing trend by rising the temperature.
Beheshti, et al. [73]	Transformer oil/ Oxidized MWCNT	30 µm × 10-20 nm Φ = 0.001-0.01 wt.%	20-80 °C	--	Newtonian 0-250	● μ_{nf} dropped remarkably at raising temperature whereas, addition of particles showed slight increase in viscosity due to low particle loading.
Ilyas, et al. [74]	Paraffin oil/ZnO	30 nm Φ = 0-1 wt.%	25-55 °C	Oleic acid	Non-Newtonian 500-1500	● Highest augmentation for μ_{nf} is observed to be ≈17% for 1 wt% the nanofluid at 55 °C
Li, et al. [75]	Waste cooking oil/ SiC /TiO_2	30 and 10 nm respectively Φ = 0.05 and 0.1 vol.%	25-65 °C	Span-80	Newtonian and Non-Newtonian 0-1000	● SiC NF performed better rheological characteristic being Newtonian fluid than Non-Newtonian TiO_2 NF. Nonetheless, μ_{nf} dropped at higher temperatures for both NFs.
Amiri, et al. [76]	Transformer oil/ MWNCT-HA	5-15 µm × 30 nm Φ = 0.001-0.005 wt.%	20-80 ºC	DMF, H_2SO_4 and hexylamine	Newtonian 35-235	● Maximum μ_{nf} enhances ~9% @ T = 40 °C and φ = 0.05 wt. %. Nevertheless, Newtonian behavior is dominant in the NFs with and without dispersants and μ_{nf} dropped above 70% at 80 ºC.
Akhter, et al. [92]	Therminol-66/Titania	30 nm Φ =0.25-1 wt.%	30-130 °C	--	Newtonian 20-200	● NF showed non-linear relation to raising temperature and μ_{nf} increased with added particles. While NF showed dominant Newtonian behaviour except at lower temperatures.
Nabeel Rashin and Hemalatha [106]	Coconut oil/ZnO	26 nm Φ = 0.08-0.48 vol.%	308-328 K	--	Non-Newtonian 3.67-14.68	● Prepared nanofluid showed share thinning behaviour for varying concentrations. μ_{nf} raises linearly with addition of nanoparticles and dropped at raising temperatures.

Moghaddam and Motahari [178]	Engine oil (SAE40)/ MWCNT-CuO	40 and 50 µm × 5-15 nm respectively Φ = 0.0625-1 vol.%	25-50 ºC	--	Non-Newtonian 666.5–9331	● Maximum μ_{nf} increases 29.47% at 30 °C and φ = 1 vol. %. The study conducted on flow behavior established that nano-lubricant and base oil followed Ostwald de Waele relationship.
Asadi and Asadi [179]	Engine oil (10 W40)/ MWCNT-ZnO/	30 nm Φ = 0.125-1 vol.%	5-55 ºC	--	Newtonian 100-900	● Maximum μ_{nf} rises of 45% at 55 °C and φ = 1 vol. %. While least μ_{nf} increases of 19.5% at 5 °C and φ = 0.125 vol. %
Alirezaie, et al. [180]	Engine oil/ MWCNT-MgO	10 µm × 10-30 and 40 nm respectively Φ = 0.0625-1 vol.%	25-50 ºC	Gum Arabic	Non-Newtonian 670-8700	● Non-Newtonian behaviour is dominant at lower temperatures and higher volume fractions. Increasing the temperature from 25 to 50 °C leads to 75% decrease in μ_{nf}.
Hemmat Esfe, et al. [181]	Engine oil (SAE40)/ MWCNT-SiO_2	5-15 and 20-30 nm respectively Φ = 0.0625 to 2 vol.%	25-50 ºC	--	Newtonian and on-Newtonian 100-500	● NF showed Newtonian performance at up to 1 vol.% and non-Newtonian for 1.5% and 2%. Maximum μ_{nf} rises of 30.2% @ T = 40 °C and φ = 0.5 wt. %
Hemmat Esfe and Rostamian [182]	Engine oil (SAE50)/ TiO_2	30 nm Φ = 0.125-1.5	25-50 ºC	--	Non-Newtonian 666.5-9331	● NF exhibited shear thinning behaviour. The sensitivity analysis showed that the maximum sensitivity was occurred at the solid concertation of 1 vol. % and temperature of 25°C.
Ahmadi Nadooshan, et al. [183]	Engine oil (10 W40)/ MWCNT-SiO_2	5-20 and 20-30 nm respectively Φ = 0.05 to 1 vol.%	5-55 ºC	--	Non-Newtonian 666.5 to 11997	● Data implies that NFs and 10W40 oil are non-Newtonian fluids with shear thinning behavior, while 10W40 oil at low temperatures performs like Newtonian fluids
Hemmat Esfe, et al. [184]	Engine oil (SAE40)/ MWCNT-ZnO	50 µm × 3-5 nm and 10-30 nm respectively Φ = 0.05-1 vol.%	25-60 ºC	--	Newtonian 333-13333	● Maximum μ_{nf} increases 33.3% @ T = 40 °C and φ = 1 vol. %. NFs are observed to be very sensitive ot temperature and it declines at elevated temperatures. However, effect of temperature on rheological behavior is not analyzed.
Motahari, et al. [185]	Engine oil (20 W50)/MWCNT-SiO_2	20 and 40 nm respectively Φ = 0.05-1 vol.%	40-100 ºC	--	Newtonian 6-68	● All the NF samples showed Newtonian flow characteristic. Maximum μ_{nf} increases 171% @ T = 100 °C and φ = 1 vol. %

Table. 7. A summary of reviewed correlations proposed based on experimental data to estimate the viscosity of oil-based nanofluids.

Reference	Nanofluid	Correlation	Applicability	Accuracy
Aberoumand, et al. [28]	Oil/ Ag	$\mu_{nf} = \mu_{bf}(1.15 + 1.061\varphi - 0.5442\varphi^2 + 0.1181\varphi^3)$	Φ = 0.12-0.72 wt.% T = 25-60 °C	Max. error = 1.2%
Ilyas, et al. [67]	Thermal oil/ MWCNT	$\mu_{nf} = -1.8231 - \frac{0.0686}{T} + 1.7235(1-\varphi) + 3.329(1-\varphi)^2 + 136.7838\frac{(1-\varphi)^2}{T^2} - 3.2363(1-\varphi)^3 - 2347.39\frac{(1-\varphi)}{T^3}$	Φ = 0.5-3 wt.% T = 25-90 °C Shear-rate = 100 s^{-1}	Max. error = 4.91% R^2 = 0.97
Asadi and Asadi [179]	Engine oil (10W40)/ MWCNT-ZnO	$\mu_{nf} = 796.8 + 76.26\varphi + 12.88T + 0.7695\varphi T + \frac{-196.9T - 16 - 53\varphi T}{\sqrt{T}}$	Φ = 0.125-2 wt.% T = 5-55 °C	R^2 = 0.9803
Asadi, et al. [56]	Thermal oil/ MWCNT-$Mg(OH)_2$	$\frac{\mu_{nf}}{\mu_{bf}} = 1604 + 256.8\varphi + 24.73\varphi^3 + 1.615T^2 + 0.07343\varphi T^2 - 83.2T - 7.389\varphi T - 0.1123T^3 - 74.19\varphi^2$	Φ = 0.25-2 vol.% T = 25-60 °C	Max. error = 6.5%
Fakoor Pakdaman, et al. [54]	Heat transfer oil/ MWCNT	$\frac{\vartheta_{nf} - \vartheta_{bf}}{\vartheta_{bf}} = (-11.23T + 5926.5)\varphi^{1.43}$	Φ = 0.1-0.4 wt.% T = 40-100 °C	R^2 = 0.91
Hemmat Esfe and Rostamian [182]	Engine oil (20 W50)/ MWCNT-SiO_2	$\frac{\mu_{nf}}{\mu_{bf}} = 0.09422 - \left[\left(\frac{T}{\varphi}\right)^2 + 0.100556T^{0.8827}\varphi^{0.3148}\right] e^{(72474.75T\varphi^{3.7951})}$	Φ = 0.05-1 vol.% T = 40-100 °C	Max. error < 5% R^2 = 0.9943
Attari, et al. [186]	Crude oil/ TiO_2, Fe_2O_3, ZnO, NiO and WO_3	$\ln[A_1(\frac{\mu_{nf}}{\mu_{bf}} + A_2)] = \left(\frac{\rho_p}{\rho_{bf}}\right)^a + A_3(w)^b\left(\frac{T}{T_0}\right)^c + A_4\left(\frac{T}{T_0}\right)^c$	Φ = 0.2-2 wt.% T = 40-100 °C	Max. error = 20% R^2 = 0.96
Dardan, et al. [187]	Engine oil (SAE40)/ Al_2O_3-MWCNT	$\frac{\mu_{nf}}{\mu_{bf}} = 1.123 + 0.3251\varphi - 0.08994T + 0.002552T^2 - 0.00002386T^3 + 0.9695\left(\frac{T}{\varphi}\right)^{0.01719}$	Φ = 0.0625-1 vol.% T = 25-50 °C	Max. error = 2%
Asadi, et al. [45]	Thermal oil/ MWCNT-Al_2O_3	$\mu_{nf} = A + B\varphi$	Φ = 0.125-.5 vol.% T = 25-50 °C	Max. error < 5%
Hemmat Esfe and Esfandeh [188]	Engine oil (SAE40)/ MWCNT-MgO	$\frac{\mu_{nf}}{\mu_{bf}} = 1.10780 - 0.10873\varphi - 1.18666E - 0.003T - 1.76723E - 0.005\gamma + 3.93936E - 0.003\varphi T + 1.14589E -$	Φ = 0.25-2 vol.% T =25-45 °C Shear-rate = 1000 s^{-1}	Max. error < 3% R^2 = 0.9565

		$0.005\varphi\gamma - 1.90857E - 0.007\gamma T + 0.037831\varphi^2 + 1.58759E - 0.005T^2 + 2.17677E - 0.009\gamma^2 - 3.83867E - 0.007\varphi T\gamma$		
Moghaddam and Motahari [178]	Engine oil (SAE40)/ MWCNT-CuO	$\frac{\mu_{nf}}{\mu_{bf}} = a_0 + a_1\varphi e^{\varphi} + a_2\varphi^2 + a_3\varphi^3$	Φ = 0.0625-1 vol.% T = 25-50 °C	Max. error < 2% R^2 = 0.9803
Asadi, et al. [80]	Engine oil (SAE50)/ MWCNT-MgO	$\mu_{nf} = 328201 \times T^{-2.053} \times \varphi^{0.09359}$	Φ = 0.25-2 vol.% T = 25-50 °C	Max. error < 8%
Hemmat Esfe and Rostamian [182]	Engine oil (SAE50)/ TiO_2	$\frac{\mu_{nf}}{\mu_{bf}} = 1.2854 + 0.1444\varphi - 0.013802T - 0.00175\varphi T$	Φ = 0.125-1.5 vol.% T = 15-55 °C	Max. error = 1.52% R^2 = 0.9751
Li, et al. [75]	Waste cooking oil/ SiC and TiO_2	$\frac{\mu_{nf}}{\mu_{bf}} = 0.15 + 2.4\varphi - 0.23\varphi^2$	Φ = 0-0.1 vol.% T = 55 °C	n/a
Ilyas, et al. [63]	Mineral oil/ Al_2O_3	$\mu_{nf} = -1.6752 - \frac{0.7856}{T} + 0.9125(1-\varphi) + 3.4862(1-\varphi)^2 + 134.8479\frac{(1-\varphi)^2}{T^2} - 2.7263(1-\varphi)^3 - 2347.62\frac{(1-\varphi)}{T^3}$	Φ = 0.5-3 wt.% T = 25-80 °C Shear-rate = 100 to 2000 s^{-1}	Max. error = 15% R^2 = 0.9814
Alirezaie, et al. [180]	Engine oil (SAE50)/ MWCNT-MgO/	$\mu_{nf} = 4 \times 10^4 + 145\varphi - 240T - 0.061\gamma + 1.9 \times 10^6\varphi^2 + 0.36T^2$	Φ = 0.0625-1 vol.% T = 25-50 °C Shear-rate = 670 to 8700 s^{-1}	R^2 = 0.98
Hemmat Esfe, et al. [189]	Engine oil (5W50)/ MWCNT-Al_2O_3	$\mu_{nf} = -744.8 + \frac{1806\varphi^{0.01382}}{T^{0.2}}$	Φ = 0.05-2 vol.% T =5-55 °C	R^2 = 0.9923

Table. 8. Summary of classical models of viscosity estimation for NFs.

Reference	**Model**	**Applicability**
Einstein [190]	$\mu_{eff} = \mu_{bf}(1 + 2.5\varphi)$	Dilute suspension of spherical particle with low solid concentration of < 1 vol.%
Brinkman [191]	$\mu_{eff} = \mu_{bf}(1-\varphi)^{-2.5}$	Extended form of Einstein model, applicable for even less dilute suspensions.
Roscoe [192]	$\mu_{eff} = \mu_{bf}\left(1 - \frac{\varphi}{\varphi_m}\right)^{-2.5}$	This model is appropriate for suspensions of equal sized rigid sphere particles at low to high concentrations.

Krieger and Dougherty [193]	$\mu_{eff} = \mu_{bf}\left(1 - \frac{\varphi}{\varphi_m}\right)^{-[\mu]\varphi_m}$	Power law-based semi-empirical to predict viscosity containing any volumetric concentration of particles.
Brenner and Condiff [194]	$\mu_{eff} = \mu_{bf}(1 + \eta\varphi)$	Suitable for rod-shaped particles suspensions at higher shear rate. Applicable for up to $1/r^2$ volume concentration.
Jeffrey and Acrivos [195]	$\mu_{eff} = \mu_{bf}\left[3 + \frac{4}{3}\left(\frac{\varphi r^2}{\ln(\frac{\pi}{\varphi})}\right)\right]$	To predict the viscosity of non-dilute suspension rod-shaped in extensional flow.
Batchelor [196]	$\mu_{eff} = \mu_{bf}(1 + 2.5\varphi + 6.2\varphi^2)$	Brownian motion is considered in this model to predict viscosity of dilute suspensions.
Graham [197]	$\mu_{eff} = \mu_{bf}[(1 + 2.5\varphi) + \frac{2.25}{\left(1 + \frac{h}{2a}\right)} \times \left[\frac{1}{\frac{h}{a}} - \frac{1}{\left(1 + \frac{h}{a}\right)} - \frac{1}{\left(1 + \frac{h}{a}\right)^2}\right]$	This model is applicable for spherical particles. Intermolecular spacing and particle radius is considered to predict viscosity by this formula.

6. Application of nanofluids on concentrating solar collectors

Solar collectors (SCs) are engineered as advanced kinds of heat exchangers that are capable of spontaneously capturing and converting solar irradiation into useful thermal energy in the case of thermal collectors and into thermal and electrical energy in the case of photovoltaic/thermal hybrid SCs. The solar energy incident on the surface of SC is captured as heat and transformed via working fluid passing through integrated tubes in the SCs [198]. SC is one of the most convenient, sustainable, eco-friendly, and efficient resources of renewable thermal energy conversion systems that can be employed in multifarious applications, including but not constrained to domestic and engineering heating processes. Primarily, SCs can be classified into thermal and hybrid collectors (combination of photovoltaic panel and thermal collector). Moreover, thermal collectors are grouped into non-concentrating and concentrating collectors based on the concentration of incident solar radiations on specific surface area of SC. Several types of SCs are classified and depicted in **Fig. 20**.

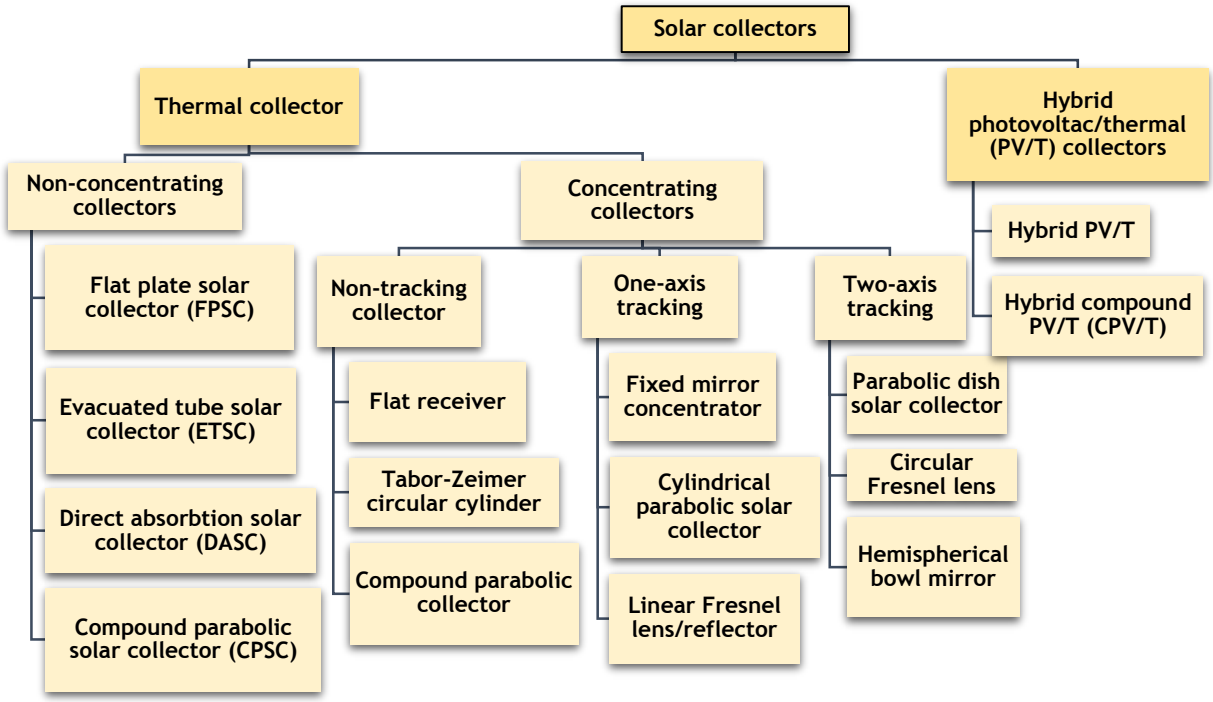

Fig. 20. Classification of solar thermal collectors.

Concentrating i.e., high flux SC devices can be categorized into non-tracking and tracking based collectors depending on the concentrator and receiver configuration of the collectors. Thermal energy efficiency of the SCs dictated notably by heat transfer performance of the working fluids. Research has been carried out over the last decade implementing many high temperature thermal oil adopted NFs replacing conventional fluids in concentrating SC technology [199]. Oil-based NFs are the most eminent and effective class of NF that can be deployed in concentrating SCs due to their suitable heat transport properties at high operating temperatures up to 400-500 ℃ [200, 201]. The present review focuses on the implementation and impact of oil-based NFs as working fluid instead of traditional fluids in various solar collector systems. NF based prominent concentrating solar collectors i.e., Concentrating direct absorption solar collector (C-DASC), Parabolic trough solar collector (PTSC), Parabolic dish collector (PDC), Compound parabolic collector (CPC) and concentrating photovoltaic/thermal (CPV/T) collector are scrutinized considering crucial parameters.

6.1. Concentrated direct absorption solar collector (C-DASC)

DASC systems provide volumetric assimilation of concentrated solar irradiations directly to working fluid. Concentrated i.e., high-flux (above 1367 W/m^2) DASC is an advanced version of conventional low-flux DASC with a reflector/concentrator which captures solar irradiation and consequently focuses the radiation on a fluid flowing receiver of the systems. Convective heat loss in C-DASCs is minimal relative to conventional indirect absorption solar collectors where, significant radiation loss is observed due to high temperature difference between absorber plate and operating fluid [11]. However, the effectiveness of DASCs is restricted due to poor solar absorption property of regular working fluids used in the systems. To optimize the performance of C-DASCs, nanotechnology offers a potential opportunity to enhance the energy output of the collectors utilizing nanoparticle dispersed working fluids, i.e., nanofluids.

Oil-based NFs are suitable for C-DASC implementation due to high temperature operating conditions.

In a combined numerical and experimental investigation, Lenert, et al. [202] offered a one dimensional transient model for a volumetric receiver to study the impacts of solar concentration (C) level, geometry of the receiver and thickness of the medium on efficiency of the collector using Therminol VP-1 based carbon-coated cobalt NF. The results indicate that volumetric receivers can gain greater power generation at higher levels of solar concentrations and receiver heights compared to surface-based receiver. The obtained results are in accord with the experimental outcomes as well. In their later investigation, they [203] optimized the efficiency of the volumetric receiver considering optical thickness, solar concentration and NF height. Higher optical thickness exhibited superior volumetric absorption of the radiation. Also, higher solar concentrations, temperature and NF heights produced optimized output. 35% exceeded efficiency is predicted for the receiver, which implies potential applicability of NF-based volumetric direct absorption techniques in concentrated solar technology. Li, et al. [204] performed an experimental and numerical comparison study between volumetric and surface absorption based solar collectors operated with Therminol-55/MWCNT NF for high-temperature operation. The surface absorber was comprised of a chrome-coated copper tube. Simulation findings implied that at 50–250°C, the overall heat deficit in the NF based absorber was approximately twice greater than the coated absorber, because the glass tube has greater emissivity than the surface absorber. To improve the volumetric system, they suggested using vacuum installation across the receivers and a low emissive coating on the tubes, which resulted in significantly less convective heat loss. On-sun tests conducted on the two prototypes showed the poorer outcome of the volumetric absorber relative to the surface absorber. At 80°C, the exterior absorber had an efficiency of 68%, while the NF-based absorber gained only 54%. Considering vacuum packaging at 200°C, the outputs are 47 and 26% respectively. The

suggestions are made that NF absorbers need anti-reflective and selective coating to compete with surface absorbers.

6.1. Parabolic trough solar collector (PTSC)

The PTSC is considered as the future of sustainable resource of renewable energy that can be commercially deployed for efficient energy conversion systems. PTSC is one of the concentrating solar system of solar collector technologies comprised of a parabolic shaped mirror reflector and cylindrical absorber surrounded by an anti-reflecting glass layer to prevent heat loss due to convection and radiation (illustrated in **Fig. 21**). Solar irradiations are concentrated on the receiver and subsequently transformed into operating fluid streaming through it and then exchanged to devices involving medium-high temperature applications up to 400℃ [205]. Output of PTSCs is a function of photothermal characteristic of the working fluid employed in the cycle. Being the most innovative and efficient light-to-heat converter medium, oil-based NFs are frequently utilized in concentrating solar collectors like PTSC due to their high temperature applicability [206].

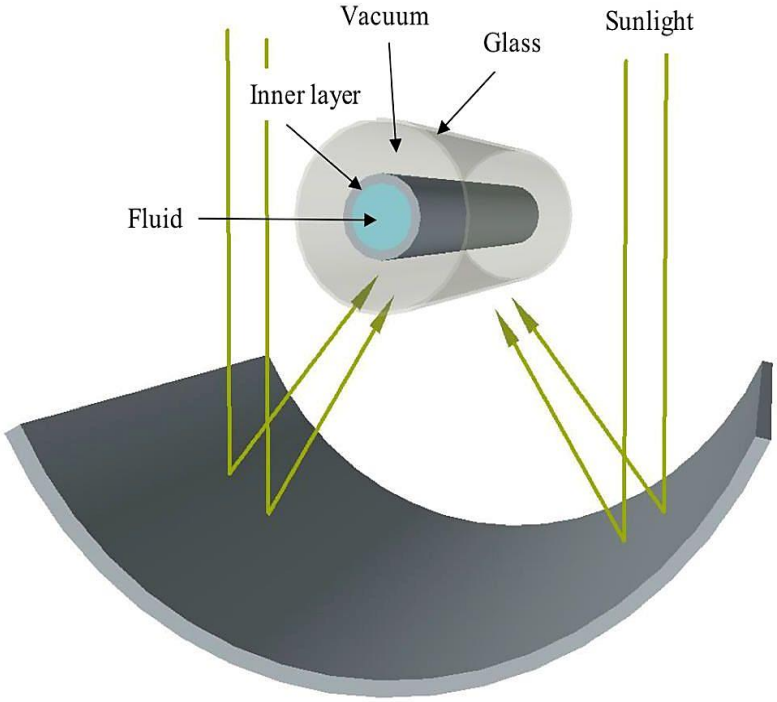

Fig. 21. Schematic illustration of the PTSC [206].

Menbari, et al. [207] experimented with low-temperature direct absorption PTSC deploying water/CuO NF at 0.002-0.008 vol.% and 10-100 L/h flow rate to augment thermal effectiveness and absorption property of the collector. The outcomes expose up to 52% increment in thermal efficiency relative to BF at highest loading of 0.008 vol.% and a flow rate of 100 L/h. Mwesigye and Meyer [208] studied the impact of Therminol®VP-1 oil based NFs, concentration ratios and flow-rates on high temperature PTSC. Along with improved thermodynamic properties, a maximum 13.9% enhancement is obtained operating Therminol®VP-1/Ag NF at optimized conditions of highest NP loading (6 vol.%), 22.5 m^3/h and a concentration ratio of 113. An analogous effect of NF on PTSC is reported for synthetic oil/A_2O_3 NF determined by a 3D coupling model [209]. Kaloudis, et al. [210] performed a numerical study to assess its performance by a two-phase computational model using Syltherm-800/Al_2O_3 NF as operating working fluid. Their obtained results reveal that the LS-2 module of PTSC performed 10% augmentation in overall efficiency operating with 4 vol.% of the particles. Furthermore, multiple parabolic concentrators are used in compound parabolic solar collector (CPSC) for medium high flux applications [211-213]. Some recent experimental and numerical studies on performance enhancement of PTSC utilizing various NFs are reviewed with key findings in **Table. 9**.

6.3. Parabolic dish solar collector (PDSC)

PDSC energy conversion systems are one of the important types of developing concentrating solar collector technology. The dish structured parabolic point-focus concentrator/reflector is located on the support structure based on a two-axis tracking system so that the parabolic dish can adjust its position according to the direction of the radiations from the sun (**Fig. 22**). PDSCs provide concentrated radiation due to greater concentration ratio. Hence, they are suitable for high temperature receivers to produce power such as Brayton engine or electric generator

[214]. In recent years, the use of NF as working fluid in PDSC has exhibited significant improvement in the energy efficiency relative to traditional fluids.

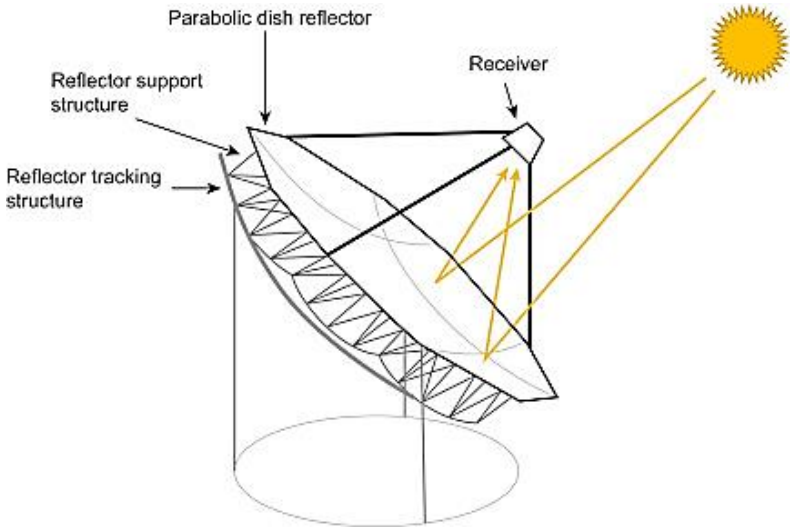

Fig. 22. Schematic illustration of the PDSC system [215].

In an outdoor experiment, Loni, et al. [216] evaluated the impact of thermal oil/MWCNT (0.8 wt.%) NF on a dish concentrator with a cylindrical cavity receiver. Achieved outcomes reveal thermal performance of the receiver augmented by 13.12% replacing pure oil by the NF. They reported similar outcomes with other oil-based NF as well [217], [218], [109], [219] (for details see in **Table. 9**). Pavlovic, et al. [220] studied the effect of four different thermal oil-based NFs on PDSC integrated with a corrugated tube receiver. The NFs had the highest energetic efficiency of 12.29% and 2.51% higher energetic efficiency using dispersion of Cu NPs in the pure oil. However, research on NF-based PDSC systems is somewhat limited, particularly the implementation and impacts of carbon-based NFs as a potential working fluid for further improving the thermal energy performance of these collectors.

6.4. Concentrated photovoltaic/thermal (CPV/T) collector

CPV/T solar collectors are capable of concurrent thermal and electrical energy generation from photovoltaic (PV) module and thermal collector harnessing solar irradiation. Unlike restricted low temperature hybrid PV/T system, CPV/T collector are equipped with a concentrating

reflector. Therefore, the solar concentration ratio is higher and suitable for medium to high temperature applications. The performance of PVT collector depends on the cooling capacity of the working fluid to reduce the temperature of the PV module. Nanofluid cooling of PV unit is one of the potential techniques to eliminate overheating issue in hybrid PV/T systems [221, 222]. **Fig. 23** represents the configuration of a standard hybrid CPV/T solar collector.

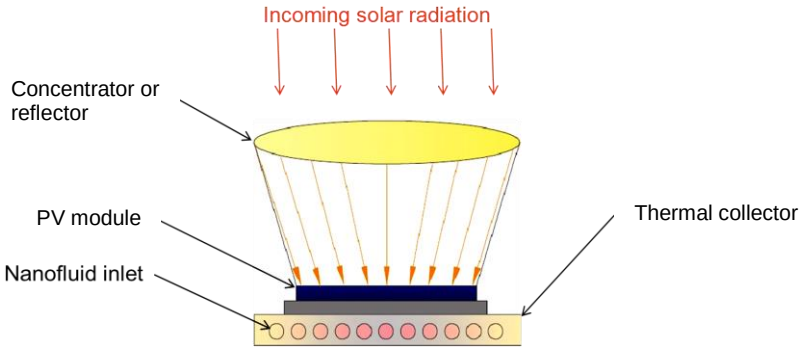

Fig. 23. A typical nanofluid based CPV/T solar collector (modified from [222]).

Rubbi, et al. [32] revealed that deploying SO/MXene NF in a hybrid PV/T caused a 14℃higher temperature drop relative to the water operated system. Acquired results also elucidate optimized performance of the NF based collector as thermal and efficiencies elevated considerably. An, et al. [223] investigated performance enhancement of the CPV/T collector which consists of the Fresnel reflector to concentrate the radiation on the receiver and oleyl-amine/Cu_9S_5 NF is utilized as cooling fluid. The collector reached a maximum operating temperature of more than 100℃. Attained experimental results confirm 17.9% increment in overall efficiency using the NF. Aslfattahi, et al. [69] applied experimentally formulated silicon oil/MXene (0.05-0.1 wt.%) to intensify the performance of CPV/T system at solar concentration of 1-8. Numerical outcomes showed highest thermal and electrical efficiency amplified by 11.95 and 69.24% at 0.1 wt.% and concentration ratio of 8 when PV surface temperature was reduced by 12.45%. Ju, et al. [224] numerically studied thermal, optical, and electrical output of CPV/T system by a new 2D:3D coupling method employing Therminol

VP-1/ITO as operating fluid. Addition of the NPs in caused 62.5% improved absorption of solar irradiation. Hassani, et al. [225] numerically optimized the performance of the cascading CPV/T system for two different configurations. The first proposed design (D-1) consists of sperate channels for optical and thermal NF while the second design (D-2) i.e., double pass configuration allows a common flow. The optical and thermal NFs are developed by dispersing Ag NPs in Therminol VP-1 and water, respectively. The achieved results indicate that NFs absorb 82% of the desired UV and IR spectra. D-1 outstripped the D-2 configuration as it exhibited 8.6% enhanced electrical efficiency in addition to advanced cooling of GaAs and Si based PV modules. Bellos and Tzivanidis [226] assessed parabolic reflector equipped CPV/T analysing effect of various combinations flow rate and temperature using Syltherm-800/CuO NF at 5 vol.%. Maximum 60.07% overall thermal output is noted deploying the NF at 720 L/h flow rate and 16.58% improved exergy efficiency at 125 °C.

6.5. Linear Fresnel Reflector (LFR)

LFR consists of multiple primary optical reflectors integrated with an absorber tube partially enclosed by a secondary reflector as demonstrated in **Fig. 24**. The curved primary concentrators or reflectors can rotate around a pivot to track and capture solar radiations to concentrate on the secondary reflector and receiver tube where soler heat is transformed to a working fluid. LFR functions based on one axis tracing system where only the primary reflector can move. These collectors can operate up to 400°C due to concentrated heat generation and are considered more effective and cheaper than PTSC [227]. Since conversion efficiency of LFR collector significantly depends on the effectiveness of the operating fluid, utilization of improved NFs in LFR energy conversion systems provides substantial augmentation in energy efficiency due to their superior photo-thermal characteristics.

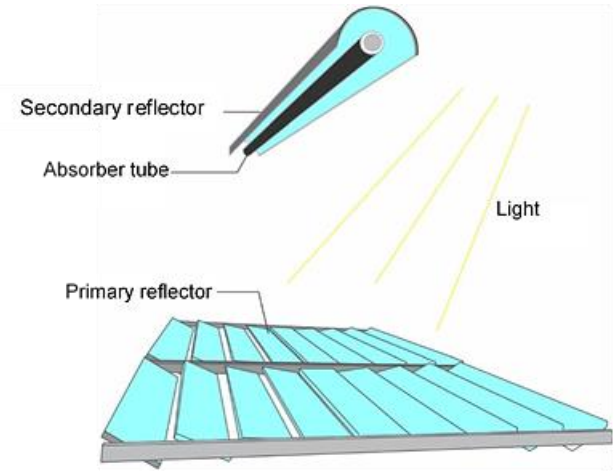

Fig. 24. Diagram of LFR solar collector system [228].

However, execution of NFs on LFRs has not been performed much except for a few numerical endeavours. Huang and Marefati [229] numerically investigated the performance of the LFR collector at a concentration ratio of 28 using thermal oil based CuO and Al_2O_3 NFs and compared to flat-plate collector and PTSC. Achieved results show that the LFR produced better outcomes in terms of energetic, energetic, and entropic aspects. The Bellos and Tzivanidis [230] studied several criteria (entropy, energy, and exergy efficiency) on performance of LFR using Syltherm-800/CuO (6 vol.%) NF. Their flow simulation indicated effective utilization of the NF at higher temperatures as heat transfer coefficient improved up to 35% along with energy and exergy efficiencies of the LFR. Using same NF at 4 vol.% in LFR integrated with internal finned absorber showed produced further increment in performance at 600K temperature [231].

According to the current review on NF based concentrating solar collector technology, it is evident to state that NFs have considerable positive impacts on performance improvement of these collectors. However, the majority of the studies are confined to mathematical modelling or numerical simulation while only a few attempts experimental implementation of the NFs. Furthermore, metal and their oxide-based NFs are frequently practiced in these collectors relative to carbon materials, although recent experimental characterizations revealed superior

optical absorption property and thermal conductivity of carbon-based NFs. Therefore, the authors suggest further experimental research on concentrating solar collectors implementing carbon-based nanomaterials.

Table. 9. Summary of key findings from recent experimental and numerical studies on various oil-based NFs on concentrating thermal solar collectors.

Reference	Nanofluids	Particle size and concentration (φ)	Solar collector	Operating temperature	Flow rate	Key findings
Mwesigye and Meyer [208]	TherminolVP-1/ /Ag /Cu /Al_2O_3	< 100 nm Φ = 0-6 vol.%	PTSC	400-600 K (inlet temp.)	20-40 m^3/h	● Thermal efficiency enhanced using NFs, maximum 13.9% improvement is found with silver/therminalVP-1 NF.
Mwesigye, et al. [232]	TherminolVP-1/ Cu	< 100 nm Φ = 0-6 vol.%	PTSC	350-650 K	1.22-135 m^3/h	● Heat transfer performance of the collector improved with increasing particles loading. ● Thermal efficiency increased up to 12.5% and entropy generation decreased at low Reynold number.
Bellos, et al. [233]	Thermal oil/Al_2O_3	20 nm Φ = 2 vol.%	PTSC	10-350 ºC	0.21 kg/s	● Overall efficiency of the solar collector is improved by 4.25% with addition Al_2O_3 particles. Besides, modified geometry of the collector enhanced the efficiency of the collector by 4.55%.
Bellos and Tzivanidis [234]	Syltherm-800/Cu /CuO /Fe_2O_3 /TiO_2 /Al_2O_3 /SiO_2	-- Φ = 1-6 vol.%	PTSC	300-650 K	50-300 L/min	● Improved efficiency of the collector is attained at higher particle loading, greater inlet temperature and lower flow rate. Cu particles exhibited optimized output than other particles.
Khan, et al. [235]	TherminolVP-1 /TiO_2-MWCNT /TiO_2 /MWCNT	-- Φ = 3 vol.%	PTSC	350-600 K	0.6 kg/s	● Maximum thermal efficiency is increased by 5.27% at higher inlet temperature of 600 K. Heat transfer coefficient improved by 197.09% using the hybrid NF in converging-diverging absorber tube.
Mohammad Zadeh, et al. [236]	Synthetic oil/ Al_2O_3	-- Φ = 0.02 and 0.04 vol.%	PTSC	300-500 K	0.61-0.66 kg/s	● Heat transfer coefficient exhibited linear increment with addition of nanoparticles in the base fluid.
Mwesigye, et al. [237]	TherminolVP-1/ SWCNT	Φ = 0.25-2.5 vol.%	PTSC	400-650 K	0-70 m^3/h	● Heat transport performance augmented 234% whereas only 4.4% improvement is noted in thermal

						efficiency using NF at 2.5 vol.%. Also, entropy generation declined by 70%.
Kaloudis, et al. [210]	Syltherm-800/ Al_2O_3	Φ = 0.5-4 vol.%	PTSC	375-570 K	0.6229-0.6522 kg/s	● Good accuracy is observed using two-phase model. Temperature, convection effect and thermal efficiency enhanced linearly with φ.
Loni, et al. [217]	Thermal oil/ Cu /SiO_2 /TiO_2 /Al_2O_3	n/a Φ = 0-5 vol.%	PDSC	60-362.4 ºC	0.02-0.2 kg/s	● Output temperature increased with particle inclusion being maximum for Oil/Cu and minimum for Oil/ Al_2O_3 NF. ● Thermal efficiency decreased with particle loading as heat capacity of the NFs declined at higher temperature. However, pressure drop decreased.
Khullar, et al. [213]	Therminol VP-1/ Aluminum	5 nm Φ = 0.05 vol.%	CPSC	0-250 ºC	0.342-0.358 L/s	● Thermal efficiency of nanofluid based CPC is about 5–10% higher compared to a conventional parabolic solar collector.
Korres, et al. [211]	Syltherm-800/CuO	-- Φ = 5 vol.%	CPSC	25-300 ºC	0.05 m/s	● Maximum thermal efficiency augmented by 2.76% while pressure drop is intensified by 16%. Also, temperature is found to be increased more than 150 ºC.
Xu, et al. [212]	Synthetic oil/CuO	200 nm Φ = 0.055 wt.%	CPSC	20-180 ºC	0.0475 m/s (velocity inlet)	● CPC performed better solar absorptivity with NF compared to conventional oil as working fluid.
Khan, et al. [238]	Thermal oil/Cu /TiO_2 Al_2O_3	-- Φ = 2 vol.%	PDSC	350-500 K	0.1-0.7 kg/s	● Al_2O_3/thermal oil NF showed maximum 33.73% and 36.27% energy and exergy efficiency, respectively. ● Overall efficiency increased significantly at rising mass flow rate from 0.1 to 0.3 kg/s but it increased insignificantly afterward till 0.7 kg/s.
Loni, et al. [216]	Thermal oil/ MWCNT	10 µm × 10 nm. Φ = 0.8 wt.%	PDSC	33.6-49.1 (inlet) 86.8 to 105.2 (outlet)	10 ml/s	● Average thermal efficiency improved by approximately 8% compared to pure oil alone. Cylindrical cavity receiver with MWCNT/thermal oil NF is proposed due to the advanced thermal productivity.
Loni, et al. [218]	Thermal oil/ SiO_2 /Al_2O_3	20-30 and 30-40 nm, respectively.	PDSC	25-150 ºC	n/a	● Heat loss is decreased using both NFs relative to oil. Thermal performance of the receiver is improved by

		Φ = 0.8 wt.%				3.3 and 0.3% with Oil/ Al_2O_3 and oil/ SiO_2 NF, respectively.
Loni, et al. [109]	Oil/ Alumina /Silica	30-40 and 20-30 nm Φ = 0.8 wt.%	PDSC	25-150 ºC	10 ml/s	● Alumina/oil NF exhibited 6.15% better thermal efficiency of hemispherical cavity receiver relative to base fluid.
Khan, et al. [238]	Thermal oil/Al_2O_3 /CuO /TiO_2	Φ = 2 vol.%	PDSC	280-450 K	0.1-0.7 kg/s	● Thermal oil/Al_2O_3 NF exhibited highest 33.37 and 36.274% energy and exergy efficiency. Raising particle loading in the dispersion increases the heat transfer coefficient of NFs in the receiver.
Luo, et al. [239]	Texatherm/ TiO_2 /Al_2O_3 /Ag /Cu /SiO_2 /Graphite /CNTs	10, 20, 50, 50, 50, 35 nm and 10-30 µm × 10-20 nm respectively Φ =0.01-0.5 vol.%	C-DASC	30-100 K	9.5-47.5 mL/min	● NFs could enhance the outlet temperature and absorption efficiency. Due to the aggregation, size and shape of NPs, the experimental extinction of the incident light was greater than the estimates. Highest 122.7% photo-conversion effectiveness is found for 0.01% graphite NF.
Hordy, et al. [240]	MWCNT/water /EG /PG /Therminol VP-1	4 µm × 30 nm Φ = 5.6-53 mg/L	C-DASC	up to 220 ºC	--	● NFs were stable up to 8 months at higher temperatures. Absorption capacity reached to almost 100% using MWCNT particles due to superior suspension stability.
Wang, et al. [241]	Silicon oil/ZnO-Au	13.3 nm and 0.75 µm × 0.08 µm respectively Φ = 0.1-1 mg/ml	C-DASC	up to 125 ºC	--	● The NF at 1.0 mg/ml displayed outstanding stability and good optical absorption properties and reached to 125°C within 1 h of heating at a solar power of 10 kW/m^2. Relative to base oil, an efficiency boost of 240% was attained by NF.
Taylor, et al. [242]	Therminol VP-1/ Graphite /Aluminum /Cu /Ag	20 nm Φ = 0.001 vol.%	C-DASC	0-300 ºC	10^{-4} kg/s	● Maximum efficiency increased up to 10% by using graphite/Therminol VP-1 nanofluid in the receiver. ● Economic evaluation indicates that a nanofluid-based 100 MWe thermal plant operating in Tucson, AZ could add $3.5 million to the revenue per year for large-scale plants under favourable conditions.

Bellos and Tzivanidis [230]	Syltherm-800/CuO	Φ = 6 vol.%	LFR	350-650 K	200 L/min	● Thermal output and Nusselt number augmented by 0.78 and 5% respectively. NF is found to be more effective at elevated temperature.
Huang and Marefati [229]	Thermal oil B /CuO /Al_2O_3	Φ = 5 vol.%	LFR	298-346 K	0.025 kg/s	● Energy and exergy efficiencies are intensified by 1.75, 1.46 and 1.27, 0.93% for CuO and Al_2O_3 NF, respectively.
Rubbi, et al. [32]	Soybean oil/ MXene	1–10 µm × 1 nm Φ = 0.025-0.125 wt.%	PV/T	25-80 ºC	0.01-0.07 kg/s	● 15.51 and 15.41% intensified thermal and electrical efficiency is obtained using the NFs relative to water-alumina NF. PV panel temperature dropped by 14 ºC relative to conventional water-cooling system.
Samylingam, et al. [65]	Soybean oil/ MXene	1–10 µm × 1 nm Φ = 0.025-0.125 wt.%	PV/T	25-80 ºC	0.01-0.07 kg/s	● 15.83% thermal output is attained using the NF instead of water. PV surface temperature reduced approximately 10℃ at 0.2 wt.% and 0.07 kg/s.
Aslfattahi, et al. [69]	Silicon oil/ MXene	1–10 µm × 1 nm Φ = 0.05-0.1 wt.%	CPV/T	30-200 ºC	0.005 kg/s	● Average temperature reduced by 12.45% for the PV unit alongside 11.92% improved energy gain by the CPV/T using NF at 0.1wt.%.
Hassani, et al. [225]	Therminol VP-1/ Ag	Φ = 0.001-1.5 vol.%	CPV/T	324.8-402.7 ºC	0.08 kg/s	● Overall efficiency increased using the NF. Raising the φ of coolant NF, highest increment is noted 5.8 and 4.6% for GaAs and Si based module, respectively.
Srivastava and Reddy [243]	Al_2O_3/Therminol VP-1, Syltherm-800, Therminol 59	Φ = 1-6 vol.%	CPV/T	315-484.2 K	0.1 m/s (velocity)	● Optimum thermal output is attained employing Syltherm-800/ Al_2O_3 NF while electrical output deteriorated by 9.8%.
Bellos and Tzivanidis [226]	Syltherm-800/CuO	Φ = 5 vol.%	CPV/T	25-200 ºC	300-720 L/h	● At 100 ℃ and 560 L/h, thermal, electrical, exergy and overall efficiency increments are 1.66, 5.17, 3.05 and 2.08% respectively.

7. Challenges with nanofluids application

NFs are the most recent promising technologies that are evolving at an unprecedented rate in order to establish their place in impending practical applications. Nevertheless, researchers and engineers have discovered some crucial issues with NF over the last decade concerning its effective application in real fields of solar thermal engineering. Various sophisticated challenges declared in numerous studies of NF properties and implementation in SCs are rendered in the subsequent discussions (also depicted in **Fig. 25**).

- Inadequate stability of NF degrades major properties described in (**Section 3**) is a fundamental shortcoming as stability dictates essential feasibility of NFs in any sensible system. Most of the techniques available to stabilize NF suspensions up to this point have proven to fall short of providing industrial standard nano-scale suspension. Some techniques, including surfactant or chemical stabilizers addition and pH modulation are reported to have positive impacts on stability within certain conditions. Yet, consequences (i.e., thermal, and optical properties degradation, foam formation, corrosion, and fouling factors) of these methods are responsible for overall deficiency of the systems at critical conditions like high temperature and particle loading. Conventional NP synthesis and NF formulation should be improved to produce more stable suspension. Furthermore, there are no standard indicator for reporting stability that can indisputably interpret suspension stability characteristics in terms of time (days or months). Hence, rigorous observation approach is essential to report accurate assessment. Zeta potential is often suggested as an indication of NF stability in literature; however, it is not appropriate since high ζ value does not necessary imply high stability. Rather, it indicates electrostatic repulsion potential between NPs whereas, in the case of steric stabilization technique, ζ can be low and entirely stable at the same time [244]. Therefore, reporting of stability is still in an ambiguous state and

needs to be construed with generic standard so that comparisons can be obtained among a wide range of NFs.

- Dispersion of nanoscale particles results in considerable increment in density and viscosity (μ) of the BF which in turn escalates the pressure drop in the NF operated dynamic systems like solar collectors. The drop expands further at greater particle loading and mass flow rate inevitably. Since the pumping power of a dynamic system is explicitly connected with pressure drop and flow rate, the increase in pressure drop implies a corresponding requirement for more pumping power [245].
- Surfactants or chemical stabilizing additives are deployed to ameliorate the stability of NFs. However, stabilizers often have penalties in terms of thermo-optical properties and performance. Although most of the studies concur on positive impact on stabilization, notable limitations (i.e., ineffectiveness at high temperature and non-Newtonian flow property) and conflicts among reported studies due to diverse classification of the surfactants make it difficult to pick the ideal stabilizer for a particular NF. In addition, employing NFs absorption characteristics of solar NFs revealed noteworthy variation in performance of non-concentrating SCs [200, 246].
- Theoretical unpredictability of experimental data reflected in literature regarding interactions among thermophysical properties (particularly, TC and c_p) and affecting constraints is another crucial challenge to conquer. Numerical based models and correlations developed for an individual combination of BF and NP i.e., NF under specific conditions could not provide accurate estimation of data for other NFs due to interactions of the extensive number of independent variables. Therefore, advanced ANN and machine learning models must be established integrating multifarious variables with NF properties utilizing accumulated practical data to reinforce the prediction.

- Several NFs exhibited perceptible corrosivity operating as working fluid in various thermal devices which can lead to significant damage to the entire system. Chemical interactions, pH value variation and mechanical stabilization of the fluids are the culpable factors that cause surface degradation [247]. Additional maintenance is required to prevent this sort of inconvenience.
- NFs consisting of nanoscale particles may cause toxic environmental and biological effects. Due to tiny size of NPs, it is plausible that the particles can get into human skin and cause respiratory, inflammation and carcinogenic infections [248]. In future studies on NF, scientists and engineers ought to consider green synthesis techniques to develop NFs that are non-toxic, ecologically beneficial, and safe for industrial usage. Besides, the potential challenge of high production cost hinders application of NF on energy conversion systems, including but not restricted to concentrating SCs.

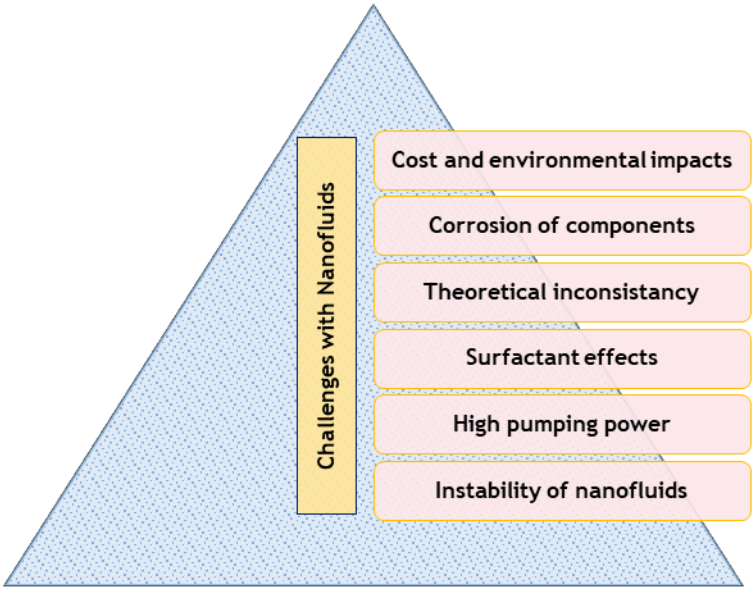

Fig. 25. Identified challenges with nanofluids.

8. Conclusions and recommendations

This review of causes, effects, thermo-physical characteristics, stability phenomena and developments of NFs on solar thermal systems is compiled with extensive experimental and

numerical investigations for better understanding for developing optimized NFs and their application on SCs. This review is particularly focused on usefully used oil-based and hybrid NFs and their implementation on concentrating solar collector technology. Some of the crucial areas are studied and reviewed, including thermo-physical properties, stability and stability mechanisms and application on medium-high temperature concentrating solar collector devices. Nevertheless, research needs to progress further in the right direction for more advancement in the field of NF and its utilization on thermal solar collector devices. In this regard, authors have drawn few crucial conclusions and recommendations on existing research gap and future research directions in this area. Based on the research investigations reviewed in this study, subsequent conclusions and recommendations are drawn:

On synthesis and formulation of NF:

- NF prepared in the single step method is found to be more stable while the two-step technique manufactures NF with more efficient thermal properties. Since both conventional methods have limitations to concurrently formulate stable and thermally optimized NF, a systematic approach should be selected considering key parameters (i.e., type of nanomaterials and BF) and operating conditions (described in **Section 2**). Further research is required to develop a sustainable, cost effective and large-scalable NF production process. Carrillo-Berdugo, et al. [249] recently revealed a novel interface based three step techniques to formulate stable NF that own optimized thermo-optical properties.

On thermophysical characteristics of NF:

- Effective TC of oil-based NFs amplifies prominently dispersing carbon contained nanomaterials rather than traditional metal and metal-oxides. Nevertheless, numerous works reveal chaotic conflicts with respect to few sophisticated factors (mentioned in **Section 3**) emerged from the diverse operating conditions. Therefore, a comprehensive

systematic approach should be performed considering the wide-ranging finite variable operating conditions to establish fundamental relationship with TC of diverse NFs.

- While TC intensifies dispersing nanomaterial in BF, c_p drops for most of the NFs due to lower heat capacity of solid particles relative to liquids. Nevertheless, opposite trends are reported in few studies using carbon-based particles. Since higher c_p value has remarkable impact on renewable energy sector particularly energy storage and SC devices. Comprehensive experiments are required to come up with detailed understanding of c_p enhancement of NFs.
- The dynamic viscosity (μ) of NF enhances with the inclusion of nanoscale materials and oil-based NFs are relatively viscous compared to other NFs at low temperatures, while μ declines considerably at higher temperatures. Moreover, Newtonian, and non-Newtonian property is dominant at low to high φ respectively. NFs with high μ BF (i.e., oil) and carbon nanotubes are often exhibit Newtonian up to an optimum loading of nanomaterials.
- Existing theoretical and empirical models derived for a specific NF are inaccurate to estimate heat transfer behavior (Nusselt number, pressure drop and performance factor), thermal conductivity, μ, and c_p of other water NFs when compared to experimental data. This could be due to considering only few influential parameters limited working conditions. Rigorous analytical studies are inferred to develop accurate models analyzing potential factors to precisely estimate these essential properties.

On suspension stability of NF:

- Stability dictates the overall performance of NF and the entire thermal system it is operating, i.e., better stability provides improved efficiency of the systems. Generally, most of the formulated oil-based NFs reported in the studies exhibit short-term stability due to agglomeration of dispersed particles caused by various factors. Instability of NFs

is identified as a function of multifarious variables, for instance formulation techniques, BF, NPs (φ, size and shape), temperature, and stabilization methods (physical and chemical). However, NFs containing very low φ of carbon nanomaterials in water and oil medium offer prominent suspension stability and effective performance boost deployed in SC based energy conversion applications. Further investigations should emphasis on rigorous tracking of stability for longer periods employing techniques associated with stabilizers and functionalization to provide explicit reports about the impacts of stabilizing additives.

- Comparisons among several stabilization strategies of NF (e.g., ionic, and non-ionic stabilizers, surface adjustment and functionalization) should be rendered by analyzing relevant destabilization factors. Deployment of advanced particle functionalization using irreversible polymers grafting during the synthesis of NP may evade limitations and provide robust protection against the undermining factors. Furthermore, there are no explicit analytical correlations integrating stability, operating conditions and properties of NFs which can be addressed in future studies.

On implementation and performance evaluation of NF on concentrating solar collector systems:

- Selection of stable NF (i.e., BF and NP) is a critical precondition to implement them on solar energy conversion operation. Performance of several concentrating and concentrating SCs exhibits noteworthy augmentation while operating with NFs replacing conventional HTFs. Desired properties for SC application of NF include high heat transport and energy storage capacity (i.e., TC and c_p) alongside low viscosity and Newtonian flow behavior which are observed to have a prominent impact on the performance.

- Oil based NFs consist of carbon materials are more effective relative to metal and metal oxide-based NFs. However, there is shortage of experimental execution of the carbon-based NFs which can be addressed in future research in this field. Besides, most of the numerical studies on NF-based concentrating SCs are performed using single phase models even though multi-phase models are more accurate for NFs. Therefore, more studies using multi-phase model are expected in upcoming research on the topic.
- Inadequate studies are performed estimating production cost, surface deterioration, safety, and ecological aspects of NFs. Such instructive statistics would provide essential assistance to determine prospective execution of the NFs in industrial sectors.

Acknowledgement

We appreciate financial support from Yayasan Universiti Teknologi Petronas (research grant no. 015LC0-118). Fazlay Rubbi wishes to dedicate his efforts to this endeavor to his adoring parents (Rahima Khatun and Md. Altaf Hossain).

References

[1] H. Masuda, A. Ebata, K. Teramae, and N. Hishinuma, "Alteration of thermal conductivity and viscosity of liquid by dispersing ultra-fine particles. dispersion of Al2O3, SiO2 and TiO2 ultra-fine particles," *Netsu Bussei,* vol. 7, no. 4, pp. 227-233, 1993.

[2] S. U. S. Choi and J. A. Eastman, "Enhancing thermal conductivity of fluids with nanoparticles," United States, 1995, Research Org.: Argonne National Lab., IL (United States), Sponsor Org.: USDOE, Washington, DC (United States).

[3] S. Kakaç and A. Pramuanjaroenkij, "Review of convective heat transfer enhancement with nanofluids," *International Journal of Heat and Mass Transfer,* vol. 52, no. 13, pp. 3187-3196, 2009/06/01/ 2009.

[4] L. Qiu *et al.*, "A review of recent advances in thermophysical properties at the nanoscale: From solid state to colloids," *Physics Reports,* vol. 843, pp. 1-81, 2020/02/13/ 2020.

[5] B. Wang, X. Wang, W. Lou, and J. Hao, "Thermal conductivity and rheological properties of graphite/oil nanofluids," *Colloids and Surfaces A: Physicochemical and Engineering Aspects,* vol. 414, pp. 125-131, 2012/11/20/ 2012.

[6] M. E. Nakhchi and J. A. Esfahani, "Cu-water nanofluid flow and heat transfer in a heat exchanger tube equipped with cross-cut twisted tape," *Powder Technology,* vol. 339, pp. 985-994, 2018/11/01/ 2018.

[7] S. Chakraborty, I. Sarkar, A. Ashok, I. Sengupta, S. K. Pal, and S. Chakraborty, "Synthesis of Cu-Al LDH nanofluid and its application in spray cooling heat transfer of a hot steel plate," *Powder Technology*, vol. 335, pp. 285-300, 2018/07/15/ 2018.
[8] S. Chakraborty and P. K. Panigrahi, "Stability of nanofluid: A review," *Applied Thermal Engineering*, vol. 174, p. 115259, 2020/06/25/ 2020.
[9] N. A. Che Sidik, M. Mahmud Jamil, W. M. A. Aziz Japar, and I. Muhammad Adamu, "A review on preparation methods, stability and applications of hybrid nanofluids," *Renewable and Sustainable Energy Reviews*, vol. 80, pp. 1112-1122, 2017/12/01/ 2017.
[10] Y. Xu, S. Qian, Q. Liu, and Z. D. Wang, "Oxidation stability assessment of a vegetable transformer oil under thermal aging," *IEEE Transactions on Dielectrics and Electrical Insulation*, vol. 21, no. 2, pp. 683-692, 2014.
[11] R. A. Rasih, N. A. C. Sidik, and S. Samion, "Recent progress on concentrating direct absorption solar collector using nanofluids," *Journal of Thermal Analysis and Calorimetry*, vol. 137, no. 3, pp. 903-922, 2019/08/01 2019.
[12] A. H. Elsheikh, S. W. Sharshir, M. E. Mostafa, F. A. Essa, and M. K. Ahmed Ali, "Applications of nanofluids in solar energy: A review of recent advances," *Renewable and Sustainable Energy Reviews*, vol. 82, pp. 3483-3502, 2018/02/01/ 2018.
[13] T. R. Shah and H. M. Ali, "Applications of hybrid nanofluids in solar energy, practical limitations and challenges: A critical review," *Solar Energy*, vol. 183, pp. 173-203, 2019/05/01/ 2019.
[14] L. Das, K. Habib, R. Saidur, N. Aslfattahi, S. M. Yahya, and F. Rubbi, "Improved Thermophysical Properties and Energy Efficiency of Aqueous Ionic Liquid/MXene Nanofluid in a Hybrid PV/T Solar System," *Nanomaterials*, vol. 10, no. 7, 2020.
[15] N. Goel, R. A. Taylor, and T. Otanicar, "A review of nanofluid-based direct absorption solar collectors: Design considerations and experiments with hybrid PV/Thermal and direct steam generation collectors," *Renewable Energy*, vol. 145, pp. 903-913, 2020/01/01/ 2020.
[16] E. Bellos, Z. Said, and C. Tzivanidis, "The use of nanofluids in solar concentrating technologies: A comprehensive review," *Journal of Cleaner Production*, vol. 196, pp. 84-99, 2018/09/20/ 2018.
[17] S. H. A. Ahmad, R. Saidur, I. M. Mahbubul, and F. A. Al-Sulaiman, "Optical properties of various nanofluids used in solar collector: A review," *Renewable and Sustainable Energy Reviews*, vol. 73, pp. 1014-1030, 2017/06/01/ 2017.
[18] T. B. Gorji and A. A. Ranjbar, "A review on optical properties and application of nanofluids in direct absorption solar collectors (DASCs)," *Renewable and Sustainable Energy Reviews*, vol. 72, pp. 10-32, 2017/05/01/ 2017.
[19] F. Yu *et al.*, "Dispersion stability of thermal nanofluids," *Progress in Natural Science: Materials International*, vol. 27, no. 5, pp. 531-542, 2017/10/01/ 2017.
[20] J. A. Ranga Babu, K. K. Kumar, and S. Srinivasa Rao, "State-of-art review on hybrid nanofluids," *Renewable and Sustainable Energy Reviews*, vol. 77, pp. 551-565, 2017/09/01/ 2017.
[21] L. Das *et al.*, "State-of-the-art ionic liquid & ionanofluids incorporated with advanced nanomaterials for solar energy applications," *Journal of Molecular Liquids*, vol. 336, p. 116563, 2021/08/15/ 2021.
[22] M. Mohammadpoor, S. Sabbaghi, M. M. Zerafat, and Z. Manafi, "Investigating heat transfer properties of copper nanofluid in ethylene glycol synthesized through single and two-step routes," *International Journal of Refrigeration*, vol. 99, pp. 243-250, 2019/03/01/ 2019.

[23] Y. Zhang, Y. Chen, P. Westerhoff, K. Hristovski, and J. C. Crittenden, "Stability of commercial metal oxide nanoparticles in water," *Water Research*, vol. 42, no. 8, pp. 2204-2212, 2008/04/01/ 2008.
[24] T.-P. Teng, C.-M. Cheng, and F.-Y. Pai, "Preparation and characterization of carbon nanofluid by a plasma arc nanoparticles synthesis system," *Nanoscale Research Letters*, vol. 6, no. 1, p. 293, 2011/04/05 2011.
[25] Y. Hwang *et al.*, "Production and dispersion stability of nanoparticles in nanofluids," *Powder Technology*, vol. 186, no. 2, pp. 145-153, 2008/08/11/ 2008.
[26] H. J. Kim, I. C. Bang, and J. Onoe, "Characteristic stability of bare Au-water nanofluids fabricated by pulsed laser ablation in liquids," *Optics and Lasers in Engineering*, vol. 47, no. 5, pp. 532-538, 2009/05/01/ 2009.
[27] S. Aberoumand and A. Jafarimoghaddam, "Experimental study on synthesis, stability, thermal conductivity and viscosity of Cu–engine oil nanofluid," *Journal of the Taiwan Institute of Chemical Engineers*, vol. 71, pp. 315-322, 2017/02/01/ 2017.
[28] S. Aberoumand, A. Jafarimoghaddam, M. Moravej, H. Aberoumand, and K. Javaherdeh, "Experimental study on the rheological behavior of silver-heat transfer oil nanofluid and suggesting two empirical based correlations for thermal conductivity and viscosity of oil based nanofluids," *Applied Thermal Engineering*, vol. 101, pp. 362-372, 2016/05/25/ 2016.
[29] Y. Chen *et al.*, "Stably dispersed high-temperature Fe3O4/silicone-oil nanofluids for direct solar thermal energy harvesting," *Journal of Materials Chemistry A*, 10.1039/C6TA07773K vol. 4, no. 44, pp. 17503-17511, 2016.
[30] M. Seyedzavvar, H. Abbasi, M. Kiyasatfar, and R. N. Ilkhchi, "Investigation on tribological performance of CuO vegetable-oil based nanofluids for grinding operations," *Advances in Manufacturing*, vol. 8, no. 3, pp. 344-360, 2020/09/01 2020.
[31] A. Hameed *et al.*, "Experimental investigation on synthesis, characterization, stability, thermo-physical properties and rheological behavior of MWCNTs-kapok seed oil based nanofluid," *Journal of Molecular Liquids*, vol. 277, pp. 812-824, 2019/03/01/ 2019.
[32] F. Rubbi, K. Habib, R. Saidur, N. Aslfattahi, S. M. Yahya, and L. Das, "Performance optimization of a hybrid PV/T solar system using Soybean oil/MXene nanofluids as A new class of heat transfer fluids," *Solar Energy*, vol. 208, pp. 124-138, 2020/09/15/ 2020.
[33] J. Qu, R. Zhang, L. Shang, and Z. Wang, "Graphene oxide/multi-walled carbon nanotube—Therminol®66 hybrid nanofluids for low-to-medium temperature volumetric solar collectors," *International Journal of Energy Research*, https://doi.org/10.1002/er.5420 vol. 44, no. 9, pp. 7216-7228, 2020/07/01 2020.
[34] O. Gulzar, A. Qayoum, and R. Gupta, "Experimental study on thermal conductivity of mono and hybrid Al2O3–TiO2 nanofluids for concentrating solar collectors," *International Journal of Energy Research*, https://doi.org/10.1002/er.6105 vol. n/a, no. n/a, 2020/10/20 2020.
[35] S. Aberoumand and A. Jafarimoghaddam, "Tungsten (III) oxide (WO3) – Silver/transformer oil hybrid nanofluid: Preparation, stability, thermal conductivity and dielectric strength," *Alexandria Engineering Journal*, vol. 57, no. 1, pp. 169-174, 2018/03/01/ 2018.
[36] M. Gupta, V. Singh, R. Kumar, and Z. Said, "A review on thermophysical properties of nanofluids and heat transfer applications," *Renewable and Sustainable Energy Reviews*, vol. 74, pp. 638-670, 2017/07/01/ 2017.
[37] A. Asadi *et al.*, "Recent advances in preparation methods and thermophysical properties of oil-based nanofluids: A state-of-the-art review," *Powder Technology*, vol. 352, pp. 209-226, 2019/06/15/ 2019.

[38] R. V. Pinto and F. A. S. Fiorelli, "Review of the mechanisms responsible for heat transfer enhancement using nanofluids," *Applied Thermal Engineering,* vol. 108, pp. 720-739, 2016/09/05/ 2016.
[39] M. M. Tawfik, "Experimental studies of nanofluid thermal conductivity enhancement and applications: A review," *Renewable and Sustainable Energy Reviews,* vol. 75, pp. 1239-1253, 2017/08/01/ 2017.
[40] M. Chandrasekar and S. Suresh, "A Review on the Mechanisms of Heat Transport in Nanofluids," *Heat Transfer Engineering,* vol. 30, no. 14, pp. 1136-1150, 2009/12/01 2009.
[41] M. U. Sajid and H. M. Ali, "Recent advances in application of nanofluids in heat transfer devices: A critical review," *Renewable and Sustainable Energy Reviews,* vol. 103, pp. 556-592, 2019/04/01/ 2019.
[42] S. M. S. Murshed and C. A. Nieto de Castro, "Superior thermal features of carbon nanotubes-based nanofluids – A review," *Renewable and Sustainable Energy Reviews,* vol. 37, pp. 155-167, 2014/09/01/ 2014.
[43] M. Afrand, D. Toghraie, and N. Sina, "Experimental study on thermal conductivity of water-based Fe3O4 nanofluid: Development of a new correlation and modeled by artificial neural network," *International Communications in Heat and Mass Transfer,* vol. 75, pp. 262-269, 2016/07/01/ 2016.
[44] T. Ambreen and M.-H. Kim, "Influence of particle size on the effective thermal conductivity of nanofluids: A critical review," *Applied Energy,* vol. 264, p. 114684, 2020/04/15/ 2020.
[45] A. Asadi, M. Asadi, A. Rezaniakolaei, L. A. Rosendahl, M. Afrand, and S. Wongwises, "Heat transfer efficiency of Al2O3-MWCNT/thermal oil hybrid nanofluid as a cooling fluid in thermal and energy management applications: An experimental and theoretical investigation," *International Journal of Heat and Mass Transfer,* vol. 117, pp. 474-486, 2018/02/01/ 2018.
[46] L. Yang, W. Ji, J.-n. Huang, and G. Xu, "An updated review on the influential parameters on thermal conductivity of nano-fluids," *Journal of Molecular Liquids,* vol. 296, p. 111780, 2019/12/15/ 2019.
[47] E. V. Timofeeva, M. R. Moravek, and D. Singh, "Improving the heat transfer efficiency of synthetic oil with silica nanoparticles," *Journal of Colloid and Interface Science,* vol. 364, no. 1, pp. 71-79, 2011/12/01/ 2011.
[48] A. K. Tiwari, N. S. Pandya, Z. Said, S. H. Chhatbar, Y. A. Al-Turki, and A. R. Patel, "3S (sonication, surfactant, stability) impact on the viscosity of hybrid nanofluid with different base fluids: An experimental study," *Journal of Molecular Liquids,* p. 115455, 2021/01/23/ 2021.
[49] G. Colangelo, E. Favale, P. Miglietta, M. Milanese, and A. de Risi, "Thermal conductivity, viscosity and stability of Al2O3-diathermic oil nanofluids for solar energy systems," *Energy,* vol. 95, pp. 124-136, 2016/01/15/ 2016.
[50] S. H. Qing, W. Rashmi, M. Khalid, T. C. S. M. Gupta, M. Nabipoor, and M. T. Hajibeigy, "Thermal conductivity and electrical properties of hybrid SiO2-graphene naphthenic mineral oil nanofluid as potential transformer oil," *Materials Research Express,* vol. 4, no. 1, p. 015504, 2017/01/24 2017.
[51] F. Garoosi, "Presenting two new empirical models for calculating the effective dynamic viscosity and thermal conductivity of nanofluids," *Powder Technology,* vol. 366, pp. 788-820, 2020/04/15/ 2020.
[52] W. Cui, Z. Shen, J. Yang, S. Wu, and M. Bai, "Influence of nanoparticle properties on the thermal conductivity of nanofluids by molecular dynamics simulation," *RSC Advances,* 10.1039/C4RA07736A vol. 4, no. 98, pp. 55580-55589, 2014.

[53] A. Zendehboudi, R. Saidur, I. M. Mahbubul, and S. H. Hosseini, "Data-driven methods for estimating the effective thermal conductivity of nanofluids: A comprehensive review," *International Journal of Heat and Mass Transfer,* vol. 131, pp. 1211-1231, 2019/03/01/ 2019.

[54] M. Fakoor Pakdaman, M. A. Akhavan-Behabadi, and P. Razi, "An experimental investigation on thermo-physical properties and overall performance of MWCNT/heat transfer oil nanofluid flow inside vertical helically coiled tubes," *Experimental Thermal and Fluid Science,* vol. 40, pp. 103-111, 2012/07/01/ 2012.

[55] S. U. S. Choi, Z. G. Zhang, W. Yu, F. E. Lockwood, and E. A. Grulke, "Anomalous thermal conductivity enhancement in nanotube suspensions," *Applied Physics Letters,* vol. 79, no. 14, pp. 2252-2254, 2001/10/01 2001.

[56] A. Asadi, M. Asadi, A. Rezaniakolaei, L. A. Rosendahl, and S. Wongwises, "An experimental and theoretical investigation on heat transfer capability of Mg (OH)2/MWCNT-engine oil hybrid nano-lubricant adopted as a coolant and lubricant fluid," *Applied Thermal Engineering,* vol. 129, pp. 577-586, 2018/01/25/ 2018.

[57] M. S. Kumar, V. Vasu, and A. V. Gopal, "Thermal conductivity and rheological studies for Cu–Zn hybrid nanofluids with various basefluids," *Journal of the Taiwan Institute of Chemical Engineers,* vol. 66, pp. 321-327, 2016/09/01/ 2016.

[58] Y. H. Chai, S. Yusup, V. S. Chok, S. Irawan, and J. S. D. B. Singh, "Thermophysical properties of graphene nanosheets – Hydrogenated oil based nanofluid for drilling fluid improvements," *Applied Thermal Engineering,* vol. 122, pp. 794-805, 2017/07/25/ 2017.

[59] M. Saeedinia, M. A. Akhavan-Behabadi, and P. Razi, "Thermal and rheological characteristics of CuO–Base oil nanofluid flow inside a circular tube," *International Communications in Heat and Mass Transfer,* vol. 39, no. 1, pp. 152-159, 2012/01/01/ 2012.

[60] J. J. Taha-Tijerina, T. N. Narayanan, C. S. Tiwary, K. Lozano, M. Chipara, and P. M. Ajayan, "Nanodiamond-Based Thermal Fluids," *ACS Applied Materials & Interfaces,* vol. 6, no. 7, pp. 4778-4785, 2014/04/09 2014.

[61] M. Farbod, R. Kouhpeymani asl, and A. R. Noghreh abadi, "Morphology dependence of thermal and rheological properties of oil-based nanofluids of CuO nanostructures," *Colloids and Surfaces A: Physicochemical and Engineering Aspects,* vol. 474, pp. 71-75, 2015/06/05/ 2015.

[62] A. Asadi and F. Pourfattah, "Heat transfer performance of two oil-based nanofluids containing ZnO and MgO nanoparticles; a comparative experimental investigation," *Powder Technology,* vol. 343, pp. 296-308, 2019/02/01/ 2019.

[63] S. U. Ilyas, R. Pendyala, M. Narahari, and L. Susin, "Stability, rheology and thermal analysis of functionalized alumina- thermal oil-based nanofluids for advanced cooling systems," *Energy Conversion and Management,* vol. 142, pp. 215-229, 2017/06/15/ 2017.

[64] A. Ghaffarkhah *et al.,* "On evaluation of thermophysical properties of transformer oil-based nanofluids: A comprehensive modeling and experimental study," *Journal of Molecular Liquids,* vol. 300, p. 112249, 2020/02/15/ 2020.

[65] L. Samylingam *et al.,* "Thermal and energy performance improvement of hybrid PV/T system by using olein palm oil with MXene as a new class of heat transfer fluid," *Solar Energy Materials and Solar Cells,* vol. 218, p. 110754, 2020/12/01/ 2020.

[66] X. Li, C. Zou, L. Zhou, and A. Qi, "Experimental study on the thermo-physical properties of diathermic oil based SiC nanofluids for high temperature applications," *International Journal of Heat and Mass Transfer,* vol. 97, pp. 631-637, 2016/06/01/ 2016.

[67] S. U. Ilyas, R. Pendyala, and M. Narahari, "Stability and thermal analysis of MWCNT-thermal oil-based nanofluids," *Colloids and Surfaces A: Physicochemical and Engineering Aspects*, vol. 527, pp. 11-22, 2017/08/20/ 2017.

[68] E.-o.-l. Ettefaghi, H. Ahmadi, A. Rashidi, A. Nouralishahi, and S. S. Mohtasebi, "Preparation and thermal properties of oil-based nanofluid from multi-walled carbon nanotubes and engine oil as nano-lubricant," *International Communications in Heat and Mass Transfer*, vol. 46, pp. 142-147, 2013/08/01/ 2013.

[69] N. Aslfattahi, L. Samylingam, A. S. Abdelrazik, A. Arifutzzaman, and R. Saidur, "MXene based new class of silicone oil nanofluids for the performance improvement of concentrated photovoltaic thermal collector," *Solar Energy Materials and Solar Cells*, vol. 211, p. 110526, 2020/07/01/ 2020.

[70] A. Naddaf and S. Zeinali Heris, "Experimental study on thermal conductivity and electrical conductivity of diesel oil-based nanofluids of graphene nanoplatelets and carbon nanotubes," *International Communications in Heat and Mass Transfer*, vol. 95, pp. 116-122, 2018/07/01/ 2018.

[71] A. Mukhtar *et al.*, "Experimental and comparative theoretical study of thermal conductivity of MWCNTs-kapok seed oil-based nanofluid," *International Communications in Heat and Mass Transfer*, vol. 110, p. 104402, 2020/01/01/ 2020.

[72] B. Wei, C. Zou, X. Yuan, and X. Li, "Thermo-physical property evaluation of diathermic oil based hybrid nanofluids for heat transfer applications," *International Journal of Heat and Mass Transfer*, vol. 107, pp. 281-287, 2017/04/01/ 2017.

[73] A. Beheshti, M. Shanbedi, and S. Z. Heris, "Heat transfer and rheological properties of transformer oil-oxidized MWCNT nanofluid," *Journal of Thermal Analysis and Calorimetry*, vol. 118, no. 3, pp. 1451-1460, 2014/12/01 2014.

[74] S. U. Ilyas, M. Narahari, J. T. Y. Theng, and R. Pendyala, "Experimental evaluation of dispersion behavior, rheology and thermal analysis of functionalized zinc oxide-paraffin oil nanofluids," *Journal of Molecular Liquids*, vol. 294, p. 111613, 2019/11/15/ 2019.

[75] W. Li, C. Zou, and X. Li, "Thermo-physical properties of waste cooking oil-based nanofluids," *Applied Thermal Engineering*, vol. 112, pp. 784-792, 2017/02/05/ 2017.

[76] A. Amiri, S. N. Kazi, M. Shanbedi, M. N. Mohd Zubir, H. Yarmand, and B. T. Chew, "Transformer oil based multi-walled carbon nanotube–hexylamine coolant with optimized electrical, thermal and rheological enhancements," *RSC Advances*, 10.1039/C5RA17687E vol. 5, no. 130, pp. 107222-107236, 2015.

[77] A. Asadi, "A guideline towards easing the decision-making process in selecting an effective nanofluid as a heat transfer fluid," *Energy Conversion and Management*, vol. 175, pp. 1-10, 2018/11/01/ 2018.

[78] F. Soltani, D. Toghraie, and A. Karimipour, "Experimental measurements of thermal conductivity of engine oil-based hybrid and mono nanofluids with tungsten oxide (WO3) and MWCNTs inclusions," *Powder Technology*, vol. 371, pp. 37-44, 2020/06/30/ 2020.

[79] W. U. Rehman *et al.*, "Synthesis, characterization, stability and thermal conductivity of multi-walled carbon nanotubes (MWCNTs) and eco-friendly jatropha seed oil based nanofluid: An experimental investigation and modeling approach," *Journal of Molecular Liquids*, vol. 293, p. 111534, 2019/11/01/ 2019.

[80] A. Asadi, M. Asadi, M. Rezaei, M. Siahmargoi, and F. Asadi, "The effect of temperature and solid concentration on dynamic viscosity of MWCNT/MgO (20–80)–SAE50 hybrid nano-lubricant and proposing a new correlation: An experimental study," *International Communications in Heat and Mass Transfer*, vol. 78, pp. 48-53, 2016/11/01/ 2016.

[81] E. De Robertis *et al.*, "Application of the modulated temperature differential scanning calorimetry technique for the determination of the specific heat of copper nanofluids," *Applied Thermal Engineering*, vol. 41, pp. 10-17, 2012/08/01/ 2012.
[82] S. Sonawane, K. Patankar, A. Fogla, B. Puranik, U. Bhandarkar, and S. Sunil Kumar, "An experimental investigation of thermo-physical properties and heat transfer performance of Al2O3-Aviation Turbine Fuel nanofluids," *Applied Thermal Engineering*, vol. 31, no. 14, pp. 2841-2849, 2011/10/01/ 2011.
[83] A. K. Tiwari, N. S. Pandya, H. Shah, and Z. Said, "Experimental comparison of specific heat capacity of three different metal oxides with MWCNT/ water-based hybrid nanofluids: proposing a new correlation," *Applied Nanoscience*, 2020/10/21 2020.
[84] A. K. Starace, J. C. Gomez, J. Wang, S. Pradhan, and G. C. Glatzmaier, "Nanofluid heat capacities," *Journal of Applied Physics*, vol. 110, no. 12, p. 124323, 2011/12/15 2011.
[85] T. Singh, I. W. Almanassra, A. Ghani Olabi, T. Al-Ansari, G. McKay, and M. Ali Atieh, "Performance investigation of multiwall carbon nanotubes based water/oil nanofluids for high pressure and high temperature solar thermal technologies for sustainable energy systems," *Energy Conversion and Management*, vol. 225, p. 113453, 2020/12/01/ 2020.
[86] B. C. Pak and Y. I. Cho, "HYDRODYNAMIC AND HEAT TRANSFER STUDY OF DISPERSED FLUIDS WITH SUBMICRON METALLIC OXIDE PARTICLES," *Experimental Heat Transfer*, vol. 11, no. 2, pp. 151-170, 1998/04/01 1998.
[87] Y. Xuan and W. Roetzel, "Conceptions for heat transfer correlation of nanofluids," *International Journal of Heat and Mass Transfer*, vol. 43, no. 19, pp. 3701-3707, 2000/10/01/ 2000.
[88] H. O'Hanley, J. Buongiorno, T. McKrell, and L.-w. Hu, "Measurement and Model Validation of Nanofluid Specific Heat Capacity with Differential Scanning Calorimetry," *Advances in Mechanical Engineering*, vol. 4, p. 181079, 2012/01/01 2012.
[89] S. M. S. Murshed, "Determination of effective specific heat of nanofluids," *Journal of Experimental Nanoscience*, vol. 6, no. 5, pp. 539-546, 2011/10/01 2011.
[90] Y. R. Sekhar and K. V. Sharma, "Study of viscosity and specific heat capacity characteristics of water-based Al2O3 nanofluids at low particle concentrations," *Journal of Experimental Nanoscience*, vol. 10, no. 2, pp. 86-102, 2015/01/22 2015.
[91] J. Gil-Font *et al.*, "Improving heat transfer of stabilised thermal oil-based tin nanofluids using biosurfactant and molecular layer deposition," *Applied Thermal Engineering*, vol. 178, p. 115559, 2020/09/01/ 2020.
[92] J. Akhter, S. I. Gilani, H. H. Al-Kayiem, M. Ali, and F. Masood, "Experimental evaluation of thermophysical properties of oil-based titania nanofluids for medium temperature solar collectors," *Materialwissenschaft und Werkstofftechnik*, https://doi.org/10.1002/mawe.201900244 vol. 51, no. 6, pp. 792-802, 2020/06/01 2020.
[93] I. C. Nelson, D. Banerjee, and R. Ponnappan, "Flow Loop Experiments Using Polyalphaolefin Nanofluids," *Journal of Thermophysics and Heat Transfer*, vol. 23, no. 4, pp. 752-761, 2009/10/01 2009.
[94] A. Safaei, A. Hossein Nezhad, and A. Rashidi, "High temperature nanofluids based on therminol 66 for improving the heat exchangers power in gas refineries," *Applied Thermal Engineering*, vol. 170, p. 114991, 2020/04/01/ 2020.
[95] I. Popa, G. Gillies, G. Papastavrou, and M. Borkovec, "Attractive and Repulsive Electrostatic Forces between Positively Charged Latex Particles in the Presence of Anionic Linear Polyelectrolytes," *The Journal of Physical Chemistry B*, vol. 114, no. 9, pp. 3170-3177, 2010/03/11 2010.

[96] M. Uematsu and E. U. Frank, "Static Dielectric Constant of Water and Steam," *Journal of Physical and Chemical Reference Data*, vol. 9, no. 4, pp. 1291-1306, 1980/10/01 1980.
[97] A. R. Akash, S. Abraham, A. Pattamatta, and S. K. Das, "Experimental Assessment of the Thermo-Hydraulic Performance of Automobile Radiator with Metallic and Nonmetallic Nanofluids," *Heat Transfer Engineering*, vol. 41, no. 3, pp. 235-251, 2020/02/04 2020.
[98] D. Wen and Y. Ding, "Effective Thermal Conductivity of Aqueous Suspensions of Carbon Nanotubes (Carbon Nanotube Nanofluids)," *Journal of Thermophysics and Heat Transfer*, vol. 18, no. 4, pp. 481-485, 2004/10/01 2004.
[99] T. Gao *et al.*, "Dispersing mechanism and tribological performance of vegetable oil-based CNT nanofluids with different surfactants," *Tribology International*, vol. 131, pp. 51-63, 2019/03/01/ 2019.
[100] O. Gulzar, A. Qayoum, and R. Gupta, "Experimental study on stability and rheological behaviour of hybrid Al2O3-TiO2 Therminol-55 nanofluids for concentrating solar collectors," *Powder Technology*, vol. 352, pp. 436-444, 2019/06/15/ 2019.
[101] S. Mesgari, R. A. Taylor, N. E. Hjerrild, F. Crisostomo, Q. Li, and J. Scott, "An investigation of thermal stability of carbon nanofluids for solar thermal applications," *Solar Energy Materials and Solar Cells*, vol. 157, pp. 652-659, 2016/12/01/ 2016.
[102] A. Dhanola and H. C. Garg, "Influence of different surfactants on the stability and varying concentrations of TiO2 nanoparticles on the rheological properties of canola oil-based nanolubricants," *Applied Nanoscience*, vol. 10, no. 9, pp. 3617-3637, 2020/09/01 2020.
[103] M. Javed *et al.*, "Synthesis of stable waste palm oil based CuO nanofluid for heat transfer applications," *Heat and Mass Transfer*, vol. 54, no. 12, pp. 3739-3745, 2018/12/01 2018.
[104] A. Amiri *et al.*, "Laminar convective heat transfer of hexylamine-treated MWCNTs-based turbine oil nanofluid," *Energy Conversion and Management*, vol. 105, pp. 355-367, 2015/11/15/ 2015.
[105] J. Akhter, S. I. Gilani, H. H. Al-kayiem, M. Ali, and F. Masood, "Characterization and stability analysis of oil-based copper oxide nanofluids for medium temperature solar collectors," *Materialwissenschaft und Werkstofftechnik*, vol. 50, no. 3, pp. 311-319, 2019/03/01 2019.
[106] M. Nabeel Rashin and J. Hemalatha, "Synthesis and viscosity studies of novel ecofriendly ZnO–coconut oil nanofluid," *Experimental Thermal and Fluid Science*, vol. 51, pp. 312-318, 2013/11/01/ 2013.
[107] F. S. Shariatmadar and S. G. Pakdehi, "Effect of various surfactants on the stability time of kerosene–boron nanofluids," *Micro & Nano Letters*, vol. 11, no. 9, pp. 498-502Available: https://digital-library.theiet.org/content/journals/10.1049/mnl.2016.0223
[108] W. Yu, H. Xie, L. Chen, and Y. Li, "Enhancement of thermal conductivity of kerosene-based Fe3O4 nanofluids prepared via phase-transfer method," *Colloids and Surfaces A: Physicochemical and Engineering Aspects*, vol. 355, no. 1, pp. 109-113, 2010/02/20/ 2010.
[109] R. Loni, E. A. Asli-Ardeh, B. Ghobadian, A. B. Kasaeian, and E. Bellos, "Energy and exergy investigation of alumina/oil and silica/oil nanofluids in hemispherical cavity receiver: Experimental Study," *Energy*, vol. 164, pp. 275-287, 2018/12/01/ 2018.
[110] B. Wei, C. Zou, and X. Li, "Experimental investigation on stability and thermal conductivity of diathermic oil based TiO2 nanofluids," *International Journal of Heat and Mass Transfer*, vol. 104, pp. 537-543, 2017/01/01/ 2017.

[111] D. Li, B. Hong, W. Fang, Y. Guo, and R. Lin, "Preparation of Well-Dispersed Silver Nanoparticles for Oil-Based Nanofluids," *Industrial & Engineering Chemistry Research,* vol. 49, no. 4, pp. 1697-1702, 2010/02/17 2010.
[112] S. U. Ilyas, R. Pendyala, and N. Marneni, "Preparation, Sedimentation, and Agglomeration of Nanofluids," *Chemical Engineering & Technology,* vol. 37, no. 12, pp. 2011-2021, 2014/12/01 2014.
[113] S. U. Ilyas, S. Ridha, and F. A. Abdul Kareem, "Dispersion stability and surface tension of SDS-Stabilized saline nanofluids with graphene nanoplatelets," *Colloids and Surfaces A: Physicochemical and Engineering Aspects,* vol. 592, p. 124584, 2020/05/05/ 2020.
[114] A. Gallego, K. Cacua, B. Herrera, D. Cabaleiro, M. M. Piñeiro, and L. Lugo, "Experimental evaluation of the effect in the stability and thermophysical properties of water-Al2O3 based nanofluids using SDBS as dispersant agent," *Advanced Powder Technology,* vol. 31, no. 2, pp. 560-570, 2020/02/01/ 2020.
[115] Z. Said, "Thermophysical and optical properties of SWCNTs nanofluids," *International Communications in Heat and Mass Transfer,* vol. 78, pp. 207-213, 2016/11/01/ 2016.
[116] R. Choudhary, D. Khurana, A. Kumar, and S. Subudhi, "Stability analysis of Al2O3/water nanofluids," *Journal of Experimental Nanoscience,* vol. 12, no. 1, pp. 140-151, 2017/01/01 2017.
[117] S. Bhattacharjee, "DLS and zeta potential – What they are and what they are not?," *Journal of Controlled Release,* vol. 235, pp. 337-351, 2016/08/10/ 2016.
[118] C. Anushree and J. Philip, "Assessment of long term stability of aqueous nanofluids using different experimental techniques," *Journal of Molecular Liquids,* vol. 222, pp. 350-358, 2016/10/01/ 2016.
[119] N. Navarrete, A. Gimeno-Furió, J. Forner-Escrig, J. E. Juliá, and R. Mondragón, "Colloidal stability of molten salt –based nanofluids: Dynamic Light Scattering tests at high temperature conditions," *Powder Technology,* vol. 352, pp. 1-10, 2019/06/15/ 2019.
[120] W. Chamsa-ard, S. Brundavanam, C. C. Fung, D. Fawcett, and G. Poinern, "Nanofluid Types, Their Synthesis, Properties and Incorporation in Direct Solar Thermal Collectors: A Review," *Nanomaterials,* vol. 7, no. 6, 2017.
[121] R. Li, L. Zhang, L. Shi, and P. Wang, "MXene Ti3C2: An Effective 2D Light-to-Heat Conversion Material," *ACS Nano,* vol. 11, no. 4, pp. 3752-3759, 2017/04/25 2017.
[122] A. Ghadimi, R. Saidur, and H. S. C. Metselaar, "A review of nanofluid stability properties and characterization in stationary conditions," *International Journal of Heat and Mass Transfer,* vol. 54, no. 17, pp. 4051-4068, 2011/08/01/ 2011.
[123] D. C. Gregg, "Practical organic chemistry (Vogel, Arthur I.)," *J. Chem. Educ.*, vol. 29, p. 320, 1952.
[124] I. M. Mahbubul *et al.*, "Effect of Ultrasonication Duration on Colloidal Structure and Viscosity of Alumina–Water Nanofluid," *Industrial & Engineering Chemistry Research,* vol. 53, no. 16, pp. 6677-6684, 2014/04/23 2014.
[125] A. Asadi *et al.*, "Effect of sonication characteristics on stability, thermophysical properties, and heat transfer of nanofluids: A comprehensive review," *Ultrasonics Sonochemistry,* vol. 58, p. 104701, 2019/11/01/ 2019.
[126] H. Chen and X. Guo, "Weave structures effect on the shear deformation of annular shaped woven fabrics," in *Advanced Materials Research* vol. 331, ed, 2011, pp. 198-201.
[127] Z. Chen, A. Shahsavar, A. A. A. A. Al-Rashed, and M. Afrand, "The impact of sonication and stirring durations on the thermal conductivity of alumina-liquid paraffin

nanofluid: An experimental assessment," *Powder Technology,* vol. 360, pp. 1134-1142, 2020/01/15/ 2020.
[128] D. H. Fontes, G. Ribatski, and E. P. Bandarra Filho, "Experimental evaluation of thermal conductivity, viscosity and breakdown voltage AC of nanofluids of carbon nanotubes and diamond in transformer oil," *Diamond and Related Materials,* vol. 58, pp. 115-121, 2015/09/01/ 2015.
[129] B. Munkhbayar, M. R. Tanshen, J. Jeoun, H. Chung, and H. Jeong, "Surfactant-free dispersion of silver nanoparticles into MWCNT-aqueous nanofluids prepared by one-step technique and their thermal characteristics," *Ceramics International,* vol. 39, no. 6, pp. 6415-6425, 2013/08/01/ 2013.
[130] J. Boopathy, R. Pari, M. Kavitha, and P. C. Angelo, "Preparation of nano fluids by mechanical method," *AIP Conference Proceedings,* vol. 1461, no. 1, pp. 218-221, 2012/07/23 2012.
[131] S. Mukherjee, P. C. Mishra, and P. Chaudhuri, "Stability of Heat Transfer Nanofluids – A Review," *ChemBioEng Reviews,* vol. 5, no. 5, pp. 312-333, 2018/10/01 2018.
[132] B. M. Paramashivaiah and C. R. Rajashekhar, "Studies on effect of various surfactants on stable dispersion of graphene nano particles in simarouba biodiesel," *IOP Conference Series: Materials Science and Engineering,* vol. 149, p. 012083, 2016/09 2016.
[133] H. Vatanparast, F. Shahabi, A. Bahramian, A. Javadi, and R. Miller, "The Role of Electrostatic Repulsion on Increasing Surface Activity of Anionic Surfactants in the Presence of Hydrophilic Silica Nanoparticles," *Scientific Reports,* vol. 8, no. 1, p. 7251, 2018/05/08 2018.
[134] A. Amiri, M. Naraghi, G. Ahmadi, M. Soleymaniha, and M. Shanbedi, "A review on liquid-phase exfoliation for scalable production of pure graphene, wrinkled, crumpled and functionalized graphene and challenges," *FlatChem,* vol. 8, pp. 40-71, 2018/03/01/ 2018.
[135] S. S. J. Aravind, P. Baskar, T. T. Baby, R. K. Sabareesh, S. Das, and S. Ramaprabhu, "Investigation of Structural Stability, Dispersion, Viscosity, and Conductive Heat Transfer Properties of Functionalized Carbon Nanotube Based Nanofluids," *The Journal of Physical Chemistry C,* vol. 115, no. 34, pp. 16737-16744, 2011/09/01 2011.
[136] H. S. Xue, J. R. Fan, Y. C. Hu, R. H. Hong, and K. F. Cen, "The interface effect of carbon nanotube suspension on the thermal performance of a two-phase closed thermosyphon," *Journal of Applied Physics,* vol. 100, no. 10, p. 104909, 2006/11/15 2006.
[137] A. Amiri *et al.*, "Pool boiling heat transfer of CNT/water nanofluids," *Applied Thermal Engineering,* vol. 71, no. 1, pp. 450-459, 2014/10/05/ 2014.
[138] A. Amiri *et al.*, "Performance dependence of thermosyphon on the functionalization approaches: An experimental study on thermo-physical properties of graphene nanoplatelet-based water nanofluids," *Energy Conversion and Management,* vol. 92, pp. 322-330, 2015/03/01/ 2015.
[139] M. N. A. W. M. Yazid, N. A. C. Sidik, R. Mamat, and G. Najafi, "A review of the impact of preparation on stability of carbon nanotube nanofluids," *International Communications in Heat and Mass Transfer,* vol. 78, pp. 253-263, 2016/11/01/ 2016.
[140] D. Lee, J.-W. Kim, and B. G. Kim, "A New Parameter to Control Heat Transport in Nanofluids: Surface Charge State of the Particle in Suspension," *The Journal of Physical Chemistry B,* vol. 110, no. 9, pp. 4323-4328, 2006/03/01 2006.
[141] H. Xie, H. Lee, W. Youn, and M. Choi, "Nanofluids containing multiwalled carbon nanotubes and their enhanced thermal conductivities," *Journal of Applied Physics,* vol. 94, no. 8, pp. 4967-4971, 2003/10/15 2003.

[142] X.-j. Wang, D.-s. Zhu, and S. yang, "Investigation of pH and SDBS on enhancement of thermal conductivity in nanofluids," *Chemical Physics Letters,* vol. 470, no. 1, pp. 107-111, 2009/02/24/ 2009.
[143] P. I. P. Soares *et al.*, "Iron oxide nanoparticles stabilized with a bilayer of oleic acid for magnetic hyperthermia and MRI applications," *Applied Surface Science,* vol. 383, pp. 240-247, 2016/10/15/ 2016.
[144] S. Umar, F. Sulaiman, N. Abdullah, and S. N. Mohamad, "Investigation of the effect of pH adjustment on the stability of nanofluid," *AIP Conference Proceedings,* vol. 2031, no. 1, p. 020031, 2018/11/29 2018.
[145] B. Smith *et al.*, "Colloidal Properties of Aqueous Suspensions of Acid-Treated, Multi-Walled Carbon Nanotubes," *Environmental Science & Technology,* vol. 43, no. 3, pp. 819-825, 2009/02/01 2009.
[146] K. A. Wepasnick, B. A. Smith, J. L. Bitter, and D. Howard Fairbrother, "Chemical and structural characterization of carbon nanotube surfaces," *Analytical and Bioanalytical Chemistry,* vol. 396, no. 3, pp. 1003-1014, 2010/02/01 2010.
[147] A. Ghozatloo, M. Shariaty-Niasar, and A. M. Rashidi, "Preparation of nanofluids from functionalized Graphene by new alkaline method and study on the thermal conductivity and stability," *International Communications in Heat and Mass Transfer,* vol. 42, pp. 89-94, 2013/03/01/ 2013.
[148] Q. Yu, Y. J. Kim, and H. Ma, "Nanofluids with plasma treated diamond nanoparticles," *Applied Physics Letters,* vol. 92, no. 10, p. 103111, 2008/03/10 2008.
[149] M. Shanbedi, S. Zeinali Heris, M. Baniadam, and A. Amiri, "The Effect of Multi-Walled Carbon Nanotube/Water Nanofluid on Thermal Performance of a Two-Phase Closed Thermosyphon," *Experimental Heat Transfer,* vol. 26, no. 1, pp. 26-40, 2013/01/01 2013.
[150] K.-J. Park, D. Jung, and S. E. Shim, "Nucleate boiling heat transfer in aqueous solutions with carbon nanotubes up to critical heat fluxes," *International Journal of Multiphase Flow,* vol. 35, no. 6, pp. 525-532, 2009/06/01/ 2009.
[151] K. Birdi, *Handbook of surface and colloid chemistry*. CRC press, 2015.
[152] E. Piacenza, A. Presentato, and R. J. Turner, "Stability of biogenic metal(loid) nanomaterials related to the colloidal stabilization theory of chemical nanostructures," *Critical Reviews in Biotechnology,* Review vol. 38, no. 8, pp. 1137-1156, 2018.
[153] M. Shanbedi, S. Zeinali Heris, and A. Maskooki, "Experimental investigation of stability and thermophysical properties of carbon nanotubes suspension in the presence of different surfactants," *Journal of Thermal Analysis and Calorimetry,* vol. 120, no. 2, pp. 1193-1201, 2015/05/01 2015.
[154] Q. Y. Tang, I. Shafiq, Y. C. Chan, N. B. Wong, and R. Cheung, "Study of the Dispersion and Electrical Properties of Carbon Nanotubes Treated by Surfactants in Dimethylacetamide," *Journal of Nanoscience and Nanotechnology,* vol. 10, no. 8, pp. 4967-4974, // 2010.
[155] M. Sahooli, S. Sabbaghi, and M. Shariaty Niassar, "Preparation of CuO/Water Nanofluids Using Polyvinylpyrolidone and a Survey on Its Stability and Thermal Conductivity," (in en), *International Journal of Nanoscience and Nanotechnology,* vol. 8, no. 1, pp. 27-34, 2012.
[156] S. Biggs and T. W. Healy, "Electrosteric stabilisation of colloidal zirconia with low-molecular-weight polyacrylic acid. An atomic force microscopy study," *Journal of the Chemical Society, Faraday Transactions,* 10.1039/FT9949003415 vol. 90, no. 22, pp. 3415-3421, 1994.

[157] E. González, M. Paulis, and M. J. Barandiaran, "Effect of controlled length acrylic acid-based electrosteric stabilizers on latex film properties," *European Polymer Journal,* vol. 59, pp. 122-128, 2014/10/01/ 2014.
[158] K. Manojkumar, A. Sivaramakrishna, and K. Vijayakrishna, "A short review on stable metal nanoparticles using ionic liquids, supported ionic liquids, and poly(ionic liquids)," *Journal of Nanoparticle Research,* vol. 18, no. 4, p. 103, 2016/04/12 2016.
[159] H. J. Kong, S. G. Bike, and V. C. Li, "Electrosteric stabilization of concentrated cement suspensions imparted by a strong anionic polyelectrolyte and a non-ionic polymer," *Cement and Concrete Research,* vol. 36, no. 5, pp. 842-850, 2006/05/01/ 2006.
[160] K. Cacua, F. Ordoñez, C. Zapata, B. Herrera, E. Pabón, and R. Buitrago-Sierra, "Surfactant concentration and pH effects on the zeta potential values of alumina nanofluids to inspect stability," *Colloids and Surfaces A: Physicochemical and Engineering Aspects,* vol. 583, p. 123960, 2019/12/20/ 2019.
[161] S. Al-Anssari, M. Arif, S. Wang, A. Barifcani, and S. Iglauer, "Stabilising nanofluids in saline environments," *Journal of Colloid and Interface Science,* vol. 508, pp. 222-229, 2017/12/15/ 2017.
[162] M. Ma, Y. Zhai, P. Yao, Y. Li, and H. Wang, "Effect of surfactant on the rheological behavior and thermophysical properties of hybrid nanofluids," *Powder Technology,* vol. 379, pp. 373-383, 2021/02/01/ 2021.
[163] K. Cacua, R. Buitrago-Sierra, B. Herrera, F. Chejne, and E. Pabón, "Influence of different parameters and their coupled effects on the stability of alumina nanofluids by a fractional factorial design approach," *Advanced Powder Technology,* vol. 28, no. 10, pp. 2581-2588, 2017/10/01/ 2017.
[164] L. Chen, H. Xie, Y. Li, and W. Yu, "Applications of cationic gemini surfactant in preparing multi-walled carbon nanotube contained nanofluids," *Colloids and Surfaces A: Physicochemical and Engineering Aspects,* vol. 330, no. 2, pp. 176-179, 2008/12/01/ 2008.
[165] H. Chen, S. Witharana, Y. Jin, C. Kim, and Y. Ding, "Predicting thermal conductivity of liquid suspensions of nanoparticles (nanofluids) based on rheology," *Particuology,* vol. 7, no. 2, pp. 151-157, 2009/04/01/ 2009.
[166] M. Hojjat, S. G. Etemad, R. Bagheri, and J. Thibault, "Rheological characteristics of non-Newtonian nanofluids: Experimental investigation," *International Communications in Heat and Mass Transfer,* vol. 38, no. 2, pp. 144-148, 2011/02/01/ 2011.
[167] A. Turgut, I. Tavman, M. Chirtoc, H. P. Schuchmann, C. Sauter, and S. Tavman, "Thermal Conductivity and Viscosity Measurements of Water-Based TiO2 Nanofluids," *International Journal of Thermophysics,* vol. 30, no. 4, pp. 1213-1226, 2009/08/01 2009.
[168] V. Penkavova, J. Tihon, and O. Wein, "Stability and rheology of dilute TiO2-water nanofluids," *Nanoscale Research Letters,* vol. 6, no. 1, p. 273, 2011/03/31 2011.
[169] H. Chen, Y. Ding, and C. Tan, "Rheological behaviour of nanofluids," *New Journal of Physics,* vol. 9, no. 10, pp. 367-367, 2007/10/09 2007.
[170] P. C. Mishra, S. Mukherjee, S. K. Nayak, and A. Panda, "A brief review on viscosity of nanofluids," *International Nano Letters,* vol. 4, no. 4, pp. 109-120, 2014/12/01 2014.
[171] S. Hamze, D. Cabaleiro, and P. Estellé, "Graphene-based nanofluids: A comprehensive review about rheological behavior and dynamic viscosity," *Journal of Molecular Liquids,* vol. 325, p. 115207, 2021/03/01/ 2021.
[172] A. V. Minakov, V. Y. Rudyak, and M. I. Pryazhnikov, "Systematic Experimental Study of the Viscosity of Nanofluids," *Heat Transfer Engineering,* pp. 1-17, 2020.

[173] H. D. Koca, S. Doganay, A. Turgut, I. H. Tavman, R. Saidur, and I. M. Mahbubul, "Effect of particle size on the viscosity of nanofluids: A review," *Renewable and Sustainable Energy Reviews,* vol. 82, pp. 1664-1674, 2018/02/01/ 2018.
[174] E. V. Timofeeva, J. L. Routbort, and D. Singh, "Particle shape effects on thermophysical properties of alumina nanofluids," *Journal of Applied Physics,* vol. 106, no. 1, p. 014304, 2009/07/01 2009.
[175] M. Hemmat Esfe and A. A. Abbasian Arani, "An experimental determination and accurate prediction of dynamic viscosity of MWCNT(%40)-SiO2(%60)/5W50 nano-lubricant," *Journal of Molecular Liquids,* vol. 259, pp. 227-237, 2018/06/01/ 2018.
[176] M. H. Aghahadi, M. Niknejadi, and D. Toghraie, "An experimental study on the rheological behavior of hybrid Tungsten oxide (WO3)-MWCNTs/engine oil Newtonian nanofluids," *Journal of Molecular Structure,* vol. 1197, pp. 497-507, 2019/12/05/ 2019.
[177] L. Wu, L. M. Keer, J. Lu, B. Song, and L. Gu, "Molecular dynamics simulations of the rheological properties of graphene–PAO nanofluids," *Journal of Materials Science,* vol. 53, no. 23, pp. 15969-15976, 2018/12/01 2018.
[178] M. A. Moghaddam and K. Motahari, "Experimental investigation, sensitivity analysis and modeling of rheological behavior of MWCNT-CuO (30–70)/SAE40 hybrid nano-lubricant," *Applied Thermal Engineering,* vol. 123, pp. 1419-1433, 2017/08/01/ 2017.
[179] M. Asadi and A. Asadi, "Dynamic viscosity of MWCNT/ZnO–engine oil hybrid nanofluid: An experimental investigation and new correlation in different temperatures and solid concentrations," *International Communications in Heat and Mass Transfer,* vol. 76, pp. 41-45, 2016/08/01/ 2016.
[180] A. Alirezaie, S. Saedodin, M. H. Esfe, and S. H. Rostamian, "Investigation of rheological behavior of MWCNT (COOH-functionalized)/MgO - Engine oil hybrid nanofluids and modelling the results with artificial neural networks," *Journal of Molecular Liquids,* vol. 241, pp. 173-181, 2017/09/01/ 2017.
[181] M. Hemmat Esfe, M. Afrand, W.-M. Yan, H. Yarmand, D. Toghraie, and M. Dahari, "Effects of temperature and concentration on rheological behavior of MWCNTs/SiO2(20–80)-SAE40 hybrid nano-lubricant," *International Communications in Heat and Mass Transfer,* vol. 76, pp. 133-138, 2016/08/01/ 2016.
[182] M. Hemmat Esfe and H. Rostamian, "Non-Newtonian power-law behavior of TiO2/SAE 50 nano-lubricant: An experimental report and new correlation," *Journal of Molecular Liquids,* vol. 232, pp. 219-225, 2017/04/01/ 2017.
[183] A. Ahmadi Nadooshan, M. Hemmat Esfe, and M. Afrand, "Evaluation of rheological behavior of 10W40 lubricant containing hybrid nano-material by measuring dynamic viscosity," *Physica E: Low-dimensional Systems and Nanostructures,* vol. 92, pp. 47-54, 2017/08/01/ 2017.
[184] M. Hemmat Esfe, M. Afrand, S. H. Rostamian, and D. Toghraie, "Examination of rheological behavior of MWCNTs/ZnO-SAE40 hybrid nano-lubricants under various temperatures and solid volume fractions," *Experimental Thermal and Fluid Science,* vol. 80, pp. 384-390, 2017/01/01/ 2017.
[185] K. Motahari, M. Abdollahi Moghaddam, and M. Moradian, "Experimental investigation and development of new correlation for influences of temperature and concentration on dynamic viscosity of MWCNT-SiO2 (20-80)/20W50 hybrid nano-lubricant," *Chinese Journal of Chemical Engineering,* vol. 26, no. 1, pp. 152-158, 2018/01/01/ 2018.
[186] H. Attari, F. Derakhshanfard, and M. H. K. Darvanjooghi, "Effect of temperature and mass fraction on viscosity of crude oil-based nanofluids containing oxide

nanoparticles," *International Communications in Heat and Mass Transfer,* vol. 82, pp. 103-113, 2017/03/01/ 2017.
[187] E. Dardan, M. Afrand, and A. H. Meghdadi Isfahani, "Effect of suspending hybrid nano-additives on rheological behavior of engine oil and pumping power," *Applied Thermal Engineering,* vol. 109, pp. 524-534, 2016/10/25/ 2016.
[188] M. Hemmat Esfe and S. Esfandeh, "Investigation of rheological behavior of hybrid oil based nanolubricant-coolant applied in car engines and cooling equipments," *Applied Thermal Engineering,* vol. 131, pp. 1026-1033, 2018/02/25/ 2018.
[189] M. Hemmat Esfe, R. Karimpour, A. A. Abbasian Arani, and J. Shahram, "Experimental investigation on non-Newtonian behavior of Al2O3-MWCNT/5W50 hybrid nano-lubricant affected by alterations of temperature, concentration and shear rate for engine applications," *International Communications in Heat and Mass Transfer,* vol. 82, pp. 97-102, 2017/03/01/ 2017.
[190] A. Einstein, "A new determination of molecular dimensions," *Ann. Phys.,* vol. 19, pp. 289-306, 1906 1906.
[191] H. C. Brinkman, "The viscosity of concentrated suspensions and solutions," *The Journal of Chemical Physics,* Article vol. 20, no. 4, p. 571, 1952.
[192] R. Roscoe, "The viscosity of suspensions of rigid spheres," *J. Appl. Phys.,* vol. 267, pp. 3-6, 1952.
[193] I. M. Krieger and T. J. Dougherty, "A Mechanism for Non-Newtonian Flow in Suspensions of Rigid Spheres," *Journal of Rheology,* Article vol. 3, no. 1, pp. 137-152, 1959.
[194] H. Brenner and D. W. Condiff, "Transport mechanics in systems of orientable particles. IV. convective transport," *Journal of Colloid and Interface Science,* vol. 47, no. 1, pp. 199-264, 1974/04/01/ 1974.
[195] D. J. Jeffrey and A. Acrivos, "The rheological properties of suspensions of rigid particles," *AIChE Journal,* Article vol. 22, no. 3, pp. 417-432, 1976.
[196] G. K. Batchelor, "The effect of Brownian motion on the bulk stress in a suspension of spherical particles," *Journal of Fluid Mechanics,* Article vol. 83, no. 1, pp. 97-117, 1977.
[197] A. L. Graham, "On the viscosity of suspensions of solid spheres," *Applied Scientific Research,* Article vol. 37, no. 3-4, pp. 275-286, 1981.
[198] H. Chang *et al.,* "Modeling study on the thermal performance of a modified cavity receiver with glass window and secondary reflector," *Energy Conversion and Management,* vol. 106, pp. 1362-1369, 2015/12/01/ 2015.
[199] M. J. Muhammad, I. A. Muhammad, N. A. Che Sidik, and M. N. A. W. Muhammad Yazid, "Thermal performance enhancement of flat-plate and evacuated tube solar collectors using nanofluid: A review," *International Communications in Heat and Mass Transfer,* vol. 76, pp. 6-15, 2016/08/01/ 2016.
[200] K. Farhana *et al.,* "Improvement in the performance of solar collectors with nanofluids — A state-of-the-art review," *Nano-Structures & Nano-Objects,* vol. 18, p. 100276, 2019/04/01/ 2019.
[201] E. Torres, I. Carrillo-Berdugo, D. Zorrilla, J. Sánchez-Márquez, and J. Navas, "CuO-containing oil-based nanofluids for concentrating solar power: An experimental and computational integrated insight," *Journal of Molecular Liquids,* vol. 325, p. 114643, 2021/03/01/ 2021.
[202] A. Lenert, Y. S. Perez Zuniga, and E. N. Wang, "Nanofluid-Based Absorbers for High Temperature Direct Solar Collectors," 2010. Available: https://doi.org/10.1115/IHTC14-22208

[203] A. Lenert and E. N. Wang, "Optimization of nanofluid volumetric receivers for solar thermal energy conversion," *Solar Energy*, vol. 86, no. 1, pp. 253-265, 2012/01/01/ 2012.
[204] Q. Li *et al.*, "Experimental and numerical investigation of volumetric versus surface solar absorbers for a concentrated solar thermal collector," *Solar Energy*, vol. 136, pp. 349-364, 2016/10/15/ 2016.
[205] A. Mwesigye and İ. H. Yılmaz, "Thermal and thermodynamic benchmarking of liquid heat transfer fluids in a high concentration ratio parabolic trough solar collector system," *Journal of Molecular Liquids*, vol. 319, p. 114151, 2020/12/01/ 2020.
[206] H. Olia, M. Torabi, M. Bahiraei, M. H. Ahmadi, M. Goodarzi, and M. R. Safaei, "Application of Nanofluids in Thermal Performance Enhancement of Parabolic Trough Solar Collector: State-of-the-Art," *Applied Sciences*, vol. 9, no. 3, 2019.
[207] A. Menbari, A. A. Alemrajabi, and A. Rezaei, "Heat transfer analysis and the effect of CuO/Water nanofluid on direct absorption concentrating solar collector," *Applied Thermal Engineering*, vol. 104, pp. 176-183, 2016/07/05/ 2016.
[208] A. Mwesigye and J. P. Meyer, "Optimal thermal and thermodynamic performance of a solar parabolic trough receiver with different nanofluids and at different concentration ratios," *Applied Energy*, vol. 193, pp. 393-413, 2017/05/01/ 2017.
[209] Y. Wang, J. Xu, Q. Liu, Y. Chen, and H. Liu, "Performance analysis of a parabolic trough solar collector using Al2O3/synthetic oil nanofluid," *Applied Thermal Engineering*, vol. 107, pp. 469-478, 2016/08/25/ 2016.
[210] E. Kaloudis, E. Papanicolaou, and V. Belessiotis, "Numerical simulations of a parabolic trough solar collector with nanofluid using a two-phase model," *Renewable Energy*, vol. 97, pp. 218-229, 2016/11/01/ 2016.
[211] D. Korres, E. Bellos, and C. Tzivanidis, "Investigation of a nanofluid-based compound parabolic trough solar collector under laminar flow conditions," *Applied Thermal Engineering*, vol. 149, pp. 366-376, 2019/02/25/ 2019.
[212] G. Xu, W. Chen, S. Deng, X. Zhang, and S. Zhao, "Performance Evaluation of a Nanofluid-Based Direct Absorption Solar Collector with Parabolic Trough Concentrator," *Nanomaterials*, vol. 5, no. 4, pp. 2131-2147, 2015.
[213] V. Khullar, H. Tyagi, P. E. Phelan, T. P. Otanicar, H. Singh, and R. A. Taylor, "Solar Energy Harvesting Using Nanofluids-Based Concentrating Solar Collector," *Journal of Nanotechnology in Engineering and Medicine*, vol. 3, no. 3, 2013.
[214] M. T. Islam, N. Huda, A. B. Abdullah, and R. Saidur, "A comprehensive review of state-of-the-art concentrating solar power (CSP) technologies: Current status and research trends," *Renewable and Sustainable Energy Reviews*, vol. 91, pp. 987-1018, 2018/08/01/ 2018.
[215] M. J. Blanco and S. Miller, "1 - Introduction to concentrating solar thermal (CST) technologies," in *Advances in Concentrating Solar Thermal Research and Technology*, M. J. Blanco and L. R. Santigosa, Eds.: Woodhead Publishing, 2017, pp. 3-25.
[216] R. Loni, E. A. Asli-Ardeh, B. Ghobadian, and A. Kasaeian, "Experimental study of carbon nano tube/oil nanofluid in dish concentrator using a cylindrical cavity receiver: Outdoor tests," *Energy Conversion and Management*, vol. 165, pp. 593-601, 2018/06/01/ 2018.
[217] R. Loni, E. Askari Asli-ardeh, B. Ghobadian, A. B. Kasaeian, and S. Gorjian, "Thermodynamic analysis of a solar dish receiver using different nanofluids," *Energy*, vol. 133, pp. 749-760, 2017/08/15/ 2017.
[218] R. Loni, E. Askari Asli-Ardeh, B. Ghobadian, A. B. Kasaeian, and E. Bellos, "Thermal performance comparison between Al2O3/oil and SiO2/oil nanofluids in cylindrical

cavity receiver based on experimental study," *Renewable Energy*, vol. 129, pp. 652-665, 2018/12/01/ 2018.
[219] R. Loni *et al.*, "Research and review study of solar dish concentrators with different nanofluids and different shapes of cavity receiver: Experimental tests," *Renewable Energy*, vol. 145, pp. 783-804, 2020/01/01/ 2020.
[220] S. Pavlovic, E. Bellos, and R. Loni, "Exergetic investigation of a solar dish collector with smooth and corrugated spiral absorber operating with various nanofluids," *Journal of Cleaner Production*, vol. 174, pp. 1147-1160, 2018/02/10/ 2018.
[221] R. Kumar, V. Deshmukh, and R. S. Bharj, "Performance enhancement of photovoltaic modules by nanofluid cooling: A comprehensive review," *International Journal of Energy Research*, https://doi.org/10.1002/er.5285 vol. 44, no. 8, pp. 6149-6169, 2020/06/25 2020.
[222] A. Ahmed, H. Baig, S. Sundaram, and T. K. Mallick, "Use of Nanofluids in Solar PV/Thermal Systems," *International Journal of Photoenergy*, vol. 2019, p. 8039129, 2019/06/16 2019.
[223] W. An, J. Wu, T. Zhu, and Q. Zhu, "Experimental investigation of a concentrating PV/T collector with Cu9S5 nanofluid spectral splitting filter," *Applied Energy*, vol. 184, pp. 197-206, 2016/12/15/ 2016.
[224] X. Ju, M. M. Abd El-Samie, C. Xu, H. Yu, X. Pan, and Y. Yang, "A fully coupled numerical simulation of a hybrid concentrated photovoltaic/thermal system that employs a therminol VP-1 based nanofluid as a spectral beam filter," *Applied Energy*, vol. 264, p. 114701, 2020/04/15/ 2020.
[225] S. Hassani, R. A. Taylor, S. Mekhilef, and R. Saidur, "A cascade nanofluid-based PV/T system with optimized optical and thermal properties," *Energy*, vol. 112, pp. 963-975, 2016/10/01/ 2016.
[226] E. Bellos and C. Tzivanidis, "Investigation of a nanofluid-based concentrating thermal photovoltaic with a parabolic reflector," *Energy Conversion and Management*, vol. 180, pp. 171-182, 2019/01/15/ 2019.
[227] G. Morin, J. Dersch, W. Platzer, M. Eck, and A. Häberle, "Comparison of Linear Fresnel and Parabolic Trough Collector power plants," *Solar Energy*, vol. 86, no. 1, pp. 1-12, 2012/01/01/ 2012.
[228] E. C. Okonkwo, I. Wole-Osho, I. W. Almanassra, Y. M. Abdullatif, and T. Al-Ansari, "An updated review of nanofluids in various heat transfer devices," *Journal of Thermal Analysis and Calorimetry*, 2020/06/15 2020.
[229] W. Huang and M. Marefati, "Energy, exergy, environmental and economic comparison of various solar thermal systems using water and Thermia Oil B base fluids, and CuO and Al2O3 nanofluids," *Energy Reports*, vol. 6, pp. 2919-2947, 2020/11/01/ 2020.
[230] E. Bellos and C. Tzivanidis, "Multi-criteria evaluation of a nanofluid-based linear Fresnel solar collector," *Solar Energy*, vol. 163, pp. 200-214, 2018/03/15/ 2018.
[231] E. Bellos, C. Tzivanidis, and A. Papadopoulos, "Enhancing the performance of a linear Fresnel reflector using nanofluids and internal finned absorber," *Journal of Thermal Analysis and Calorimetry*, vol. 135, no. 1, pp. 237-255, 2019/01/01 2019.
[232] A. Mwesigye, Z. Huan, and J. P. Meyer, "Thermal performance and entropy generation analysis of a high concentration ratio parabolic trough solar collector with Cu-Therminol®VP-1 nanofluid," *Energy Conversion and Management*, vol. 120, pp. 449-465, 2016/07/15/ 2016.
[233] E. Bellos, C. Tzivanidis, K. A. Antonopoulos, and G. Gkinis, "Thermal enhancement of solar parabolic trough collectors by using nanofluids and converging-diverging absorber tube," *Renewable Energy*, vol. 94, pp. 213-222, 2016/08/01/ 2016.

[234] E. Bellos and C. Tzivanidis, "Thermal efficiency enhancement of nanofluid-based parabolic trough collectors," *Journal of Thermal Analysis and Calorimetry,* vol. 135, no. 1, pp. 597-608, 2019/01/01 2019.
[235] M. S. Khan, M. Abid, M. Yan, T. A. H. Ratlamwala, and I. Mubeen, "Thermal and thermodynamic comparison of smooth and convergent-divergent parabolic trough absorber tubes with the application of mono and hybrid nanofluids," *International Journal of Energy Research,* https://doi.org/10.1002/er.6123 vol. 45, no. 3, pp. 4543-4564, 2021/03/10 2021.
[236] P. Mohammad Zadeh, T. Sokhansefat, A. B. Kasaeian, F. Kowsary, and A. Akbarzadeh, "Hybrid optimization algorithm for thermal analysis in a solar parabolic trough collector based on nanofluid," *Energy,* vol. 82, pp. 857-864, 2015/03/15/ 2015.
[237] A. Mwesigye, İ. H. Yılmaz, and J. P. Meyer, "Numerical analysis of the thermal and thermodynamic performance of a parabolic trough solar collector using SWCNTs-Therminol®VP-1 nanofluid," *Renewable Energy,* vol. 119, pp. 844-862, 2018/04/01/ 2018.
[238] M. S. Khan, M. Abid, H. M. Ali, K. P. Amber, M. A. Bashir, and S. Javed, "Comparative performance assessment of solar dish assisted s-CO2 Brayton cycle using nanofluids," *Applied Thermal Engineering,* vol. 148, pp. 295-306, 2019/02/05/ 2019.
[239] Z. Luo, C. Wang, W. Wei, G. Xiao, and M. Ni, "Performance improvement of a nanofluid solar collector based on direct absorption collection (DAC) concepts," *International Journal of Heat and Mass Transfer,* vol. 75, pp. 262-271, 2014/08/01/ 2014.
[240] N. Hordy, D. Rabilloud, J.-L. Meunier, and S. Coulombe, "High temperature and long-term stability of carbon nanotube nanofluids for direct absorption solar thermal collectors," *Solar Energy,* vol. 105, pp. 82-90, 2014/07/01/ 2014.
[241] X. Wang, Y. He, M. Chen, and Y. Hu, "ZnO-Au composite hierarchical particles dispersed oil-based nanofluids for direct absorption solar collectors," *Solar Energy Materials and Solar Cells,* vol. 179, pp. 185-193, 2018/06/01/ 2018.
[242] R. A. Taylor *et al.*, "Applicability of nanofluids in high flux solar collectors," *Journal of Renewable and Sustainable Energy,* vol. 3, no. 2, p. 023104, 2011/03/01 2011.
[243] S. Srivastava and K. S. Reddy, "Simulation studies of thermal and electrical performance of solar linear parabolic trough concentrating photovoltaic system," *Solar Energy,* vol. 149, pp. 195-213, 2017/06/01/ 2017.
[244] O. Z. Sharaf, R. A. Taylor, and E. Abu-Nada, "On the colloidal and chemical stability of solar nanofluids: From nanoscale interactions to recent advances," *Physics Reports,* vol. 867, pp. 1-84, 2020/06/25/ 2020.
[245] M. Faizal, R. Saidur, S. Mekhilef, A. Hepbasli, and I. M. Mahbubul, "Energy, economic, and environmental analysis of a flat-plate solar collector operated with SiO2 nanofluid," *Clean Technologies and Environmental Policy,* vol. 17, no. 6, pp. 1457-1473, 2015/08/01 2015.
[246] T. J. Choi, S. P. Jang, and M. A. Kedzierski, "Effect of surfactants on the stability and solar thermal absorption characteristics of water-based nanofluids with multi-walled carbon nanotubes," *International Journal of Heat and Mass Transfer,* vol. 122, pp. 483-490, 2018/07/01/ 2018.
[247] S. Fotowat, S. Askar, M. Ismail, and A. Fartaj, "A study on corrosion effects of a water based nanofluid for enhanced thermal energy applications," *Sustainable Energy Technologies and Assessments,* vol. 24, pp. 39-44, 2017/12/01/ 2017.

[248] K. Elsaid, A. G. Olabi, T. Wilberforce, M. A. Abdelkareem, and E. T. Sayed, "Environmental impacts of nanofluids: A review," *Science of The Total Environment*, vol. 763, p. 144202, 2021/04/01/ 2021.
[249] I. Carrillo-Berdugo *et al.*, "Interface-inspired formulation and molecular-level perspectives on heat conduction and energy storage of nanofluids," *Scientific Reports*, vol. 9, no. 1, p. 7595, 2019/05/20 2019.